Evaluation of nitrocatechol bearing cyclic chalcones and related analogues as dual monoamine oxidase and catechol-O-methyltransferase inhibitors

AD de Beer

orcid.org/0000-0002-5755-5969

Dissertation submitted in fulfilment of the requirements for the degree *Masters of Science in Pharmaceutical Chemistry* at the North West University

Supervisor:	Prof LJ Legoabe
Co-Supervisor:	Prof A Petzer
Co-Supervisor:	Prof JP Petzer

Examination: October 2019

Student number: 25094963

DECLARATION

This dissertation is submitted in fulfilment of the requirements for the degree *Master of Science in Pharmaceutical Chemistry*, at the North-West University, Potchefstroom campus.

I the undersigned, Andries Daniël de Beer, hereby declare that the dissertation with the title: **"Evaluation of nitrocatechol bearing cyclic chalcones and related analogues as dual monoamine oxidase and catechol-O-methyltransferase inhibitors."** is my own work and has not been submitted at any other University either whole or in part.

Andries Daniël de Beer

Signed at Potchefstroom on the 15th day of October 2019

NWU®
NORTH-WEST UNIVERSITY
NOORDWES-UNIVERSITEIT
YUNIBESITI YA BOKONE-BOPHIRIMA

Pharmacen

Private Bag X6001, Potchefstroom
South Africa 2520

Tel: +27 18 299-1111/2222
Web: http://www.nwu.ac.za

PHARMACEN™
(CENTRE OF EXCELLENCE FOR PHARMACEUTICAL SCIENCES)
Tel:
Email:

16 October 2019

Dear Sir/Madam,

CO-AUTHORSHIP ON RESEARCH ARTICLE

The undersigned are co-authors of the research article listed below, and hereby give permission to Mr. AD de Beer to submit this article as part of the degree *Magister Scientiae in Pharmaceutical Chemistry* at the North-West University (NWU) Potchefstroom campus:

- **Evaluation of nitrocatechol bearing cyclic chalcones and related analogues as dual monoamine oxidase and catechol-O-methyltransferase inhibitors.**

Yours sincerely;

Prof. L.J. Legoabe

Prof. A. Petzer

Prof. J.P. Petzer

PREFACE

ACKNOWLEDGEMENTS

I would like to present my appreciation for the following people, who helped me through this study:

- To Prof. Lesetja Legoabe; thank you for all the patience and wisdom. You have made a huge impact on me as a scientist and person. I will be forever grateful.
- To Prof. Anèl and Prof. Jacques Petzer, thank you for all your expertise and patience with all my questions.
- To my parents, Dries and Elsabè, and my whole family, thank you for your undying support and love. You are the best.
- To Arisa, Coetsee, Erick, Leroux and Safiya; you guys are my best friends and I couldn't have finished this without you.
- To all the personnel at Pharmaceutical Chemistry, thank you for a great two years, you made it a great place to work and do research.

I would also like to thank the following institutions who helped me in this study:

- The North-West University, who gave me the opportunity to do this study, and the financial support during my time here.
- Dr. D Otto for the NMR data, and Dr. J Jordaan for the MS data from the SASOL Centre for Chemistry.

"All we have to decide is what to do with the time that is given us."

- Gandalf the Grey, The Fellowship of the Ring

ABSTRACT

Parkinson's disease (PD) is one of the leading causes of disability in the world. A better understanding of the aetiology of this disorder will lead to better medications, and would improve the quality of life for millions of patients worldwide. By inhibiting the degradation of dopamine in the midbrain, enzyme inhibitors of both catechol-*O*-methyltransferase (COMT) and monoamine oxidase (MAO) are important drugs in the treatment of PD.

Dopamine is degraded both peripherally and centrally by COMT to yield 3-O-methyldopa, which can reduce L-dopa absorption at the brain-blood barrier. COMT inhibitors have shown a great promise in reducing akinesia in controlled clinical trials. The MAO-catalysed degradation of dopamine yields reactive oxygen species which may accelerate neuronal degeneration in PD. Thus, MAO-B inhibitors are specifically used for PD pharmacotherapy. MAO-B inhibitors are considered to be safe medication with excellent safety profiles.

By employing the hybrid theory for the design of new drugs, this study used the chalcone structure and the nitrocatechol moiety to design dual inhibitors for COMT and MAO. By using acid catalysed aldol condensation, aith a refluxtime of 24 – 26 hours, a series of nitrocatechol derivatives of chalcone was synthesised in good yields (71–84%). Bicyclic systems were also incorporated into the chalcone structure. An analysis of the structure-activity relationships showed an increase in MAO-B inhibition activity with the inclusion of either a methoxy or hydroxy group on the 5-position of the indanone bicyclic system. Overall the inhibition of MAO-B was moderate, with none of the compounds exhibiting IC_{50} values in the nanomolar range. The most potent IC_{50} for MAO-B inhibition was 7.26 µM for compound **G**, which bears chromanone as the bicyclic system. In contrast to their MAO inhibition potencies, the chalcones were good potency COMT inhibitors with IC_{50} values in the nanomolar range. The most potent COMT inhibitor was compound C with an IC_{50} value of 0.163 µM. The potency of this compounds can be attributed to the addition of the nitrocatechol moiety.

This study concludes that the indanone bicyclic system substituted with methoxy or hydroxy groups on the 5-position has potential for the design of dual inhibitors of MAO-B and COMT.

Keywords: COMT, MAO, Parkinson's disease, chalcone, nitrocatechol.

UITTREKSEL

Parkinson se siekte (PS) is een van die hoofoorsake van gestremdheid in die wêreld. 'n Beter begrip van die oorsake van hierdie siekte sal lei tot beter geneesmiddels, en sal gevolglik die kwaliteit van lewe vir miljoene pasiënte wêreldwyd verbeter. Deur beide katesjol-O-metieltransferase (KOMT) en monoamienoksidase (MAO) te inhibeer sal die afbraak van dopamien in die brein vertraag word. Hierdie benadering kan 'n effektiewe strategie vir die behandeling van PS wees.

Dopamien word beide perifeer en sentraal deur KOMT gemetaboliseer om 3-O-metieldopa te lewer. Hierdie metaboliet kompeteer met levodopa (L-dopa) vir opname by die bloed-brein skans. Daar is in verskeie studies gevind dat KOMT-inhibeerders akinesie in PS verminder. Die MAO-gekataliseerde afbraak van dopamien lei tot die produksie van reaktiewe suurstof spesies wat neurodegenerasie in PS kan versnel. MAO-B-inhibeerders word dus gebruik vir die farmakoterapie van PS. MAO-B inhibeerders word as veilige geneesmiddels beskou met uitstekende veiligheidsprofiele.

Deur gebruik te maak van die hibridisasieteorie vir die ontwerp van die nuwe geneesmiddels, het hierdie studie die chalkoon- en nitrokatesjolstrukture saamgevoeg om verbindings te ontwerp wat beide KOMT en MAO inhibeer. Die sinteseroete het die suurgekataliseerde aldolkondensasie reaksie behels met 'n reflukstyd van 24–26 uur. Die reeks chalkone is so gesintetiseer met goeie opbrengste (71–84%). Bisikliese chalkoonsisteme is ook in hierdie studie ingesluit. Die analise van die struktuur-aktiwiteit-verwantskappe het gewys dat MAO-B inhibisie aktiwiteit verbeter met substitusie van 'n metoksie- of hidroksiegroep op die 5-posisie van die indanoon bisikliese sisteem. Oor die algemeen was die chalkone swak MAO-B-inhibeerders en geen verbinding het nanomolaar IC_{50} waardes getoon nie. Die mees potente inhibeerder was verbinding **G** met 'n IC_{50} waarde van 7.26 µM. Hierdie verbinding het chromanoon as die bisikliese sisteem besit. In teenstelling met die MAO-inhibisie waardes, was die chalkone goeie KOMT-inhibeeredrs met nanomolaar IC_{50} waardes. Die mees potente KOMT-inhibeerder was verbinding **C** met 'n IC_{50} waarde van 0.163 µM. Hierdie goeie potensie kan toegeskryf word aan die teenwoordigheid van die nitrokatesjolgroep.

Die studie het bewys dat die indanoon bisikliese struktuur met 'n metoksie- of hidroksiegroep op die 5-posisie potensiaal besit vir die verdere ontwerp van verbindings wat beide KOMT en MAO-B inhibeer.

Sleutelwoorde: KOMT, MAO, Parkinson se siekte, chalkoon, nitrokatesjol.

TABLE OF CONTENTS

LIST OF TABLES

LIST OF FIGURES

LIST OF ABBREVIATIONS

Abbreviation	Meaning
[…]	Concentration
˚C	Degree Celsius
α-carbon	Alpha-carbon
α-helical	Alpha-helical
α-synuclein	Alpha-synuclein
λ_{em}	Emission wavelength
λ_{ex}	Excitation wavelength
µM	Micromolar
µL	Microliter
3-OMD	3-Methyldopa
^{1}H	Proton
^{13}C	Carbon-13
A	
AADC	Amino acid decarboxylase
ADME	Absorption, distribution, metabolism, excretion
$AlCl_3$	Aluminium trichloride
ALDH	Aldehyde dehydrogenase
APCI	Atmospheric pressure chemical ionisation
ATP	Adenosine triphosphate
B	
BBB	Blood-brain barrier
C	
Calc.	Calculated
CH_3OH	Methanol
$CHCl_3$	Chloroform
COMT	Catechol-O-methyltransferase
CNS	Central nervous system
D	
d	Doublet
dd	Doublet of doublets
ddd	Doublet of doublet of doublets
D_2	Dopamine-2 receptor
D_3	Dopamine-3 receptor
DA	Dopamine
DMSO	Dimethyl sulfoxide
DMSO-*d6*	Deuterated dimethyl sulfoxide
DNA	Deoxyribonucleic acid
DOPAC	3,4-Dihydroxyphenylacetic acid
DOPAL	3,4-Dihydroxyacetaldehyde
E	
E	Enzyme
EI	Enzyme-inhibitor complex
EIS	Enzyme-inhibitor-substrate complex
ES	Enzyme-substrate complex
EP	Enzyme-product complex
F	
FAD	Flavin adenine dinucleotide

FRAP	Ferric oxidation/reduction
G	
GPe	Globus pallidus (external)
GPi	Globus pallidus (internal)
H	
H	Hydrogen
H_2O	Water
H-bond	Hydrogen bond
HCl	Hydrogen chloride/hydrochloric acid
HPLC	High performance liquid chromatography
HRMS	High resolution mass spectroscopy
Hz	Hertz
I	
I	Inhibitor
IC_{50}	Inhibitor concentration at 50% inhibition
J	
J	Joules
K	
KCl	Potassium chloride
L	
LB(s)	Lewy Body(ies)
L-dopa	Levodopa
M	
m	Multiplet
MAO-A	Monoamine oxidase isoform A
MAO-B	Monoamine oxidase isoform B
Mg^{2+}	Magnesium(II) ion
$MgSO_4$	Magnesium sulphate
MH^+	Protonated molecular weight
MHz	Megahertz
min	Minute
mL	Millilitre
mM	Millimolar
mm	Millimetre
mmol	Millimole
MPP^+	1-Methyl-4-phenylpyridinium
MPTP	1-Methyl-4-phenyl-1,2,3,6-tetrahydropyridine
MS	Mass spectroscopy
MW	Molecular weight
N	
N	Molar
NADH	Nicotinamide adenine dinucleotide
NH_4^+	Ammonium ion
nM	Nanomolar
nm	Nanometre
NMR	Nuclear magnetic resonance
NWU	North-West University
O	
ORAC	Oxygen radical absorbance capacity
P	
P	Product

PD	Parkinson’s disease
PSA	Polar surface area
R	
ROS	Reactive oxygen species
S	
s	Singlet
S (capital)	Substrate
SAH	S-adenosyl-L-homocysteine
SAM	S-adenosyl-L-methionine
SAR(s)	Structure activity relationship(s)
SD	Standard deviation
SI	Selectivity index
SNc	Substantia nigra pars compacta
SNr	Substantia nigra oars reticulata
STN	Subthalamic nucleus
T	
t	Triplet
TBARS	Thioburbituric acid-reactive substances
TH	Tyrosine hydroxylase
TLC	Thin layer chromatography
tPSA	Total/topographic polar surface area
TYR	Tyrosinase
W	
WHO	World Health Organisation

CHAPTER 1 INTRODUCTION

1.1 Parkinson's disease

Parkinson's disease (PD), with motor symptoms such as resting tremor, rigidity, bradykinesia and postural instability, as well as non-motor symptoms such as depression, constipation and anxiety, is the second most common neurodegenerative disease in the age of an ever increasing geriatric population (de Lau & Breteler, 2006; Dickson, 2018; Jancovic, 2008); According to Rodrigeuz-Oros *et al.* (2009), PD is characterised by a loss of dopaminergic (DA) neurons in the area of the brain known as the substantia nigra pars compacta and this causes reduced dopamine activation in the motor cortex (Limongi, 2017). PD represents a frequent cause of morbidity that affects 1–2 per 1000 of the population at any time, clearly most often in the older age groups (Tsynes & Storstein*.,* 2017).

The WHO statistical records on chronic PD cases in the aged population raise extensive concerns amongst researchers in the pharmaceutical and medical industries. Although the exact cause of PD is unknown, evidence suggests that increased production of chemical species such as hydrogen peroxide contribute to oxidative stress, which results in neuronal degradation. In the human brain, hydrogen peroxide is the by-product of metabolism of amines such as dopamine by monoamine oxidase B (MAO-B) (Wang *et al.*, 2009).

Several strategies exist for the symptomatic treatment of PD. One treatment strategy is to conserve dopamine by inhibiting the enzymes responsible for its catabolism (Yacoubian & Standaert, 2009). MAO-A and MAO-B are flavin adenine dinucleotide (FAD)-containing enzymes that are attached to the outer membrane of the mitochondrion (Youdim & Bakhle, 2006). These enzymes catalyse the α-carbon oxidation of a variety of neurotransmitters such as dopamine (Inoue *et al.*, 1999). Clinically, inhibitors of MAO-B are considered to be a useful treatment strategy in PD, since the main pathological characteristic is a dopamine deficiency in the basal ganglia. In the basal ganglia MAO-B is the principle enzyme responsible for the catabolism of dopamine (Youdim *et al.*, 2006).

Another drug class involved in the treatment of PD is catechol-O-methyltransferase (COMT) inhibitors. COMT is a magnesium-dependent enzyme which plays an important role in the peripheral catabolism of endogenous catecholamines such as dopamine (Ehler *et al.*, 2014). Levodopa (L-dopa), the metabolic precursor of dopamine, is the drug of choice in PD treatment (Lees, 2005). Due to extensive peripheral enzymatic metabolism by COMT and other enzymes,

only a small portion of L-dopa reaches the brain (Kiss & Soares-da-Silva, 2014). Thus, the dual inhibition of MAO and COMT could not only conserve endogenous dopamine levels, but may also protect L-dopa against undesirable metabolism, thus improving its availability to the brain.

1.2 Monoamine oxidase and its inhibitors

The enzyme, MAO, is responsible for the oxidative deamination of many catecholamine compounds and is present in the central nervous system and the peripheral tissues (Johnston, 1968; Westlund *et al.*, 1988). During the MAO catalytic cycle, hydrogen peroxide and 3,4-dihydroxyphenylacetaldehyde is produced as products, as shown by degradation of dopamine in the presence of MAO (Depicted in figure 1-1).

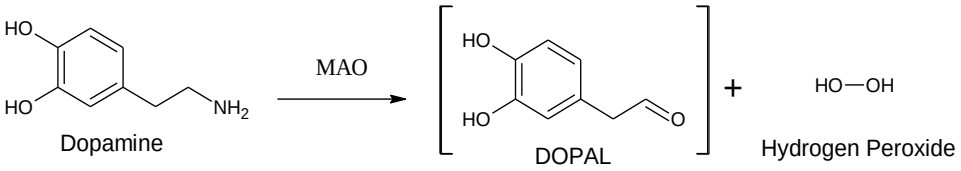

Figure 1-1: The degradation of dopamine in the presence of MAO.

Since hydrogen peroxide may be converted to reactive oxygen species (ROS), which are known to cause oxidative stress (Berman & Hastings, 1999), it may be concluded that with inhibition of MAO, less ROS will be produced and therefore oxidative stress will decrease.

MAO occurs in two isoforms, MAO-A and MAO-B, which differ in their action, distribution and substrate specificity. MAO-A is mostly present in the gut lining whereas MAO-B is more prevalent in the basal ganglia (Collins *et al.*, 1970; Johnston, 1968). MAO-A is inhibited by clorgyline and its preferred substrates are noradrenaline and serotonin, while MAO-B is unaffected by clorgyline (Johnston, 1968). Both isoforms metabolise dopamine and tyramine equally (Youdim *et al.*, 2005).

Clinically, MAO isoform inhibitors are employed for different indications. MAO-A inhibitors are used for treatment of depressive disorder and as anxiolytic agents, whereas inhibition of MAO-B inhibitors are used for the treatment of PD.

1.3 Catechol-O-methyltransferase (COMT) and its inhibitors

COMT is the enzyme that acts as the catalyst for the transfer of an activated methyl group to a catechol neurotransmitter substrate and thus renders it inactive (Vidgren *et al.*, 1994). Clinically, COMT inhibitors are usually used in conjunction with L-dopa therapy to limit the peripheral metabolism of L-dopa to 3-methyldopa (3-OMD) (Rivera-Calimlim *et al.*, 1977). By inhibiting the

peripheral metabolism of L-dopa, an increase in the amount of L-dopa that reaches the brain is obtained.

Furthermore, the reduction of the amount of 3-methyldopa (3-OMD) produced in the peripheral system will lead to increased penetration of L-dopa into the central nervous system (CNS) as 3-OMD competes directly with L-dopa for active transport across the blood-brain barrier (BBB) (Tohgi *et al.*, 1991). The general structures of clinically used COMT inhibitors (entacapone and tolcapone) bear acidic nitro catechol groups. Their mechanism of action is described as reversible yet tight binding, dose dependant inhibition, with tolcapone being more potent (Lotta *et al.*, 1995).

1.4 Dual COMT/MAO inhibitors

According to Beauchine *et al.* (2009), the degradation of dopamine in the brain is controlled by MAO and COMT, which suggests that inhibition of both enzymes will lead to elevated intrinsic dopamine concentrations and the reduction of the symptoms of PD. To achieve this, a combination of MAO and COMT inhibitors could be used or a single dual acting compound could be used to exert the same effect. However, the use of dual acting drugs can be favourable compared to the two distinct drugs since the single entity will have more predictable pharmacokinetic and pharmacodynamics properties (Wermuth, 2011).

Hybridisation is one of the approaches used in attempts to discover dual acting drugs, in which two different pharmacophores are incorporated into a new single entity which possess both initial pharmacological activities. This approach will only be appropriate when the two targeted enzymes or receptors are involved in the same disease or disorder (Wermuth, 2011), such as PD therapy, where both COMT and MAO affect the levels of dopamine, particularly with L-dopa therapy.

As depicted in figure 1-2, cyclic chalcone derivatives (**1**-**3**) have shown nanomolar activity as MAO-B inhibitors, while tolcapone and entacapone both bear the nitrocatechol moiety and are clinically used as COMT inhibitors.

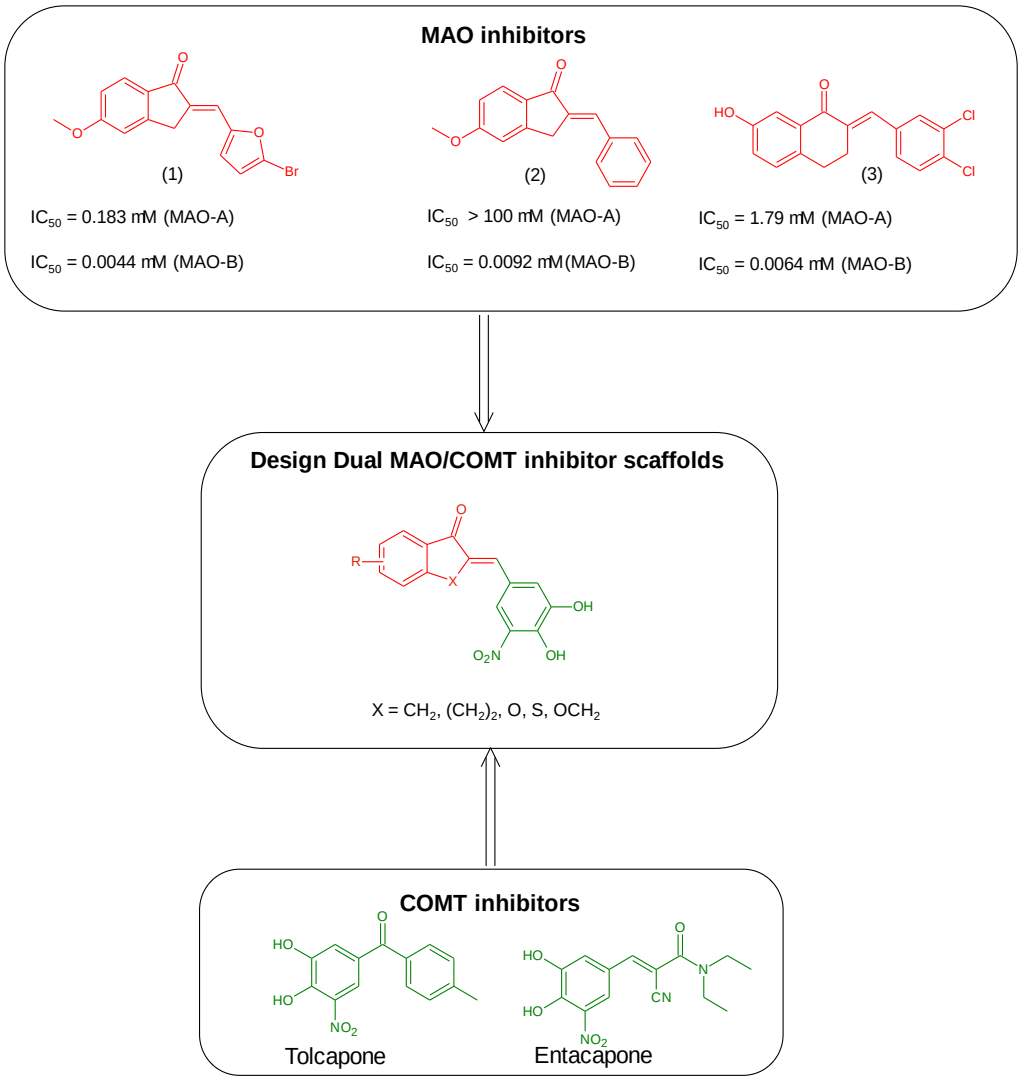

Figure 1-2: Design approach for the discovery of dual COMT/MAO inhibitors.

Based on the promising properties of chalcones as inhibitors of MAO (Chimenti *et al.*, 2009; Legoabe *et al.*, 2014; Nel *et al.*, 2016b) and nitrocatechol compounds as COMT inhibitors (Engelbrecht *et al.*, 2018; Learmonth *et al.*, 2012), we envisage to design the dual COMT/MAO inhibitors bearing both pharmacophores by employing the hybridisation approach.

Even though both centrally and peripherally acting COMT inhibitors are of value, it is a crucial that dual-acting COMT/MAO inhibitors are able to penetrate the BBB to reach the substantia nigra where it could exert MAO-B inhibitory action and thus contribute towards the conservation of dopamine. Therefore it's essential to take into account the physicochemical properties essential for crossing BBB when designing dual-acting COMT/MAO inhibitors.

In the current study, the nitrocatechol pharmacophore will be retained for all compounds that will be designed since it is essential for COMT inhibition activity. The cyclic chalcone moiety will,

however, be targeted for structural modification, particularly to determine structure-activity relationships (SARs), and to modulate physicochemical properties such as log P and polar surface area (PSA) (Singh *et al.*, 2017), which are determinants for BBB penetration.

1.5 Hypothesis

COMT is responsible for the peripheral metabolism of L-dopa, whereas more than 99% of the bioavailable dose is metabolised before it can reach the brain (Kaakkola, 2000). Furthermore, the metabolism of dopamine in the CNS by MAO further decreases the efficacy of L-dopa (Lees, 2005). Therefore it is hypothesised that, the dual inhibition of COMT and MAO will conserve endogenous dopamine levels in addition to protecting L-dopa against undesirable metabolism and thus improving its availability to the brain.

It is further envisaged that, given the known potential of cyclic chalcones as MAO-inhibitors and nitrocatechol compounds as COMT inhibitors, appropriate hybridisation of these pharmacophores could lead to dual COMT/MAO inhibition. With the presence of the nitrocatechol moiety and appropriate substitution of the cyclic chalcones, dual COMT/MAO inhibition may be obtained.

1.6 Aims and objectives

The aim of the current study is to design dual COMT/MAO inhibitors by hybridisation of the cyclic chalcone and nitrocatechol pharmacophores.

In order to achieve the above mentioned aim, the following objectives have been set:

(i) To synthesise the tetralone- and indanone-based cyclic chalcones bearing nitrocatechol as ring B (series 1).

(ii) To evaluate the synthesised compounds as inhibitors of MAO-A, MAO-B and COMT by measuring IC_{50} values.

(iii) To determine SARs for the inhibition of COMT and MAO by the synthesised compounds.

1.7 Methodology

1.7.1 Synthesis

Compounds in this series are cyclic chalcones bearing the nitrocatechol moiety as ring B. Commercially available 5-nitrovanillin dissolved in chloroform will be reacted with $AlCl_3$ in the presence of pyridine to yield 3,4-dihydroxy-5-nitrobenzaldehyde according to the method described in literature (Walz & Sundberg, 2000). The catechol thus obtained, 3,4-dihydroxy-5-

nitrobenzaldehyde, will undergo aldol condensation (Amakali, 2016; Nel *et al.*, 2016a; Nel *et al.*, 2016b) with an appropriate cyclic ketones to give the target compounds.

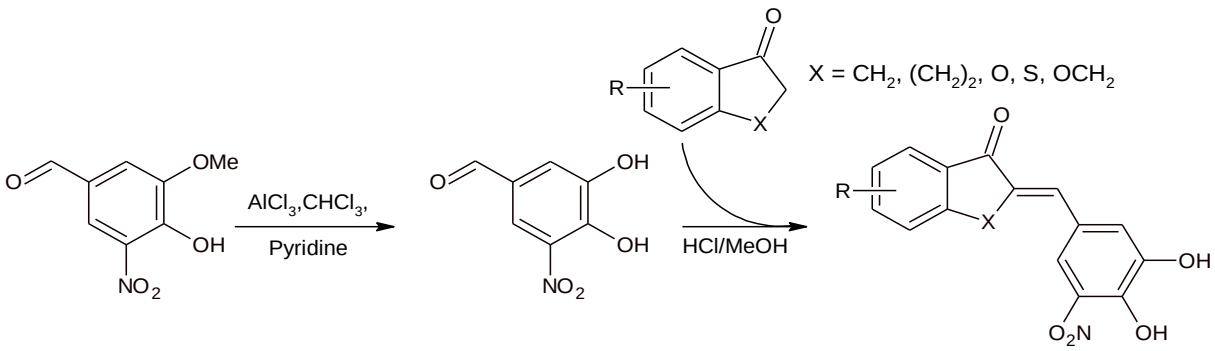

Figure 1-3: Synthetic pathway for preparation of cyclic chalcones bearing the nitrocatechol as ring B.

1.7.2 Biological Assays

1.7.2.1 MAO inhibition assay

Fluorescence spectrophotometry will be used to determine the IC_{50} values for the inhibition of the recombinant human MAOs by the synthesised inhibitors. This protocol uses kynuramine as substrate. Kynuramine is oxidised by MAO-A and MAO-B to ultimately yield 4-hydroxyquinoline, a metabolite which fluoresces (λ_{ex} = 310 nm; λ_{em} = 400 nm) in alkaline media (Strydom *et al*., 2010). From the MAO activity measurements in the presence of the test inhibitors, sigmoidal dose-response curves will be constructed and the inhibition potencies, the corresponding IC_{50} values, will be calculated. Sigmoidal dose–response curves will be constructed using the Prism 5.0 software package (GraphPad), and the IC_{50} values will be determined in triplicate and expressed as mean ± standard deviation (SD).

1.7.2.2 COMT inhibition assay

To determine whether the synthesised compounds are inhibitors of COMT, the method described in literature (Borchardt, 1974) will be used. This protocol uses esculetin (6,7-dihydroxycoumarin) as substrate for COMT. After the test inhibitor is incubated with esculetin and COMT, fluorescence spectrophotometry will be used to quantify the enzymatic product, scopoletin. Sigmoidal dose-response curves of scopoletin concentration versus the logarithm of inhibitor concentration (Log[I]) will be constructed using the Prism 5.0 software package, and the IC_{50} values will be determined in triplicate and expressed as mean ± SD. As enzyme source, the soluble fraction obtained from homogenates of rat liver tissue will be used.

1.8 Ethical considerations

Rat liver tissue will be used as an enzyme source for COMT. The rat livers will be obtained from other ongoing studies. A category 0 application to obtain and use rat liver tissue has been submitted to AnimCare, and has been approved (NWU-000564-19-S5) To process the rat livers, a previously reported literature method will be applied (Hirano *et al*., 2005; Zhu *et al*., 1994) and the soluble fraction of COMT will be used for the evaluation of the IC_{50} values of the various synthesised test compounds. Approximately 4 rat livers will be needed for this study. The recombinant mitochondrial-bound MAO enzymes, expressed in insect cells, will be purchased from a commercial supplier. For the enzyme work, HREC has been notified and approval has been obtained.

REFERENCES

Alexander, G. 2004. Biology of Parkinson's disease: pathogenesis and pathophysiology of a multisystem neurodegenerative disorder. *State of the Art*, 6(3):259.

Amakali, K.T. 2016. Synthesis and evaluation of cyclic chalcones as monoamine oxidase inhibitors. North-West University (South Africa), Potchefstroom Campus. (Dissertation – MSc).

Aoyama, N., Tsunoda, M. & Kimai, K. 2005. Improved assay for catechol-O-methyltransferase activity utilizing norepinephrine as an enzymatic substrate and reversed-phase high-performance liquid chromatography with fluorescence detection. *Journal of Chromatography A*. 1074:47-51.

Beauchaine, T.P., Klein, D.N., Crowell, S.E., Derbidge, C. & Gatzke-Kopp, L. 2009. Multifinality in the development of personality disorders: a Biology x Sex x Environment interaction model of antisocial and borderline traits. *Development and Psychopathology*, 21(3):735-770.

Berman, S.B. & Hastings, T.G. 1999. Dopamine oxidation alters mitochondrial respiration and induces permeability transition in brain mitochondria: implications for Parkinson's disease. *Journal of Neurochemistry*, 73(3):1127-1137.

Borchardt, R.T. 1974. A rapid spectrophotometric assay for catechol-O-methyltransferase. *Analytical Biochemistry*, 58(2):382-389.

Chimenti, F., Fioravanti, R., Bolasco, A., Chimenti, P., Secci, D., Rossi, F., Yanez, M., Orallo, F., Ortuso, F. & Alcaro, S. 2009. Chalcones: a valid scaffold for monoamine oxidases inhibitors. *Journal of Medicinal Chemistry*, 52(9):2818-2824.

Collins, G., Sandler, M., Williams, E. & Youdim, M.B.H. 1970. Multiple forms of human brain mitochondrial monoamine oxidase. *Nature*, 225:817–820.

Da Prada, M., Kettler, R., Keller, H.H., Cesura, A.M., Richards, J.G., Saura Marti, J., Muggli-Maniglio, D., Wyss, P.C., Kyburz, E. & Imhof, R. 1990. From moclobemide to Ro 19-6327 and Ro 41-1049: the development of a new class of reversible, selective MAO-A and MAO-B inhibitors. *Journal of Neural Transmission Supplementum*, 29(29):279-292.

De Lau, L.M. & Breteler, M.M. 2006. Epidemiology of Parkinson's disease. *The Lancet Neurology*, 5(6):525-535.

Di Pietro, O., Alencar, N., Esteban, G., Vianya, E., Szałaj, N., Vázquez, J., Juárez-Jiménez, J., Sola, I., Pérez, B., Solé, M., Unzeta, M., Muñez-Toerro, D. & Javier Luque, F. 2016. Design, synthesis and biological evalution of N-methyl¬N-[(1,2,3-triazole-4-yl)alkyl)]propargylamines as novel monoamine oxidase B inhibitors. *Bioorganic & Medicinal Chemistry*, 24::4835-4854.

Dickson, D.W. 2018. Neuropathology of Parkinson disease. *Parkinsonism & Related Disorders*, 46 Suppl 1:S30-S33.

Duarte, C.D., Barreiro, E.J. & Fraga, C.A. 2007. Privileged structures: a useful concept for the rational design of new lead drug candidates. *Mini Reviews in Medicinal Chemistry*, 7(11):1108-1119.

Ehler, A., Benz, J., Schlatter, D. & Rudolph, M.G. 2014. Mapping the conformational space accessible to catechol-O-methyltransferase. *Acta Crystallographica Section D: Biological Crystallography*, 70(8):2163-2174.

Engelbrecht, I., Petzer, J.P. & Petzer, A. 2018. Nitrocatechol Derivatives of Chalcone as Inhibitors of Monoamine Oxidase and Catechol-O-Methyltransferase. *Central Nervous System Agents Medicinal Chemistry,* 18(2):115-127.

Hirano, Y., Tsunoda, M., Funatsu, T. & Imai, K. 2005. Rapid assay for catechol-O-methyltransferase activity by high-performance liquid chromatography-fluorescence detection. *Journal of Chromatography B*. 819:41-46.

Hutschenreuter, T.U., Ehmer, P.B. & Hartmann, R.W. 2004. Synthesis of Hydroxy Derivatives of Highly Potent Non-steroidal CYP 17 Inhibitors as Potential Metabolites and Evaluation of their Activity by a Non Cellular Assay using Recombinant Human Enzyme. *Journal of Enzyme Inhibition and Medicinal Chemistry*, 19(1):17-32.

Inoue, H., Castagnoli, K., Van der Schyf, C., Mabic, S., Igarashi, K. & Castagnoli, N. 1999. Species-dependent differences in monoamine oxidase A and B-catalyzed oxidation of various C4 substituted 1-methyl-4-phenyl-1, 2, 3, 6-tetrahydropyridinyl derivatives. *Journal of Pharmacology and Experimental Therapeutics*, 291(2):856-864.

Jana, S., Sinha, M., Chanda, D., Roy, T., Banerjee, K., Munshi, S., Patro, B.S. & Chakrabarti, S. 2011. Mitochondrial dysfunction mediated by quinone oxidation products of dopamine: Implications in dopamine cytotoxicity and pathogenesis of Parkinson's disease. *Biochimica et Biophysica Acta*, 1812(6):663-673.

Jancovic, J. 2008. Parkinson's Disease: Clinical Features and diagnosis. *Journal on Neurology, Neurosurgery and Psychiatry*, 79:368-376.

Johnston, J. 1968. Some observations upon a new inhibitor of monoamine oxidase in brain tissue. *Biochemical Pharmacology*, 17(7):1985-1297.

Kaakkola, S. 2000. Clinical pharmacology, therapeutic use and potential of COMT inhibitors in Parkinson's disease. *Drugs*, 59(6):1233-1250.

Kiss, L.s.E. & Soares-da-Silva, P. 2014. Medicinal chemistry of catechol O-methyltransferase (COMT) inhibitors and their therapeutic utility. *Journal of Medicinal Chemistry*, 57(21):8692-8717.

Lazar, C., Kluczyk, A., Kiyota, T. & Konishi, Y. 2004. Drug evolution concept in drug design: 1. Hybridization method. *Journal of Medicinal Chemistry*, 47(27):6973-6982.

Learmonth, D.A., Bonifácio, M.J. & Soares-da-Silva, P. 2005. Synthesis and biological evaluation of a novel series of "ortho-nitrated" inhibitors of catechol-O-methyltransferase. *Journal of Medicinal Chemistry*, 48(25):8070-8078.

Learmonth, D.A., Kiss, L.E., Palma, P.N.L., Ferreria, H.D.S. & Silva, P.M.V.A.S.d. 2012. Nitrocatechol derivatives as COMT inhibitors . Patent number: US8168793B2.

Lees, A. 2005. Alternatives to levodopa in the initial treatment of early Parkinson's disease. *Drugs & Aging*, 22(9):731-740.

Legoabe, L.J., Petzer, A. & Petzer, J.P. 2014. α-Tetralone derivatives as inhibitors of monoamine oxidase. *Bioorganic & Medicinal Chemistry Letters*, 24(12):2758-2763.

Limongi, J.C.P., 2017. Quality of life in Parkinson's disease. *Arquivos de Neuro-Psiquiatria*, *75*(8), pp.493-498

Lotta, T., Vidgren, J., Tilgmann, C., Ulmanen, I., Melen, K., Julkunen, I. & Taskinen, J. 1995. Kinetics of human soluble and membrane-bound catechol O-methyltransferase: a revised mechanism and description of the thermolabile variant of the enzyme. *Biochemistry*, 34(13):4202-4210.

Meiser, J., Weindl, D., Hiller, K. 2013. Complexity of dopamine metabolism. *Cell Communication and Signaling*, 11(34):18.

Mostert, S., Petzer, A. & Petzer, J.P. 2015. Indanones As High-Potency Reversible Inhibitors of Monoamine Oxidase. *ChemMedChem*, 10(5):862-873.

Nel, M.S., Petzer, A., Petzer, J.P. & Legoabe, L.J. 2016. 2-Benzylidene-1-indanone derivatives as inhibitors of monoamine oxidase. *Bioorganic & Medicinal Chemistry Letters*, 26(19):4599-4605.

Nel, M.S., Petzer, A., Petzer, J.P. & Legoabe, L.J. 2016. 2-Heteroarylidene-1-indanone derivatives as inhibitors of monoamine oxidase. *Bioorganic Chemistry*, 69:20-28.

Petzer, A., Harvey, B.H., Wegener, G. & Petzer, J.P. 2012. Azure B, a metabolite of methylene blue, is a high-potency, reversible inhibitor of monoamine oxidase. *Toxicology and Applied Pharmacology*. 258(3):403-409.

Rivera-Calimlim, L., Tondon, D., Anderson, E. & Joynt, R. 1977. The clinical picture and plasma levodopa metabolite profile of Parkinsonian nonresponders. *Archives of Neurology*, 34:228-232.

Rodriguez-Oroz, M.C., Jahanshahi, M., Krack, P., Litvan, I., Macias, R., Bezard, E. and Obeso, J.A., 2009. Initial clinical manifestations of Parkinson's disease: features and pathophysiological mechanisms. *The Lancet Neurology*, 8(12), pp.1128-1139.

Santana, L., González-Díaz, H., Quezada, E.a., Uriarte, E., Yáñez, M., Vina, D. & Orallo, F. 2008. Quantitative structure− activity relationship and complex network approach to monoamine oxidase A and B inhibitors. *Journal of Medicinal Chemistry*, 51(21):6740-6751.

Singh, R.K, Prasad, D.N., Bhardwaj, T.R. 2017. Design, synthesis, chemical and biological evaluation of brain targeted alkylating agent using reversible redox prodrug approach. *Arabian Journal of Chemistry*, 10(3):420-429.

Strydom, B., Malan, S.F., Castagnoli, N., Jr., Bergh, J.J. & Petzer, J.P. 2010. Inhibition of monoamine oxidase B by 8-benzyloxycaffeine analogues. *Bioorganic & Medicinal Chemistry*. 18:1018-1028

Tohgi, H., Abe, T., Kikuchi, T., Takahashi, S. & Nozaki, Y. 1991. The significance of 3-O-methyldopa concentrations in the cerebrospinal fluid in the pathogenesis of wearing-off phenomenon in Parkinson's disease. *Neuroscience Letters*, 132(1):19-22.

Tysnes, O.-B. & Storstein, A. 2017. Epidemiology of Parkinson's disease. *Journal of Neural Transmission*, 124(8):901-905.

Vidgren, J., Svensson, L.A. & Liljas, A. 1994. Crystal structure of catechol O-methyltransferase. *Nature*, 368(6469):354.

Viegas-Junior, C., Danuello, A., da Silva Bolzani, V., Barreiro, E.J. & Fraga, C.A.M. 2007. Molecular hybridization: a useful tool in the design of new drug prototypes. *Current Medicinal Chemistry*, 14(17):1829-1852.

Walz, A.J. & Sundberg, R.J. 2000. Synthesis of 8-Methoxy-1-methyl-1 H-benzo [de][1, 6] naphthyridin-9-ol (Isoaaptamine) and Analogues. *The Journal of Organic Chemistry*, 65(23):8001-8010.

Wang, Q., Yang, Z.-Y., Qi, G.-F. & Qin, D.-D. 2009. Crystal structures, DNA-binding studies and antioxidant activities of the Ln (III) complexes with 7-methoxychromone-3-carbaldehyde-isonicotinoyl hydrazone. *Biometals*, 22(6):927.

Westlund, K., Denney, R., Rose, R. & Abell, C. 1988. Localization of distinct monoamine oxidase A and monoamine oxidase B cell populations in human brainstem. *Neuroscience*, 25(2):439-456.

Wermuth, C.G. 2011. The practice of medicinal chemistry. 3rd ed. 84 Theobald's Road, London: Academic Press.

Yacoubian, T.A. & Standaert, D.G. 2009. Targets for neuroprotection in Parkinson's disease. *Biochimica et Biophysica Acta*, 1792(7):676-687.

Youdim, M., Maruyama, W. & Naoi, M. 2005. Neuropharmacological, neuroprotective and amyloid precursor processing properties of selective MAO-B inhibitor antiparkinsonian drug, rasagiline. *Drugs Today*, 41(6):369-391.

Youdim, M.B. & Bakhle, Y. 2006. Monoamine oxidase: isoforms and inhibitors in Parkinson's disease and depressive illness. *British Journal of Pharmacology*, 147(S1).

Youdim, M.B., Edmondson, D. & Tipton, K.F. 2006. The therapeutic potential of monoamine oxidase inhibitors. *Nature Reviews Neuroscience*, 7(4):295.

Zhu, B.T., Ezell, E.L. and Liehr, J.G., 1994. Catechol-O-methyltransferase-catalyzed rapid O-methylation of mutagenic flavonoids. Metabolic inactivation as a possible reason for their lack of carcinogenicity in vivo. *Journal of Biological Chemistry*, 269(1), pp.292-299.

CHAPTER 2 LITERATURE OVERVIEW

2.1 History of Parkinson's disease

In 1817, when James Parkinson wrote "An Essay on the Shaking Palsy", he started more than a 200 year study into the illness that would bear his name. He gave descriptions of the classic motor and non-motor symptoms we know today as the clinical signs of Parkinson's disease (PD). He also had the hypothesis that the origin of the tremor is somewhere in the midbrain, as the dopaminergic pathways was unknown at that time (Parkinson, 2002). It was not until 1895 that the role of the *substantia nigra pars compacta* was implicated in the possible pathogenesis of the then newly named PD. Brissaud then dissected the brains of nine "palsy" patients and noticed that the midbrain was less pigmented than the healthy control brains that he had as reference (Brissaud, 1895).

After the discovery of the *substantia nigra pars compacta* as the origin of the illness, in 1957 an experiment with levodopa (L-dopa), the precursor to dopamine (DA), reversed the parkinsonian state induced by reserpine in rabbits. The precursor to serotonin, L-5-hydroxytryptophan, did not show the same effect, and thus L-dopa became the gold standard in the pharmacological treatment of PD (Carlsson *et al.*, 1957).

In 1997 Polymeropoulus and co-workers published a paper regarding a genetic mutation in the proteins needed to control dopamine synthesis and metabolism, thus accelerating the loss of neurons. Thus a genetic link was established and alpha-synuclein was seen as a crucial missing link in the pathogenesis of PD (Polymeropoulos *et al.*, 1997; Spillantini *et al.*, 1997).

2.2 Etiology and pathophysiology of Parkinson's disease

PD is described as a multisystem, hypokinetic neurodegenerative disorder with the progressive loss of dopamine neurons in the midbrain (Brady *et al.*, 2005). The loss of these dopaminergic neurons gives rise to the known clinical motor symptoms that are used to diagnose PD: resting tremor, stiffness, decreased movement and a loss of balance (Vijayakumar & Jankovic, 2016).

For a definitive diagnosis, post-mortem examination must show the presence of: intraneuronal inclusions – also known as Lewy bodies – and the loss of dopaminergic neurons (Alexander, 2004). Non-motor symptoms such as depression, constipation, psychosis and dementia also aid in the diagnosis (Gelb *et al.*, 1999; Gonzalez-Usigli, 2017). To understand the occurrence of these symptoms, the abnormal physiology and anatomy in patients with PD must be evaluated.

2.2.1 Neuropathological and neurochemical characteristics in Parkinson's disease

2.2.1.1 Normal anatomy

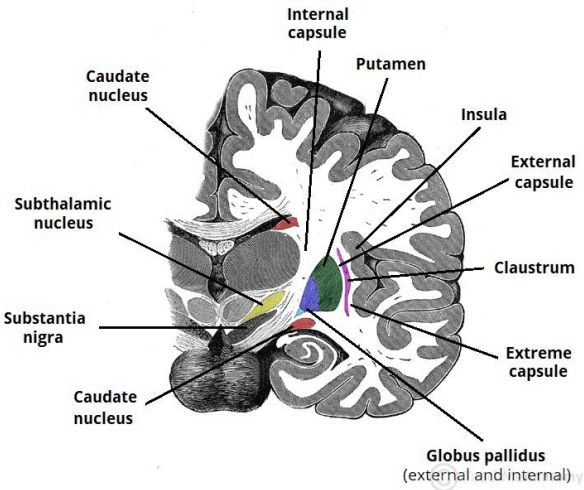

Figure 2-1: Normal anatomy of the basal ganglia and associated projections (Photos & Server).

The basal ganglia and the dopaminergic neurons in the substantia nigra are crucial to the normal functioning of the motor and cognitive areas of the brain (Brown & Marsden, 1998). The motor circuit consists of two sets of pathways: direct and indirect. A direct connection between the putamen and internal segment of the globus pallidus (GPi) and substantia nigra pars reticulata (SNr) constitutes the direct pathway. An indirect pathway from the putamen to the subthalamic nucleus (STN) via the external segment of the globus pallidus (GPe), and then back to the GPe, GPi, and SNr constitutes the indirect pathway. The GPi and SNr project to the thalamus and brainstem (Figure 2-1) (Alexander & Crutcher, 1990; Hoover & Strick, 1993).

2.2.1.2 Neuropathological and motor dysfunctions in Parkinson's disease

The striatum, which consists of both the putamen and caudate nucleus, is the major input nucleus of the basal ganglia. These projections also spread to other regions of the brain and can account for the non-motor symptoms of PD (Table 2.1) (Calabresi *et al.*, 2013). The normal basal ganglia function is activated by an input from the cortex, which stimulates the substantia nigra pars compacta (SNc) to excite the direct pathway to the subthalamic nucleus (STN) and the globus pallidus pars externa (GPE). This excitatory pathway creates impulses that move through the thalamus to the cortex, which in turns redirects impulses to the spinal cord. The spinal cords then direct the impulses to the skeletal muscle for a smooth and controlled movement (Dauer &

Przedborski, 2003; DeLong, 1990; Obeso *et al.*, 2000). This is shown in Figure 2.2 by the red arrows.

In the so-called parkinsonian state, the input from the cortex has a reduced effect on the dopamine secretion due to the destruction of dopaminergic neurons from the SNc. The lack of dopamine and inhibition of the indirect pathway reduces the impulse and causes a top-down inhibition of the entire pathway. This inhibitory effect has slow, uncontrolled movement as a result (Calabresi *et al.*, 2013; Dauer & Przedborski, 2003; Dickson, 2018; Zhai *et al.*, 2018). This shown in Figure 2.2 by the blue arrows.

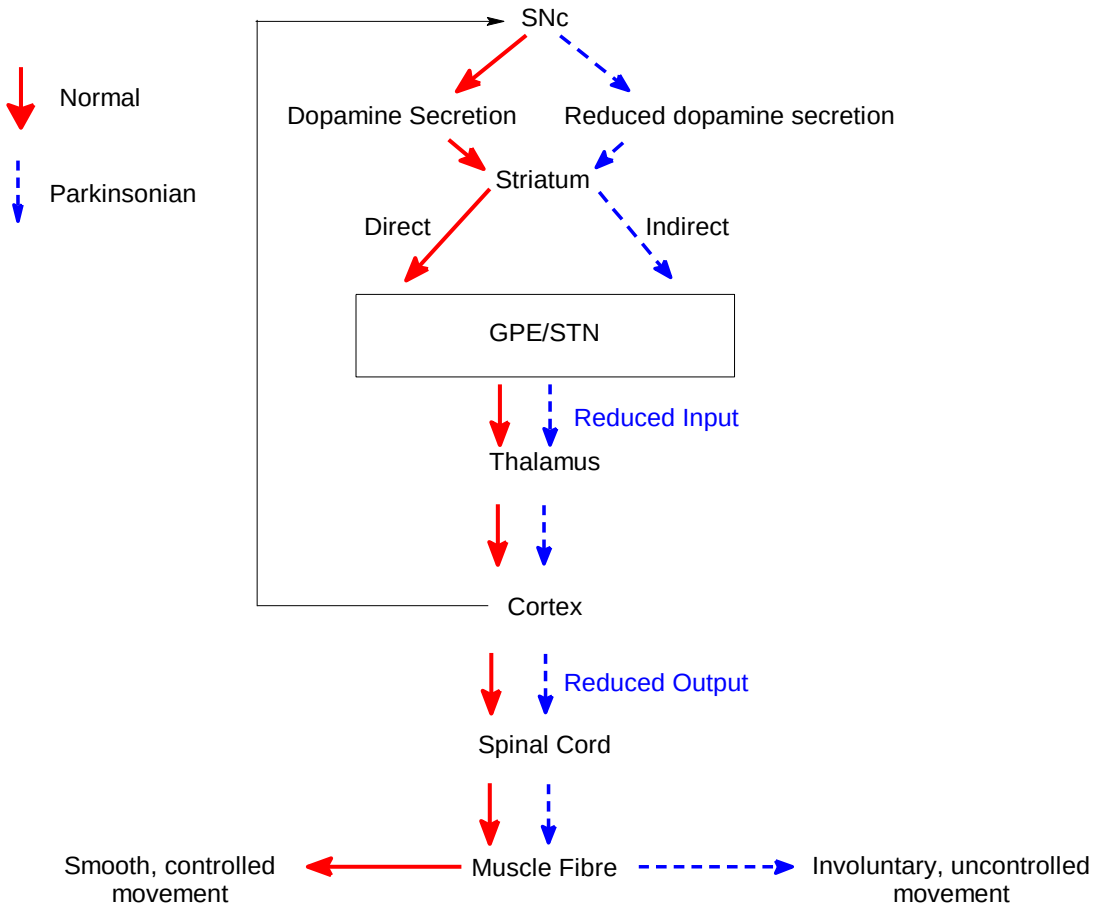

Figure 2-2: Normal and parkinsonian state movement circuits (Dauer & Przedborski, 2003; Obeso *et al.*, 2000; Zhai *et al.*, 2018).

2.2.1.3 Lewy bodies

Accompanying the loss of the dopaminergic neurons, there is also cellular inclusions called Lewy bodies (LBs). LBs are α-synuclein filled aggregates that form insoluble fibrils that infiltrate the neurons (Gonzalez-Usigli, 2017; Spillantini *et al.*, 1997). In PD, the majority of LBs are found in

the SNc and surrounding tissues. The formation and effects of LBs will be discussed later in this chapter (Dickson, 2018; Jellinger, 1987; Rocha *et al.*, 2018).

2.2.2 Neurochemical characteristics

Neurodegeneration is not only exclusive to the dopaminergic neurons, but several other types of neurons are also affected. This can account for the presence of the plethora of non-motor symptoms that can be witnessed months or years before the diagnosis of PD is made. Several studies have shown that the loss of multiple neuromodulators in the midbrain, spinal cord, thalamus and medulla oblongata are the basis of the non-motor symptoms (Gibb & Lees, 1991; Moore, 2003; Paulus & Jellinger, 1991). Table 2.1 list the neuromodulators and their effects in the clinical manifestations in PD.

Table 2-1: Clinical manifestations of multiple region neuron loss in Parkinson's disease (Alexander, 2004).

REGION	NEUROMODULATORS	MANIFESTATIONS
MIDBRAIN	Dopamine	Bradykinesia, rigidity, tremors (McRitchie *et al.*, 1997)
PONS	Noradrenaline	Hypokinesia (Paulus & Jellinger, 1991), depression (Kish *et al.*, 1984)
	Serotonin	Depression (Paulus & Jellinger, 1991), insomnia (Olson *et al.*, 2000; Onofrj *et al.*, 2002)
	Acetylcholine	Dysphagia and oesophageal dysmotility (Edwards *et al.*, 1992), insomnia (Olson *et al.*, 2000), dementia (Berridge & Waterhouse, 2003)
THALAMUS	Glutamate	Memory loss (McDonald, 1996), learning disability (Cardinal *et al.*, 2002)
AMYGDALA	Glutamate	Visual hallucinations (Masson *et al.*, 1993), hyposmia (inability to smell) (Harding *et al.*, 2002; Ponsen *et al.*, 2004)

2.2.3 Etiology of Parkinson's disease

There are several theories and hypotheses regarding the etiology of PD that include oxidative stress, environmental factors, genetic factors (including mitochondrial dysfunction and parkin mutations), neuroinflammation and gender difference (Alexander, 2004; Bourque *et al.*, 2015; Brady *et al.*, 2005; Dauer & Przedborski, 2003). These will be discussed below.

2.2.3.1 Oxidative stress

Oxidative stress is defined as "*the imbalance between oxidants produced, and anti-oxidants available, and this may lead to macromolecular damage*" (Jones, 2006; Sies, 2015).

The brain has a unique vulnerability to oxidative stress due the mismatching of weight of the brain and the total percentage of oxygen used. Even though the brain is only 2% of the total body weight, it uses about 20% of total oxygen due to high energy demand. The bulk of oxygen is used for ATP generation, the invoking of action potentials, neurotransmitter synthesis and enzymatic reactions (Frank, 2006; Patel, 2016). Oxidative stress in the brain is mostly derived from dopamine metabolism and mitochondrial dysfunction.

2.2.3.2 Dopamine metabolism

Dopamine metabolism through MAO and the intermediates that are produced may itself be a source of oxidative stress (Figure 2.3). Several ROS are produced in the complex metabolism of dopamine and these species may have a further degenerative effect on the neurons (Segura-Aguilar *et al.*, 2014).

DA synthesis is mainly controlled by two enzymes, tyrosinase (TYR) and aromatic amino acid decarboxylase (AADC), to produce dopamine from L-tyrosine and L-dopa, respectively (Blaschko, 1939). DA degradation is controlled by MAO and COMT. MAO catalysis produces hydrogen peroxide and 3,4-dihydroxyacetaldehyde (DOPAL), which may damage neuronal cells under specific conditions (Carlsson *et al.*, 1957; Meiser, 2013; Tohgi *et al.*, 1991).

DA degradation has been shown to alter many processes in the brain. These include altered mitochondrial respiration, a change in the permeability of mitochondrial organelles, deactivation of the DA transporter and inhibition of tyrosine hydroxylase (Berman & Hastings, 1999; Blesa *et al.*, 2015; Kuhn *et al.*, 1999; Whitehead *et al.*, 2001).

Dopaquinone can also be synthesised either spontaneously or in the presence of transition metals, and this compound can react with cysteine residues of certain proteins that are needed for normal cellular function (Spencer *et al.*, 1998). Dopaquinone is an electron-poor and highly reactive metabolite of DA. Dopaquinone reacts with iron to produce 6-hydroxydopamine, a potent neurotoxin (Napolitano *et al.*, 2011; Napolitano *et al.*, 1999). The effect of these quinones on proteins can be seen in the misfolding of α-synuclein into the known LB's. The misfolding of these proteins gives rise to reduced inhibition of dopamine synthesis and a subsequent increase in oxidative species (Giasson *et al.*, 2000). Aggregates of this protein cause lesions and inclusions

that can lead to an increase in cell membrane pores and cell leakages, and ultimately will lead to cell death (Winklhofer & Haass, 2010).

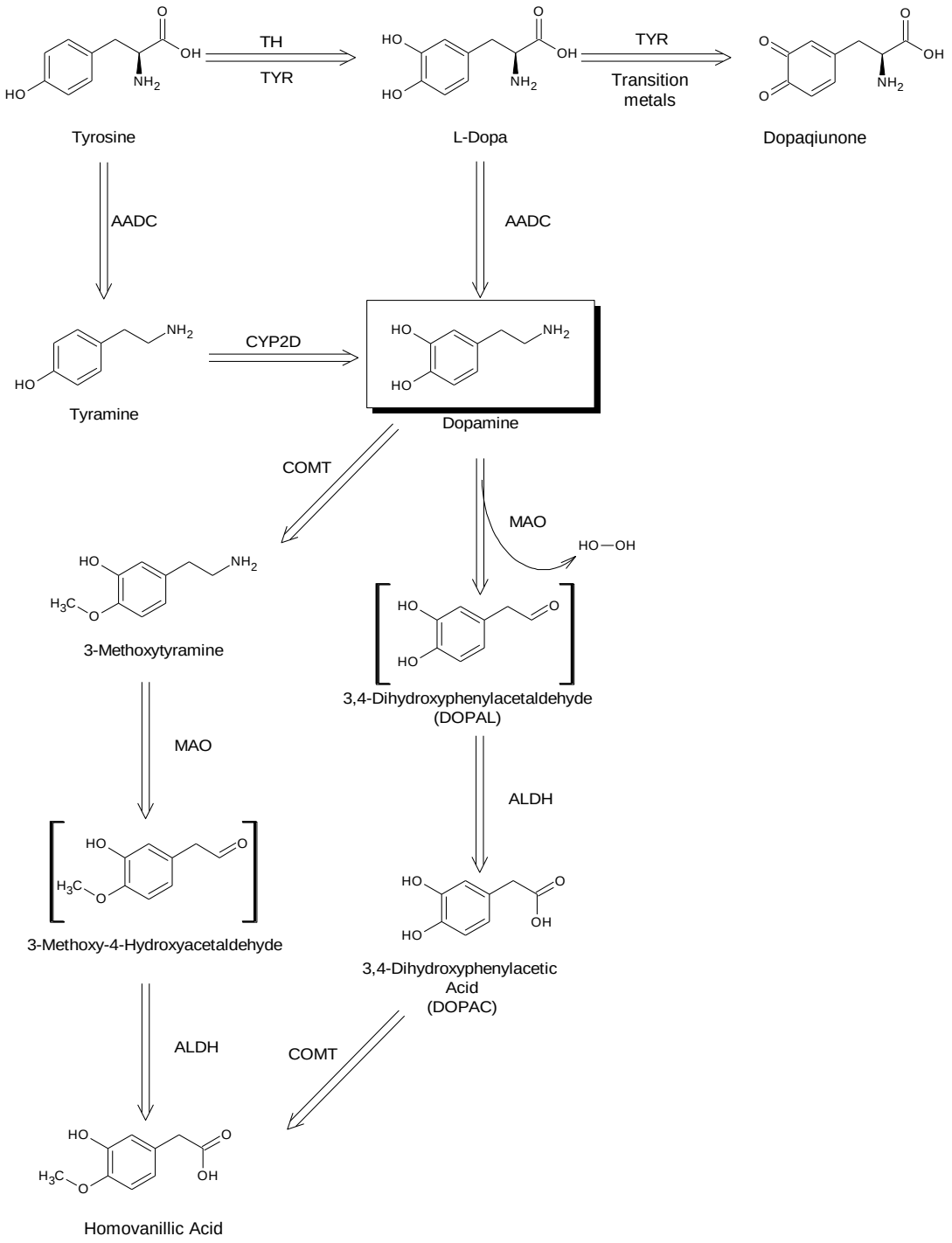

Figure 2-3: Biosynthesis and degradation of dopamine (Blaschko, 1939; Carlsson, 1959; Delcambre *et al.*, 2016; Meiser *et al.*, 2013).

2.2.3.3 Genetic mutations and mitochondrial dysfunction

The mitochondria use oxidative phosphorylation to provide energy in the form of adenosine triphosphate (ATP) to the cell. Oxidative phosphorylation synthesises ATP through the transport of electrons through several intracellular complexes (Saraste, 1999). The metabolism of nutrients to ultimately yield ATP is a significant source of superoxide and hydrogen peroxide in the neuronal cells (Hall *et al.*, 2012). In the oxidative phosphorylation pathway, complex 1 of the electron transport chain is the point where electrons enter the chain and where most of the ROS are produced (Brandt, 2006). Complex 1 is where nicotinamide adenine dinucleotide (NADH) provides electrons to the rest of the chain. Complex 1 is thus a potent source of ROS production (Halliwell, 1992; Parker Jr *et al.*, 1989).

In 1980 several patients were admitted after the intravenous admission of a complex 1 inhibitor namely MPTP (1-methyl-4-phenyl-1,2,3,6-tetrahydropyridine), an impurity from a batch of illicit drugs (Sian *et al.*, 1999). These patients presented with the characteristic parkinsonian symptoms. The findings of autopsy showed the characteristic degeneration of the *substantia nigra pars compacta*, and the consequent inhibition of the complex 1 of the oxidative phosphorylation chain. This inhibition causes a decrease in ATP production while ROS production is increased (Andreyev *et al.*, 2005; Brandt, 2006; Chan *et al.*, 1991; Davis *et al.*, 1979; Murphy, 2009; Starkov, 2008).

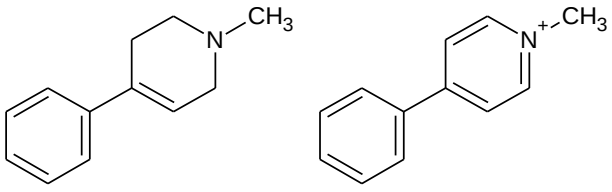

Figure 2-4: Structures of MPTP and MPP^+.

However, the inhibition of complex 1 is mainly due to the metabolite MPP^+ (1-methyl-4-phenylpyridinium) (Figure 2-4) that is produced by oxidation of MPTP by MAO-B. MPP^+ is taken up into the mitochondria where it reduces ATP formation, which results in the loss in ATP energy dependant processes such as transport and repair are impaired. The loss of these processes has degenerative effect on neuronal cells (Langston *et al.*, 1984; Markey *et al.*, 1984).

This observation led to the identification of certain genetic markers that code for complex 1 deficiency and that can lead to sporadic PD (Winklhofer & Haass, 2010). The different genes that are affected are numerous and complex, and many sources link the defects to changes in

mitochondrial DNA (due to less efficient DNA repair mechanisms and the absence of histones to protect the DNA during replication) (DiMauro & Davidzon, 2005; Reeve *et al.*, 2008; Trifunovic & Larsson, 2008).

2.2.3.4 Neuroinflammation

Oxidative stress, reduced repair and anti-oxidant capabilities, certain pro-inflammatory cytokines and macrophages all can produce innate and acute inflammatory responses in the microglial cells of certain brain regions (Frank-Cannon *et al.*, 2009). These responses can increase the permeability of the blood-brain-barrier (BBB) and can cause further oxidative damage due to the infiltration of oxidative species into the brain (McGuire *et al.*, 2001).

2.2.3.5 Gender and prevalence of PD in men and women

The incidence of PD is more in men than women (Baldereschi *et al.*, 2003; Bourque *et al.*, 2018). Men are 50% more susceptible to PD than women (Marras *et al.*, 2018). Early onset of disease and severity thereof is also less prominent in women (Haaxma *et al.*, 2007). This suggests that a higher degree of circulating estrogen level can act as protective agent to postpone the onset time of PD (Frentzel *et al.*, 2017; Yadav *et al.*, 2012). 17β-Estradiol, more prevalent in women, has a multitude of effects including the inhibition of apoptosis, maintaining the integrity of dopaminergic neurons and the suppression of protein aggregates (Arnold *et al.*, 2012; Bourque *et al.*, 2015; Brewer *et al.*, 2009).

2.3 Pharmacological treatment of Parkinson's disease

There are many pharmacological treatments for PD, and they may be classified as dopaminergic and non-dopaminergic treatments (Table 2–2).

Although there are many drugs that may be used for the treatment of PD, the most effective remains the dopaminergic options, because of either their ability to increase DA concentrations or to reduce DA metabolism (LeWitt, 2015).

Table 2-2: Current dopaminergic and non-dopaminergic treatments for Parkinson's disease (Du & Chen, 2017; Engelbrecht *et al.*, 2018)

DOPAMINERGIC TREATMENTS	NON-DOPAMINERGIC TREATMENTS
L-Dopa (Raab & Gigee, 1951) and AADC-inhibitors (Bartholini & Pletscher, 1975)	Adenosine antagonists (Bara-Jimenez *et al.*, 2003)
DA agonists (Shulman, 1999)	Anticholinergic drugs (Katzenschlager *et al.*, 2002)
MAO-inhibitors (Fagervall & Ross, 1986)	Anti-oxidant therapy (Ebadi *et al.*, 1996)
COMT-inhibitors (Nissinen *et al.*, 1988)	Gonadal hormones and derivatives (Bourque *et al.*, 2015)

2.3.1 Levodopa and aromatic amino acid decarboxylase inhibitors

In 1913 when Marcus Guggenheim isolated pure L-dopa, both he and Casimir Frank had thought they had found the parent precursor molecule to adrenaline, but later (in 1938) when Peter Holtz found it was converted to DA, L-dopa was correctly characterised and a new age in catechol research began (Guggenheim, 1913; Holtz *et al.*, 1938; Hornykiewicz, 2002).

The rationale behind L-dopa therapy is that L-dopa is converted to DA after it has passed the BBB. The conversion to DA is catalysed by amino acid decarboxylase (AADC). DA metabolism continues via metabolism by MAO and COMT (Meiser *et al.*, 2013). Furthermore, there are studies that show that, when L-dopa is metabolised peripherally via AADC, the metabolite 3-*O*-methyldopa can compete with L-dopa for active transport through the BBB [Figure 2.6] (Tohgi *et al.*, 1991).

The use of a peripheral AADC inhibitor such as carbidopa or benserazide (Figure 2.5) can lower peripheral metabolism of DA and thus result in higher circulating concentrations of L-dopa available for penetration into the brain to be converted into DA. This is useful since the brain penetration of DA is very low compared to the penetration by L-dopa (Aminoff, 2004). This effect coincides with the "wearing off" effect in L-dopa therapy. "Wearing-off" is a condition of lowered efficacy due to reduced bioavailability of L-dopa to the brain, compared to the original dosage (Lee *et al.*, 2008; Nord *et al.*, 2010; Standaert & Roberson, 2015). In addition to L-dopa induced

dyskinesia, “wearing-off” is a major limitation of L-dopa therapy. AADC inhibitor therapy can dramatically reduce these limitations (Mucklow, 2000).

The use of AADC inhibitors also lessens the peripheral side effects of L-dopa therapy, (gastrointestinal irritation, anorexia and orthostatic hypotension) (Aminoff, 2004). Patients are rarely treated by only L-dopa, since the combination of L-dopa and AADC inhibitors is highly effective in raising DA levels in the brain. However, adverse neurological effects are also very common if spikes in DA concentrations occur. Hence, controlled dosage increments must be used to achieve a level appropriate for each individual patient (Nord *et al.*, 2017).

Although DA concentrations are increased in the brain through the use of L-dopa and a AADC inhibitor, the use of MAO and COMT inhibitors can further decrease the breakdown of striatal dopamine and improve L-dopa therapy (Kaakkola, 2000; Youdim & Bakhle, 2006).

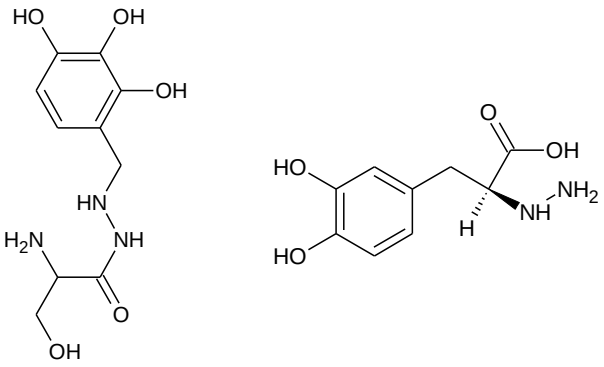

Benserazide Carbidopa

Figure 2-5: Structures of commercially used AADC inhibitors.

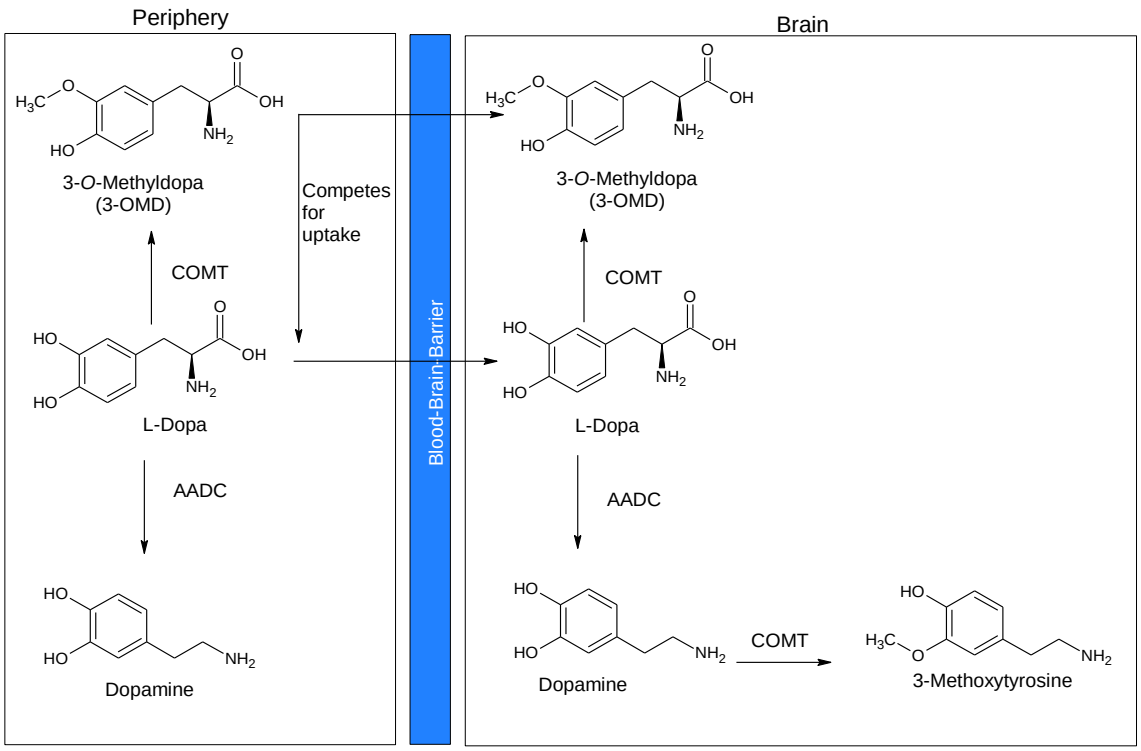

Figure 2-6: The metabolism of L-dopa by COMT and AADC (Kaakkola, 2000; Lee *et al.*, 2008; Meiser *et al.*, 2013).

2.3.2 Dopamine agonists

At present, DA agonists, instead of L-dopa are considered as first-line treatment in PD, although many uncertainties concerning long-term effects of these drugs exist (Stowe *et al.*, 2008). These uncertainties and prescribing complexities (titration of dosage up or down, as well as distressing adverse effects) make it difficult to assess the success of DA agonist treatment (Shulman, 1999). The rationale for the use of DA agonists is based on direct stimulation of DA receptors to mimic the effects of endogenous DA. Normally in PD, where reduced DA secretion in the synaptic cleft occurs, DA agonists can have a very beneficial effect if used properly (Katzung *et al.*, 2012).

2.3.2.1 Ergot derivatives

Drugs such as bromocriptine, cabergoline and pergolide (Figure 2-7) are examples of DA agonists (Olanow *et al.*, 2001). The use of these derivatives is, however, limited due to the vasospasm, fibrotic degeneration of cardiac valves and cardiac arrhythmias (Davie, 2008; Katzung *et al.*, 2012; Mucklow, 2000). Certain effects can be exacerbated with the use of L-dopa in conjunction with these drugs, mainly because L-dopa dosage should be reduced. Many prescribers overlook this dosage reduction which results in increased dyskinesia that can cripple most patients. The use of

ergot derivatives should be associated with an average of 20 – 30% reduction in L-dopa dosage (Brooks, 2000).

Ergot derivatives can also have a beneficial impact on brain chemistry since they are not oxidised by normal dopaminergic pathways and does not contribute to ROS formation. Ergot derivatives may also possess neuroprotective effects by suppressing dopamine release via negative feedback channels to prevent further neuronal damage (Rascol *et al.*, 1998; Schapira, 2002).

2.3.2.2 Non-ergot derivatives

Pramipexole, ropinirole and rotigotine (Figure 2-8) are the non-ergot derivatives currently used as DA agonists. The removal of the ergot structure has a beneficial effect on the side effect profile of DA agonists. Non-ergot derivatives allow for a reduction in L-dopa dosage and combined with peroxide scavenging properties, these drugs may have both symptomatic effects and act as neuroprotective agents (Gottwald *et al.*, 1997).

Most of these derivatives have an affinity for the dopamine 3 receptor (D_3), which means they may have certain neurorestorative properties (Pich & Collo, 2015). Evidence exists that chronic L-dopa treatment may lead to an over-expression of these D_3 receptors, which can explain certain L-dopa side effects (Chondrogiorgi *et al.*, 2014; Visanji *et al.*, 2009). Furthermore, studies showed that the use of DA agonists may lead to a reduction in dyskinesia and an enhanced quality of life due to better “wearing-off” tolerability (Group, 2000; Holloway *et al.*, 2004; Pham & Nogid, 2008; Rascol *et al.*, 2000).

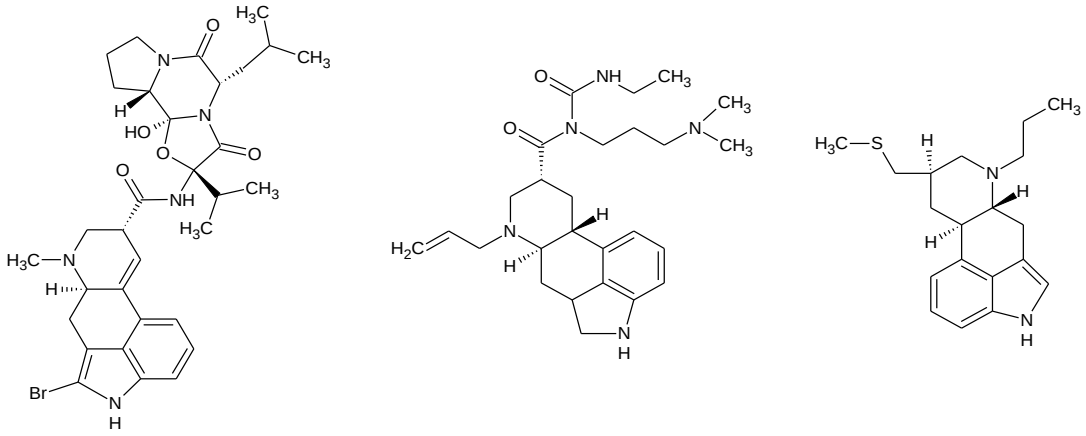

Figure 2-7: The different ergot derived dopamine agonists (Gonzalez-Usigli, 2017; Olanow *et al.*, 2001; Shulman, 1999).

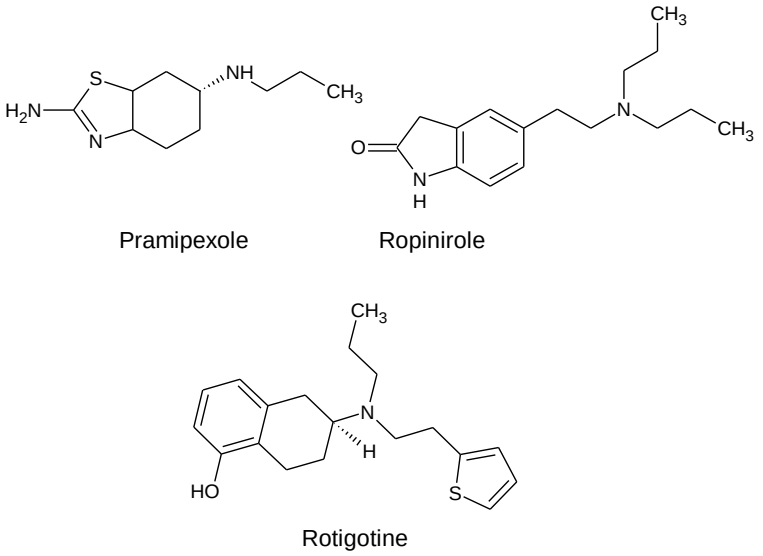

Figure 2-8: The different non-ergot derived dopamine agonists (Olanow *et al.*, 2001; Schapira, 2002; Stowe *et al.*, 2008).

2.3.3 Diverse dopaminergic and non-dopaminergic treatments

Amantadine is used as a dopamine reuptake inhibitor (Takahasi *et al.*, 1996), and was first used as an anti-viral drug for influenza (Transm, 1994). Many studies suggest the efficacy of amantadine may be reduced due to the occurrence of tolerance to the effects. The combination with L-dopa can reduce the appearance of tolerance to amantadine (Zeldowicz & Huberman, 1973).

Apomorphine is a weak D_2 receptor agonist and is almost exclusively used as a short-term rescue for “off-period” dyskinesia (Ul Haq *et al.*, 2007). It is used either as a subcutaneous injection or in

a pump system, and leads to a motor function response indistinguishable from L-dopa (Corsini *et al.*, 1979). Side effects like postural hypotension, oedema and priapism have caused a decline in the use of apomorphine as a monotherapy (Lewitt & Oertel, 1999; Porst & Buvat, 2008; Stacy & Silver, 2008).

The repurposing of gonadal hormones and derivatives are of new interest in PD therapy where the use of 17β-estradiol in men has shown certain neuroprotective effects. 17β-Estradiol in combination with spirinolactone has shown a reduction in motor and non-motor symptoms (Bourque *et al.*, 2018). In contrast, testosterone has not shown the same effects as the estrogens (Ekue *et al.*, 2002).

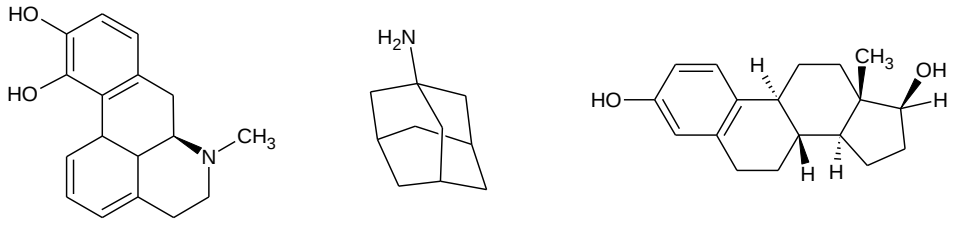

Apomorphine Amantadine 17ß-estradiol

Figure 2-9: Diverse dopaminergic and non-dopaminergic treatments of Parkinson's disease (Bourque *et al.*, 2015; Katzung *et al.*, 2012; Stacy & Silver, 2008; Stowe *et al.*, 2008).

2.3.4 Monoamine oxidase (MAO) and inhibitors

2.3.4.1 Biological importance of MAO

MAO [amine:oxygen oxidoreductase (deaminating) EC 1.4.3.4] is an enzyme that is mostly found on the outer membrane of the mitochondria, and catalyses the deamination of several neurotransmitters, including noradrenaline, serotonin and dopamine (Son *et al.*, 2008). This reaction produces a corresponding aldehyde, hydrogen peroxide and either ammonia or a substituted amine (Youdim *et al.*, 2006). MAO plays a decisive role in many neurological disorders as well as PD. Neurological pathways depend on a delicate balance of neurotransmitters, and with either an over- or under expression of this enzyme, sensitive motor states as well as emotional states can be affected (Youdim & Bakhle, 2006). Intraneuronal MAO plays a role in the metabolism of the monoamine neurotransmitters, as well as the regulation of monoamine storage and protects neurons from exogenous monoamine chemicals (Saura *et al.*, 1996; Tong *et al.*, 2013).

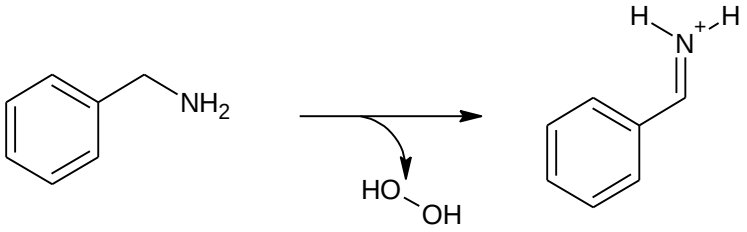

Figure 2-10: The oxidation reaction catalysed by MAO (Edmondson *et al.*, 2004).

MAO is also a key player in many neurological states, where dysfunction or polymorphism of MAO genes can lead to many altered reality states including schizophrenia (Berk *et al.*, 2007), bipolar disorder (Sun *et al.*, 2012), pathological aggression (Brunner *et al.*, 1993; Caspi *et al.*, 2002) and depression (Meyer *et al.*, 2006).

2.3.4.2 Isoforms of MAO and the impact on Parkinson's disease

MAO is present as two isoforms, MAO-A and MAO-B, which has different substrate and inhibitor specificities (Shih *et al.*, 1999; Tipton *et al.*, 2004). The redox cofactor, flavin adenine dinucleotide (FAD), is the only cofactor present in both MAO-A and MAO-B. It is absolutely needed for catalysis (Edmondson *et al.*, 2004). Figure 2.13 shows the structure of FAD as seen in MAO. Both isoforms also share a membrane binding domain, a C-terminal α-helical region that anchors the enzyme to the outer mitochondrial wall. This domain also has other hydrophobic interactions with the membrane (Binda *et al.*, 2002; Ma *et al.*, 2004; Rebrin *et al.*, 2001). This chain is shown as red in the figures that follow (Figure 2-11 & Figure 2-12).

MAO-A and MAO-B share a 70% sequence identity, and with overlapping biological functions, a high level of inhibitor specificity is needed to produce little to no adverse effects (Bach *et al.*, 1988). MAO-A is defined as being inhibited by clorgyline whilst catalysing the metabolism of norepinephrine, serotonin and tyramine. Clinical trials showed increased concentrations of norepinephrine and serotonin after treatment with this compound, which were associated with good anti-depressant properties. The development of this drug was abandoned due to a severe adverse effect called the "cheese effect" (This will be discussed later in this chapter) (Ochiai *et al.*, 2006; Youdim & Bakhle, 2006). MAO-A is mostly found in catecholaminergic neurons (Jahng *et al.*, 1997). MAO-A also mainly exists as a monomer when crystallised (Caccia *et al.*, 2006).

Figure 2-11: The structure of MAO-A with harmine as inhibitor (Gaweska & Fitzpatrick, 2011; Rose *et al.*, 2018).

MAO-B is resistant to clorgyline and favours benzylamine as substrate (Fowler *et al.*, 1982). MAO-B is abundant in serotonergic and histaminic neurons, as well as in the basal ganglia, which makes it a good target for inhibition in PD (Collins *et al.*, 1970; Luque *et al.*, 1995). MAO-B is also responsible for the oxidation of MPTP to yield MPP^+ (Chiba *et al.*, 1984). Through high resolution crystal structures, the cavity of MAO-B was shown to be hydrophobic in nature with the FAD located at the back of the binding site (Binda *et al.*, 2003; Binda *et al.*, 2002). MAO-B is naturally a dimer, with each monomer anchored with the C-helix into the mitochondrial membrane (Caccia *et al.*, 2006). The active site structure reveals the path, consisting of two cavities, that a substrate or inhibitor must follow in order to reach the FAD co-factor. The two cavities are lined with hydrophobic residues, and these connect to the FAD binding site (Binda *et al.*, 2002; Edmondson *et al.*, 2004). Present at the mitochondrial membrane is a loop of residues that act as a “gating switch”. This switch must be activated in order for the substrate or inhibitor to move into the active site (Binda *et al.*, 2003). MAO-B is the enzyme more suited for inhibition in PD.

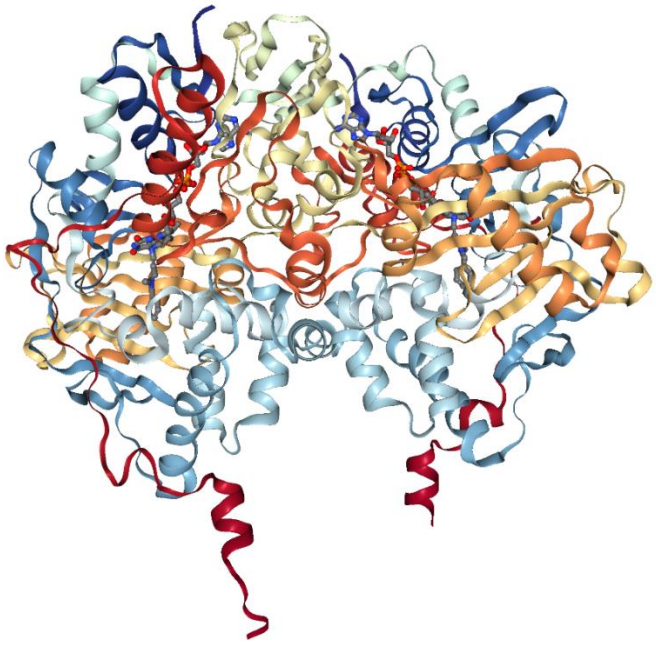

Figure 2-12: The structure of MAO-B (Gaweska & Fitzpatrick, 2011; Rose *et al.*, 2018).

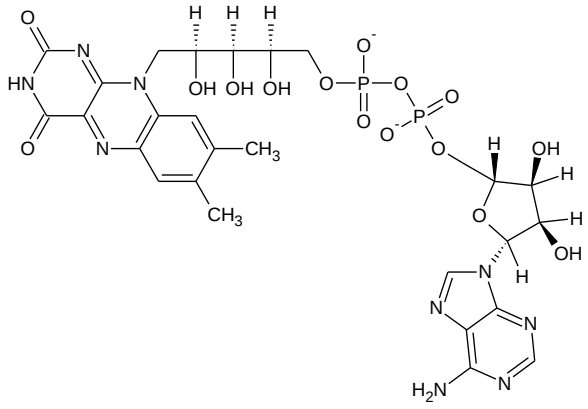

Figure 2-13: The FAD co-factor in MAO (Binda *et al.*, 2002).

Even though both isoforms of MAO oxidises DA, the concentration of the substrate is a factor in enzyme catalysis. As seen, MAO-B is more prevalent in the basal ganglia, where DA acts as a substrate (Luque *et al.*, 1995). There is evidence that MAO-B activity can increase with age (Diez & Maderdrut, 1977; Lewinsohn *et al.*, 1980). Increased activity suggests that increased amounts of DA is being metabolised, which may further reduce DA in PD. This coupled with normal cellular degeneration and multiple other etiologies, can explain why MAO-B is so important in the therapy of PD.

2.3.4.3 Inhibitors of MAO

The inhibition of MAO is associated with symptomatic benefit in PD, but adverse effects, may occur with irreversible inhibition. The earliest known inhibitor of MAO was the tuberculosis drug, isoniazid. From this compound the related compound iproniazid was developed and became the first commercially used MAO inhibitor for depressive illness. However, severe liver toxicity led to the withdrawal of the drug from the market. It was found that the hydrazine structure of the drugs was responsible for the toxicity (Fagervall & Ross, 1986; Youdim *et al.*, 1988; Youdim & Bakhle, 2006). Clogyline, selective for MAO-A, and pargyline, selective for MAO-B, were used as leads for the discovery of MAO inhibitors (Fišar *et al.*, 2010).

After the development of a non-hydrazine drug, namely tranylcypromine, a new side effect was observed, the “cheese effect”. The cheese effect is a severe hypertensive reaction to an excess of tyramine in the system after the irreversible inhibition of MAO-A. Tyramine cannot be normally metabolised when MAO in inhibited, and with a higher concentration of tyramine at the synaptic cleft, less noradrenaline is reabsorbed (Florvall *et al.*, 1986). This leads to a higher than normal noradrenaline concentration, and results in a physiological overreaction to the sympathomimetic effects of noradrenaline (Fišar, 2016; Gottwald *et al.*, 1997; Youdim & Bakhle, 2006). This side effect is mainly seen with non-selective MAO inhibitors, and MAO-A inhibitors, since tyramine is mainly metabolised by MAO-A in the periphery (Liccione & Azzaro, 1988).

Several MAO inhibitor drugs has since been tested and introduced into the market for PD. Isocarboxazid was used as a treatment for PD as well as other dementia related illnesses (Fagervall & Ross, 1986). (R)-Deprenyl (or selegiline) is a MAO-B selective irreversible inhibitor, with an added action of prolongation dopamine action (Kiray *et al.*, 2006). Rasagiline is used in the late and early stages of PD, and is effective as monotherapy (Oldfield *et al.*, 2007). Rasagiline has been shown to protect neuronal cells against cell death and may thus possess neuroprotective properties (Naoi *et al.*, 2003).

Lazabemide and safinamide are both multiple action drugs and, in addition to the inhibition of MAO-B, also act as calcium channel blockers and dopamine reuptake inhibitors, respectively (Caccia *et al.*, 2006; Henriot *et al.*, 1994).

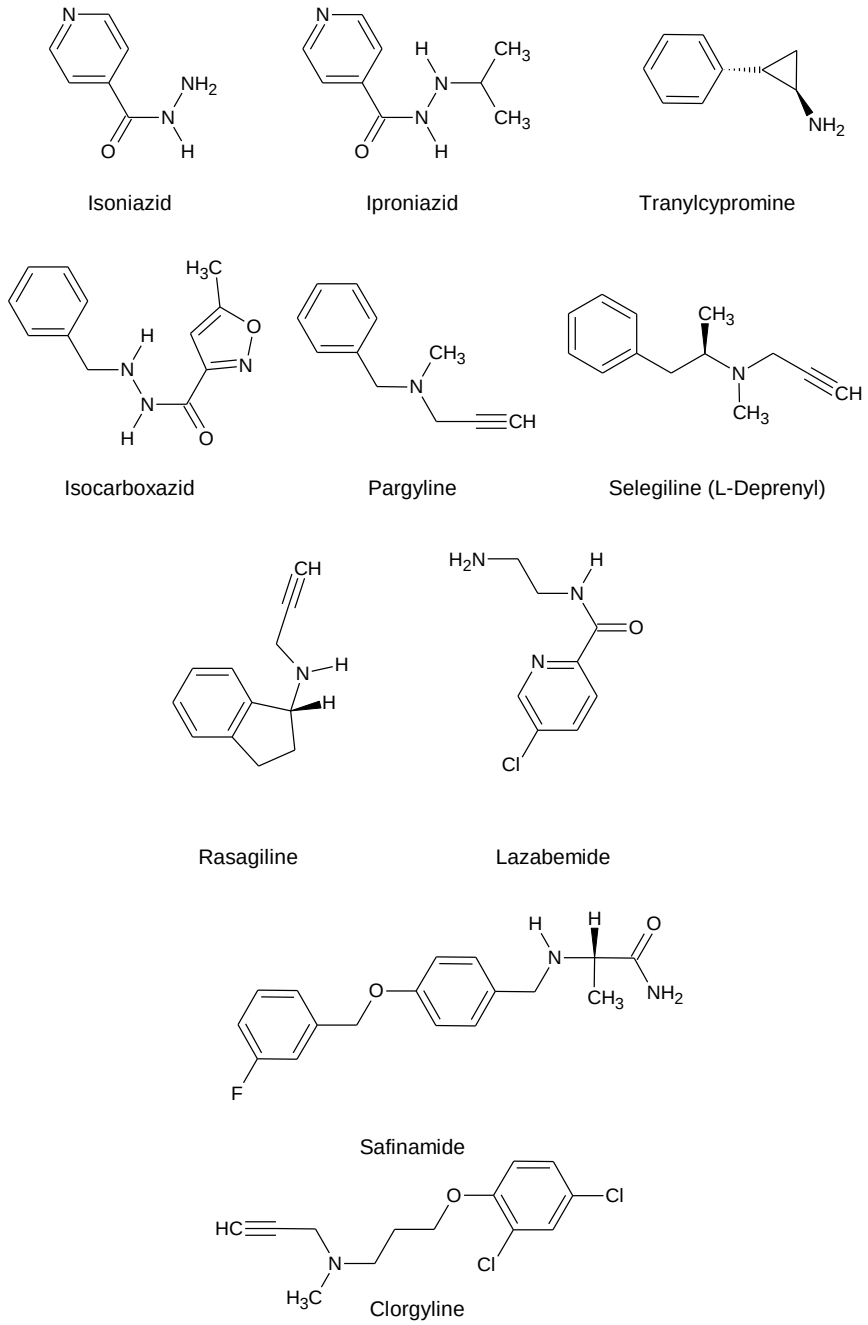

Figure 2-14: The structures of MAO inhibitors discussed in the text.

2.3.5 Catechol-*O*-methyl transferase

2.3.5.1 Structure and biological importance of COMT

COMT is an intracellular enzyme that catalyses the transfer of a methyl group from S-adenosyl-L-methionine (SAM) to one of the hydroxyl groups in a catechol neurotransmitter (Kaakkola, 2000; Vidgren *et al.*, 1994). The enzyme exists as two forms: a 221-residues soluble protein, mostly in the cytosol of the cells, and as a membrane-bound protein with 50 extra residues at the N-terminus (Backstrom *et al.*, 1989; Bai *et al.*, 2007; Huh & Friedhoff, 1979; Tenhunen *et al.*, 1994).

The catechol binding site is situated in a shallow pocket with two “gate keeping” residues. These residues use van der Waals interactions to keep the substrate in place, and adjacent the SAM and Mg^{2+} co-factor for methylation (Bonifácio *et al.*, 2002; Lerner *et al.*, 2003; Vidgren *et al.*, 1994). Figure 2.16 shows the catalysis of a catechol neurotransmitter by SAM in COMT. The Mg^{2+} co-factor binds the catechol neurotransmitter as a bidentate ligand, this deprotonates the neurotransmitter to form a nucleophile. The newly formed nucleophile attacks the activated methyl group of SAM. With the now methylated neurotransmitter, the Mg^{2+} can no longer bind and the neurotransmitter dissociates (Lotta *et al.*, 1995; Vidgren *et al.*, 1994).

The reaction of methylation is almost exclusively regioselective towards *meta*-O-methylation (Axelrod, 1966), but under certain in vivo conditions *para*-O-methylation was possible. The extent of *para*-O-methylation is dependent on experimental conditions, including the pH of the solution and the nature of the substrate (Creveling *et al.*, 1970). Catechols that bear more polar groups (like DA) are methylated at the *meta* position, whereas less polar catechol groups may undergo *para* methylation (Guldberg & Marsden, 1975). The SAM cofactor is converted to SAH (S-adenosyl-L-homocysteine) and is remethylated by vitamins B_6 or B_{12} (Müller, 2008).

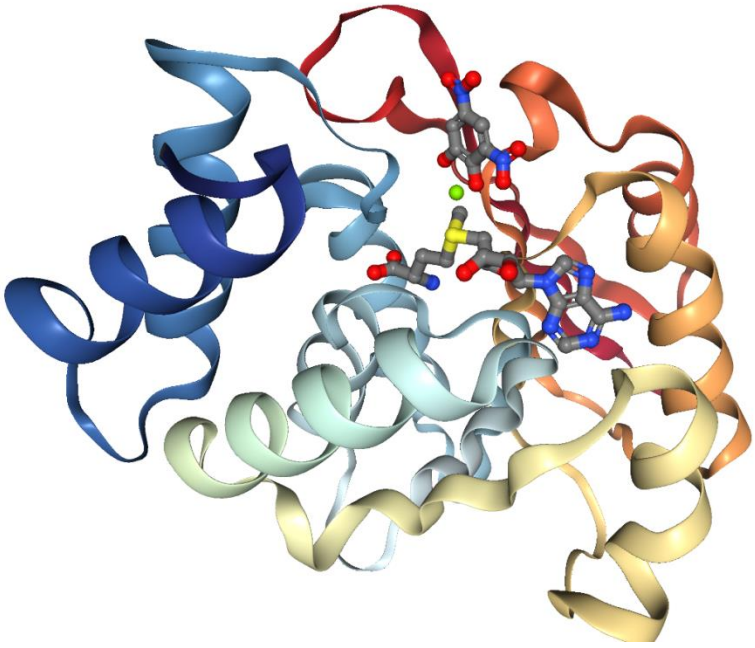

Figure 2-15: The structure of soluble COMT with SAM, the catechol substrate and the Mg^{2+} ion shown (green) (Rose *et al.*, 2018; Vidgren *et al.*, 1994).

COMT’s biological function is to metabolic inactivate various endogenous catechol neurotransmitters and xenobiotic substances (Burba & Becking, 1969; Zhu *et al.*, 1994). COMT has a wide variety of substrates, all including a catechol pharmacophore. These include

dopamine, epinephrine, norepinephrine, ascorbic acid and catechol estrogens such as 2 hydroxyestradiol and 2-hydroxyestrone (Kiss & Soares-da-Silva, 2014).

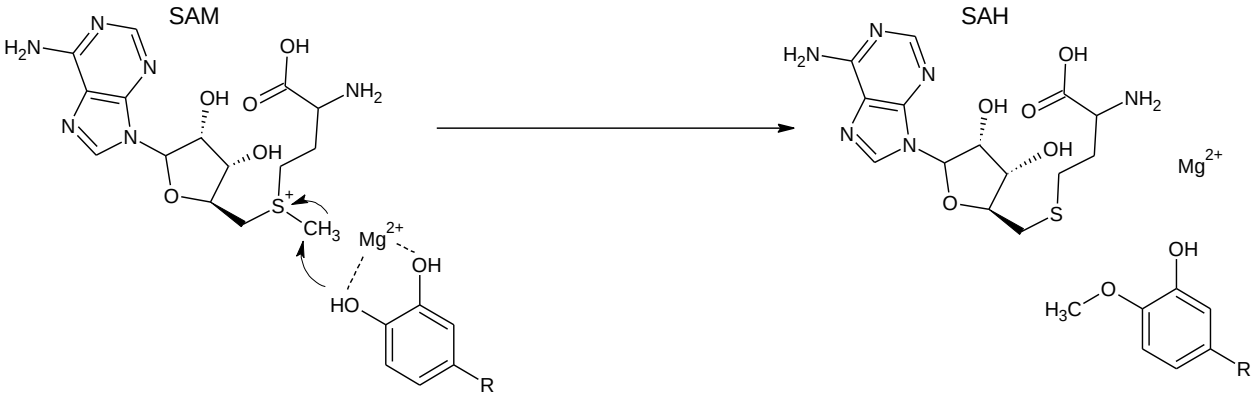

Figure 2-16: Scheme showing the catalysis of a catechol neurotransmitter by SAM in COMT (Ehler *et al.*, 2014; Vidgren *et al.*, 1994).

Many drugs are also substrates for COMT and may be metabolised. These include carbidopa (Porter *et al.*, 1962), apomorphine (Muguet *et al.*, 1995) and isoprenaline (Popa, 1984). COMT is distributed ubiquitously throughout the body and the central nervous system. It is present in the lungs, liver, spleen, stomach, intestines, uterus and gonads (Ellingson *et al.*, 1999). However, the enzymatic activity in the liver is 3-4 times higher than that of the rest of the periphery, and activity in the brain is lower compared to that of the peripheral tissues (Borchardt *et al.*, 1974).

Drug-induced inhibition of the methylation capacity by COMT can occur where anti-convulsion therapy with valproic acid, as well as long term L-dopa therapy, can consume activated methyl groups (Chuang *et al.*, 2012; Müller, 2008). Subsequently, the decrease of methyl donating vitamins such as B_6 and B_{12} also decrease, as they are needed to methylate SAH to yield SAM. These metabolic changes may, hypothetically, accelerate aging-associated brain degeneration by means of atrophy, cognitive deterioration and peripheral nerve function (Müller, 2011; Schwartz *et al.*, 2012).

2.3.5.2 Inhibitors of catechol-*O*-methyltranferase and the role in Parkinson's disease

Currently nitro-substituted catechol derivatives are the most potent COMT inhibitors available. The presence of the strong electron withdrawing nitro moiety prevents the reaction toward *O*-methylation (Backstrom *et al.*, 1989, Learmonth *et al.,* 2012). The reaction of catechol breakdown can be inhibited by acidic nitrocatechol containing drugs like tolcapone and entacapone (Ehler *et al.*, 2014). No new COMT inhibitor has passed clinical trials since entacapone (Kaakkola, 2010).

COMT-inhibitors are used in conjunction with L-dopa to prevent further peripheral metabolism of L-dopa as well as the metabolism of DA to 3-O-methoxytyramine. 3-O-Methoxytyramine can compete with L-dopa for transport at the BBB (Ehler *et al.*, 2014; Müller, 2015). Pharmacologically, COMT-inhibitors are used in conjunction with an L-dopa/AADC inhibitor combination, with tolcapone being more potent of the two drugs on the market (Männistö *et al.*, 1992). Without a COMT inhibitor, only 10% of administered L-dopa reaches the brain, even when an AADC inhibitor is used to increase the effective dose of L-dopa (Rinne & Mölsä, 1979). With COMT present in the gastro-intestinal tract, much of the administered L-dopa is metabolised as it is absorbed into the bloodstream. In contrast, with COMT inhibited, much of the dosage will enter the bloodstream intact (Kaakkola, 2000).

Animal studies with entacapone showed an increased half-life and bioavailability of L-dopa in both rats and monkeys (Cedarbaum *et al.*, 1991; Jenner & Smith, 1993; Nissinen *et al.*, 1988). In later human studies, similar results were obtained with both healthy and PD patients (Jenner & Smith, 1993; Kaakkola *et al.*, 1994; Nutt *et al.*, 1994). Side effects included a harmless urine discolouration, but fatal cases of hepatotoxicity in 1998 led to the removal of tolcapone until April of 2004. At present it can be used under strict monitoring of liver enzyme activity (Müller, 2015; Smith *et al.*, 2003).

Opicapone is a new COMT inhibitor that was clinically tested. It has shown a superior response to entacapone in phase 3 studies and has shown a longer lasting and sustained COMT inhibition (Rocha *et al.*, 2014). Opicapone also showed profound reduction cell toxicity when compared to entacapone (Kiss *et al.*, 2010). Further studies showed that opicapone results in 99% inhibition of COMT one hour after administration, with entacapone resulting in only 82% inhibition (Nuno Palma *et al.*, 2012). Opicapone has been commercially available in Europe since 2016 under the tradename Ongentys (Vasconcelos *et al.*, 2016).

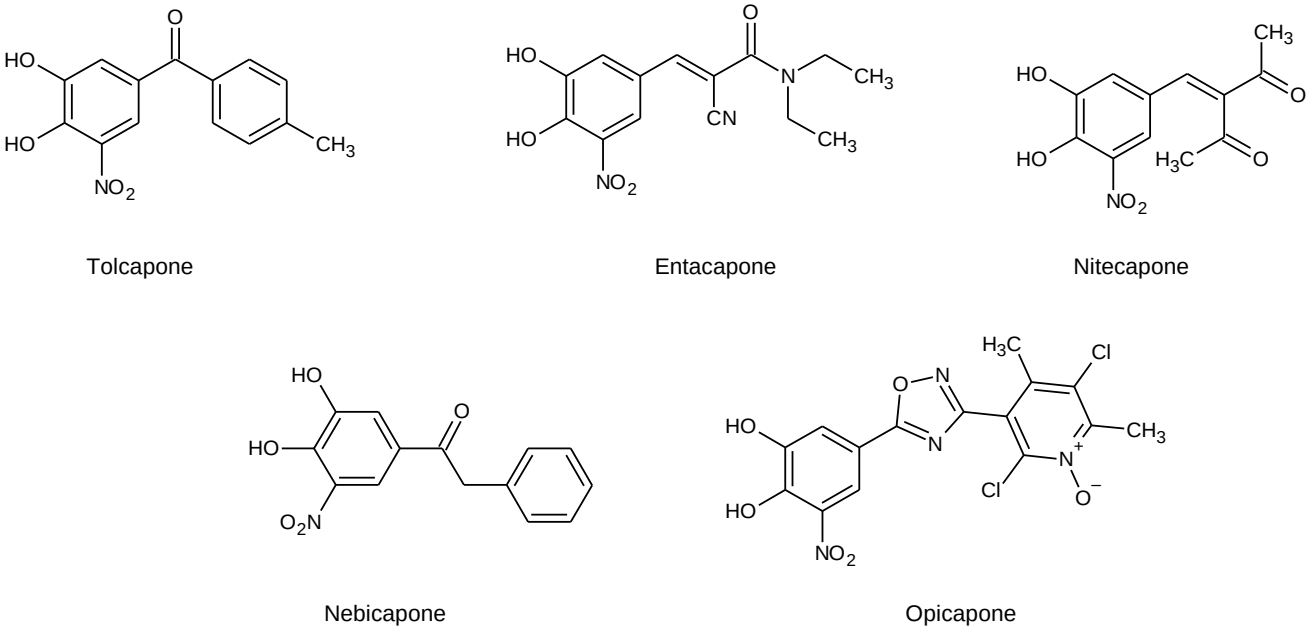

Figure 2-17: Examples of nitrocatechol containing COMT inhibitors.

2.3.6 Dual inhibition of COMT and MAO

In 1994, in a study involving MPTP-treated mice, researchers studied the synergistic effects of L-dopa with COMT/MAO-inhibitors. The mice received dual treatment with COMT and MAO inhibitors, and displayed a decrease in akinesia and an increase in overall movement when compared to control mice. Decreased DA metabolism was observed in the autopsied brain of the mice. The researchers concluded that a COMT inhibitor with L-dopa produced an anti-akinesia effect. When COMT inhibition was paired with L-dopa and a MAO-B inhibitor, an enhanced, possibly restorative, behavioural effect was seen (Fredriksson & Archer, 1995).

In a double blind, placebo controlled cross over study in 1997 further investigation of dual inhibition of both MAO and COMT was done by using selegiline as the MAO inhibitor and entacapone as the COMT inhibitor. The study concluded that, by inhibiting both enzymes, the half-life of L-dopa is significantly increased and 3-OMD formation is decreased. This enhances the brain penetration of L-dopa. The use of dual inhibitors, however, may promote catechol formation and breakdown via other metabolic pathways which may lead to adverse effects not associated with L-dopa treatment (Lyytinen *et al.*, 1997). A later study showed that motor symptoms improve with dual MAO-B/COMT inhibition, especially in the “wear-off” times of L-dopa therapy (Rinne *et al.*, 1998; Ruottinen & Rinne, 1996).

Thus with the studies on the inhibition of MAO and COMT, one can postulate that the dual inhibition of the enzymes may have significant pharmacological value in the treatment of PD (Engelbrecht *et al.*, 2018; Mostert *et al.*, 2015).

2.3.7 Theoretical blood-brain barrier values for central nervous system drugs

The blood-brain barrier (BBB) is the presence of high-resistance tight junctions between the brain endothelial capillaries that form a selective permeable barrier for certain drugs and proteins (Pardridge, 2002). The BBB prevent the uptake of almost >98% of all potential neurotherapeutics to the brain (Clark, 2003). Through several studies, certain rules of thumb have been developed to see a trend in certain structures and the brain permeability of said molecule (Atkinson *et al.*, 2002; Clark, 2001; Norinder & Haeberlein, 2002).

These rules can be summarised as follows:

1. The sum of all nitrogen and oxygen atoms (N + O) must be five or less, this increases the chance of good penetration in to the brain (Norinder & Haeberlein, 2002).

2. If ClogP – (N + O) > 0, then there could be a positive influx into the brain. ClogP is the logarithm of the octanol-water coefficient (P) of a certain compound. This coefficient denotes if a compound is more water or lipid soluble (Norinder & Haeberlein, 2002).

3. Limiting the polar surface area (PSA) to either below 90 $Å^2$ or between 60-70 $Å^2$, depending on the source. PSA is the measure of a molecule's hydrogen-bonding capacity by calculated contribution of oxygen and nitrogen atoms, as well as the hydrogens bonded to oxygen and nitrogen atoms (Kelder *et al.*, 1999; van de Waterbeemd *et al.*, 1998).

4. The molecular weight should be kept under 450 (van de Waterbeemd *et al.*, 1998).

5. The logD value must be between 1 – 3 (van de Waterbeemd *et al.*, 1998).

To summarise, successful CNS drugs are rigid, more lipophilic, with fewer hydrogen-bond donors, fewer formal charges and a PSA lower than 80 $Å^2$ (Doan *et al.*, 2002).

2.4 Enzyme kinetics and mode of inhibition

Enzymes are catalytic proteins that accelerate chemical reactions under physiological conditions favourable to that specific enzyme, without being consumed themselves (Baynes & Dominiczak, 2009). Factors such as pH and temperature are the main parameters which affect enzyme activity (Kilpatrick *et al.*, 2013). Enzyme activity was described in 1894 as "lock and key", where the substrate fits into the enzyme cavity and then the substrate is metabolised (Fisher, 1894). Today the binding and metabolism of a substrate by an enzyme is often described by the transition-state theory (Haldane, 1930; Pauling, 1948).

The transition state theory describes the activated enzyme-substrate-complex, and proposed that as the substrates binds to the enzyme, the activation energy of the system is lowered to favour the chemical reaction (Stein, 2011). This lowered activation energy is the sole driving force behind the catalysis of many enzymatic reactions (Garcia-Viloca *et al.*, 2004).

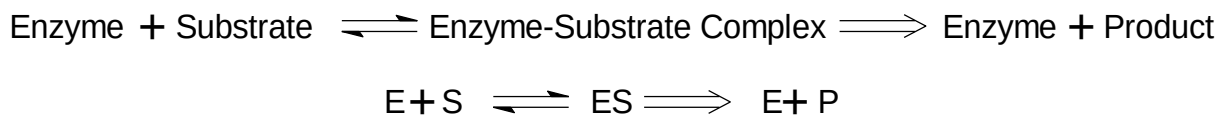

Figure 2-18: The enzyme catalysed reaction (Fersht, 1999).

As seen in Figure 2–18, the formation of the product is the rate limiting step in any reaction (thus the arrow from ES to E + P) (Baynes & Dominiczak, 2009). There are certain factors in the Enzyme-Substrate Complex (ES) that affects the enzyme induced reaction, and includes but is not limited to: reaction surface, reagent positioning and participation in the reaction (Garcia-Viloca *et al.*, 2004; Kilpatrick *et al.*, 2013).

Reaction surface and *reagent positioning* relates to the active site of the enzyme where the amino acids and certain cofactors play a role. Characteristics such as the level of hydrophobicity as well as the size of the cavity are all factors in enzyme kinetics as well as the design of inhibitors. This in turn also has an effect on the intra- and intermolecular forces used to stabilise the substrate in either a stereospecific position or orientation that is favourable for the reaction to take place (Benkovic & Hammes-Schiffer, 2003; Cannon *et al.*, 1996; Kilpatrick *et al.*, 2013; Knowles, 1991).

Reaction participation refers to certain inorganic cofactors (for example Zinc or Mg^{2+}) or organic molecules called coenzymes (for example NAD^{+}) used as part of the reaction either as a catalyst or as a substrate in the reaction (Broderick, 2001).

By using these factors one can inhibit an enzyme, so that the forward reaction of E+P is either reduced or totally inhibited, and this depends on the mode of inhibition. As a chemist one can look at the substrate or product structures of the reaction to design an inhibitor (Radzicka & Wolfenden, 1995). Enzyme inhibitors may act as either reversible or irreversible inhibitors, where reversible inhibitors can be explained as competitive, non-competitive or uncompetitive in terms of interaction with an inhibitor (Hollenberg, 2002).

Reversible inhibition states that the enzyme is inhibited for a short period in a dose dependant manner. When the drug has passed though the liver or kidneys, the rate and extent of inhibition begins to diminish (Lin *et al.*, 2000).

Competitive inhibition states that the binding of the inhibitor to the enzyme prevents the substrate from entering the active site. The inhibitor mostly has some level of structural similarity to the endogenous substrate. When the substrate concentration is increased, the substrate will displace the inhibitor from the active site and normal product formation will continue (de Montellano & Correia, 1995).

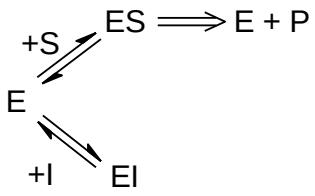

Figure 2-19: Competitive inhibition of an enzyme catalysed reaction [E = Enzyme, S = Substrate, I = Inhibitor, P = Product]. Adapted from (Wharton, 2013).

Non-competitive inhibition states that the inhibitor binds not the free enzyme, but rather to the enzyme-substrate-complex (ES), and not always in the active site but on an allosteric binding site that induces a conformational change in the active site (Silverman & Holladay, 2014). The allosteric binding site is distinct and physically separate from the active site (Baynes & Dominiczak, 2009). This in turn produces a non-productive complex in which the catalytic power has been reduced (Schenkman *et al.*, 1981). In this instance, when the concentration of substrate is increased, the concentration of the complex increases, thus more inhibited complexes are present, which increases the rate and extent of inhibition (Baynes & Dominiczak, 2009).

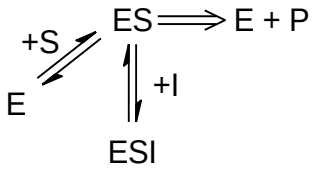

Figure 2-20: Non-competitive inhibition of an enzyme catalysed reaction [E = Enzyme, S = Substrate, I = Inhibitor, P = Product]. Adapted from (Baynes & Dominiczak, 2009).

Uncompetitive inhibitors states that the inhibitor can either bind to the free enzyme at the active site, or with the enzyme-substrate-complex to reduce the metabolism of the substrate (Burlingham & Widlanski, 2003). The concentration of the substrate has no effect as this type of inhibition does not differentiate between free enzyme or enzyme-substrate-complexes (Kilpatrick *et al.*, 2013).

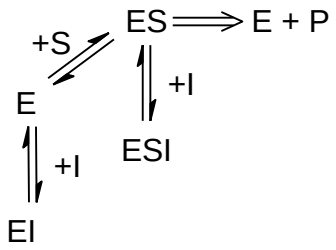

Figure 2-21: Uncompetitive inhibition of an enzyme catalysed reaction [E = Enzyme, S = Substrate, I = Inhibitor, P = Product]. Adapted from (Silverman & Holladay, 2014).

The potency of enzyme inhibition is expressed as the IC_{50} value, which is the concentration of inhibitor needed to inhibit enzyme activity with 50%. The lower the value, the more potent the compound. Normally good potency inhibitors possess IC_{50} values in the micro to nanomolar range (Kilpatrick *et al.*, 2013).

2.5 Molecular hybridisation and lead structure

Choosing the correct structure to synthesise can be a daunting task, but by using molecular hybridisation and lead discovery, one is able to hypothesise that the possible addition of certain substituents to a pharmacophore will produce active compounds (Viegas-Junior *et al.*, 2007).

Lead discovery is when one looks at the natural occurring substrate for the enzyme/receptor in question, and breaks it down into the smallest active configuration, the *pharmacophore*, which are the minimum structural features needed for enzyme binding. This can be used to isolate structures with pharmacological activity (Milne *et al.*, 1998). To ensure the possibility of a good match, novel compounds must be structurally and chemically compliant to the natural substrate (Dean, 1988).

Upon the identification of the lead pharmacophore, one can look at existing drugs and use the method of molecular hybridisation, to design bioactive derivatives. Two strategies exists; 1) the development of new ligands by the fusion of two pharmacophoric sub-structures, and this fusion leads to the forming of a new hybrid structure that maintain the characteristics of the pre-selected templates (Kuntz, 1992; Viegas-Junior *et al.*, 2007), or 2) the use of two pharmacophoric entities, which is linked with a linker to merge the entities as a new chemical compound (Fraga, 2009).

The process of finding an active compound is explained in Figure 2-22. In this scheme an approach to design biological inhibitors is described. This design approach states that, to develop an inhibitor, one must have the structure of the receptor/enzyme. By considering the structures of the naturally occurring ligands, one may propose new ligands with the help of either SARs. After

newly designed compounds are synthesised, they are subjected to thorough biological evaluation. The active compounds are identified, and can be used to start again and build on the knowledge gained (Kuntz, 1992).

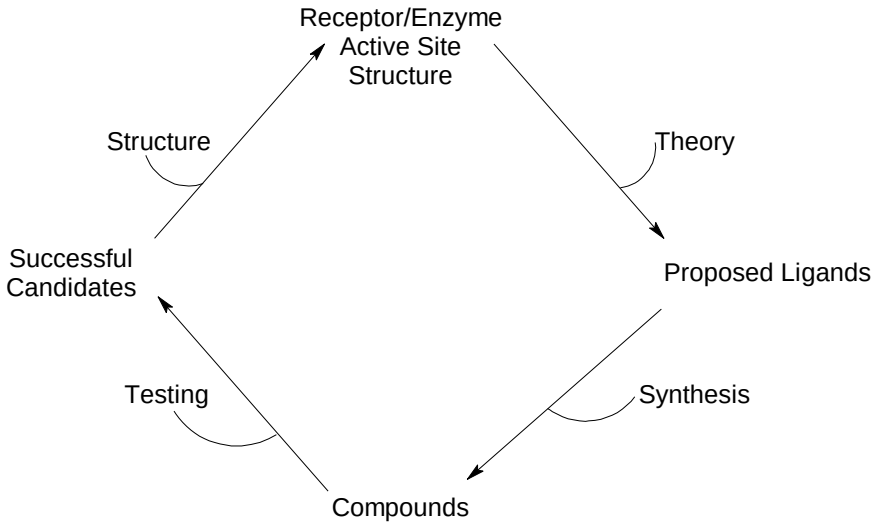

Figure 2-22: Approach to the design of biological inhibitors (Kuntz, 1992; Milne *et al.*, 1998).

To obtain a good candidate drug can be difficult, but via drug hybridisation studies, it is possible to arrive at active compounds with minimal effort (Amakali, 2016; Engelbrecht *et al.*, 2018; Legoabe *et al.*, 2014).

With this in mind, one must also have a scaffold as a starting point. For the purpose of this study the chalcone structure was selected as scaffold, for multiple reasons, which include their ease of synthesis, simple chemistry and their variety of biological activities (Gomes *et al.*, 2017). Chalcones are very interesting chemical scaffolds, and have been used to design a large array of structures with many possible uses. Chalcones may exist as either the trans (*E*, **1**) or the cis (*Z*, **2**) isomers, while having two aromatic rings joined via a three-carbon α,β-unsaturated carbonyl system (Aksöz & Ertan, 2011). With the two aromatic rings, there is a large possible number of replaceable hydrogens that can be used for a large variety of derivatives (Gomes *et al.*, 2017). The *E* isomer is more stable from a thermodynamic perspective, with the *Z* isomer being unfavourable due to strong steric effects between the carbonyl group and the B-ring (Aksöz & Ertan, 2011; Amslinger *et al.*, 2013).

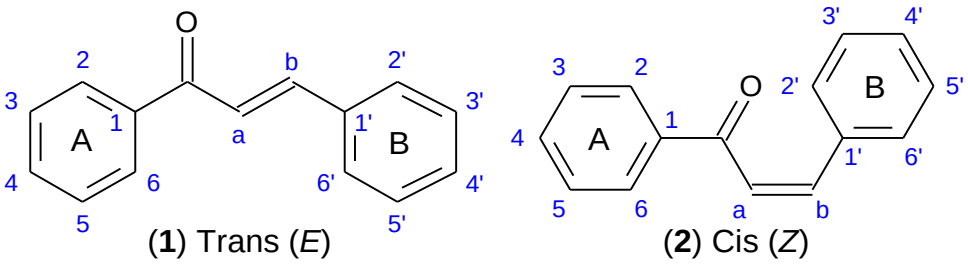

Figure 2-23: Structural representations of the chalcone scaffold (Gomes *et al.*, 2017).

BIBLIOGRAPHY

Aksöz, B.E. & Ertan, R. 2011. Chemical and structural properties of chalcones. *FABAD Journal of Pharmaceutical Science*, 36:223-242.

Alexander, G. 2004. Biology of Parkinson's Disease: pathogenesis and pathophysiology of a multisystem neurodegenerative disorder. *State of the Art*, 6.

Alexander, G.E. & Crutcher, M.D. 1990. Functional architecture of basal ganglia circuits: neural substrates of parallel processing. *Trends in Neurosciences*, 13(7):266-271.

Amakali, K.T. 2016. Synthesis and evaluation of cyclic chalcones as monoamine oxidase inhibitors. North-West University (South Africa), Potchefstroom Campus. Dissertation – MSc.

Aminoff, M. 2004. Pharmacologic Management of Parkinsonism & Other Movement Katzung Pharmacology Katzung, Basic and Clinical Pharmacology: Lang Medical Books, McGraw-Hill, New York, NY, USA.

Amslinger, S., Al-Rifai, N., Winter, K., Wörmann, K., Scholz, R., Baumeister, P., et al. 2013. Reactivity assessment of chalcones by a kinetic thiol assay. *Organic & Biomolecular Chemistry*, 11(4):549-554.

Andreyev, A.Y., Kushnareva, Y.E. & Starkov, A. 2005. Mitochondrial metabolism of reactive oxygen species. *Biochemistry (Moscow),* 70(2):200-214.

Arnold, S., Victor, M.B. & Beyer, C. 2012. Estrogen and the regulation of mitochondrial structure and function in the brain. *The Journal of Steroid Biochemistry and Molecular Biology*, 131(1-2):2-9.

Atkinson, F., Cole, S., Green, C. & Van de Waterbeemd, H. 2002. Lipophilicity and other parameters affecting brain penetration. C*urrent Medicinal Chemistry-Central Nervous System Agents*, 2(3):229-240.

Axelrod, J. 1966. Methylation Reactions in the Formation and Metabolism of Catecholamines and Other Biogenic Amines. *Pharmacological Reviews*, 18(1):95-113.

Bach, A., Lan, N.C., Johnson, D.L., Abell, C.W., Bembenek, M.E., Kwan, S.-W., et al. 1988. cDNA cloning of human liver monoamine oxidase A and B: molecular basis of differences in enzymatic properties. *Proceedings of the National Academy of Sciences*, 85(13):4934-4938.

Backstrom, R., Honkanen, E., Pippuri, A., Kairisalo, P., Pystynen, J., Heinola, K., et al. 1989. Synthesis of some novel potent and selective catechol O-methyltransferase inhibitors. *Journal of Medicinal Chemistry*, 32(4):841-846.

Bai, H.W., Shim, J.Y., Yu, J. & Zhu, B.T. 2007. Biochemical and molecular modeling studies of the O-methylation of various endogenous and exogenous catechol substrates catalyzed by recombinant human soluble and membrane-bound catechol-O-methyltransferases. *Chemical Research in Toxicology*, 20(10):1409-1425.

Baldereschi, M., Di Carlo, A., Vanni, P., Ghetti, A., Carbonin, P. & Amaducci, L. 2003. Lifestyle-related risk factors for Parkinson's disease: a population-based study. *Acta Neurologica Scandinavica,* 108(4):239-244.

Bara-Jimenez, W., Sherzai, A., Dimitrova, T., Favit, A., Bibbiani, F., Gillespie, M., et al. 2003. Adenosine A2A receptor antagonist treatment of Parkinson's disease. *Neurology*, 61(3):293-296.

Bartholini, G. & Pletscher, A. 1975. Decarboxylase inhibitors. *Pharmacology & Therapeutics. Part B: General and Systematic Pharmacology,* 1(3):407-421.

Baynes, J. & Dominiczak, M.H. 2009. Medical biochemistry. 4th ed. London: Elsevier.

Benkovic, S.J. & Hammes-Schiffer, S. 2003. A perspective on enzyme catalysis. *Science*, 301(5637):1196-1202.

Berk, M., Dodd, S., Kauer-Sant'anna, M., Malhi, G., Bourin, M., Kapczinski, F., et al. 2007. Dopamine dysregulation syndrome: implications for a dopamine hypothesis of bipolar disorder. *Acta Psychiatrica Scandinavica*, 116:41-49.

Berman, S.B. & Hastings, T.G. 1999. Dopamine oxidation alters mitochondrial respiration and induces permeability transition in brain mitochondria: implications for Parkinson's disease. *Journal of Neurochemistry*, 73(3):1127-1137.

Berridge, C.W. & Waterhouse, B.D. 2003. The locus coeruleus–noradrenergic system: modulation of behavioral state and state-dependent cognitive processes. *Brain Research Reviews*, 42(1):33-84.

Binda, C., Li, M., Hubálek, F., Restelli, N., Edmondson, D.E. & Mattevi, A. 2003. Insights into the mode of inhibition of human mitochondrial monoamine oxidase B from high-resolution crystal structures. P*roceedings of the National Academy of Sciences*, 100(17):9750-9755.

Binda, C., Newton-Vinson, P., Hubálek, F., Edmondson, D.E. & Mattevi, A. 2002. Structure of human monoamine oxidase B, a drug target for the treatment of neurological disorders. *Nature Structural and Molecular Biology*, 9(1):22.

Blaschko, H. 1939. The specific action of L-dopa decarboxylase. *Journal of physiology*, 96:50P-51P.

Blesa, J., Trigo-Damas, I., Quiroga-Varela, A. & Jackson-Lewis, V.R. 2015. Oxidative stress and Parkinson's disease. *Frontiers in Neuroanatomy*, 9:91.

Bonifácio, M.J., Archer, M., Rodrigues, M.L., Matias, P.M., Learmonth, D.A., Carrondo, M.A., et al. 2002. Kinetics and crystal structure of catechol-o-methyltransferase complex with co-substrate and a novel inhibitor with potential therapeutic application. *Molecular Pharmacology*, 62(4):795-805.

Borchardt, R.T., Cheng, C.-F., Cooke, P.H. & Creveling, C. 1974. The purification and kinetic properties of liver microsomal-catechol-O-methyltransferase. *Life Sciences*, 14(6):1089-1100.

Bourque, M., Morissette, M. & Di Paolo, T. 2015. Neuroprotection in Parkinsonian-treated mice via estrogen receptor α activation requires G protein-coupled estrogen receptor 1. *Neuropharmacology*, 95:343-352.

Bourque, M., Morissette, M. & Di Paolo, T. 2018. Repurposing sex steroids and related drugs as potential treatment for Parkinson's disease. *Neuropharmacology*, 147:37-54.

Brady, S., Siegel, G., Albers, R. & Price, D. 2005. Inherited and Neurodegenerative Diseases. In Technology. *Basic Neurochemistry: Molecular, Cellular and Medical Aspects* 1:766 - 778.

Brandt, U. 2006. Energy converting NADH: quinone oxidoreductase (complex I). *Annual Review of Biochemistry*, 75:69-92.

Brewer, L.D., Dowling, A.L., Curran-Rauhut, M.A., Landfield, P.W., Porter, N.M. & Blalock, E.M. 2009. Estradiol reverses a calcium-related biomarker of brain aging in female rats. *Journal of Neuroscience*, 29(19):6058-6067.

Brissaud, E. 1895. Clinical Lessons on Mental and Nervous Diseases. *Salpêtrière*, 1893-94.

Broderick, J.B. 2001. Coenzymes and cofactors. (*in* Encyclopedia of life sciences).

Brooks, D. 2000. Dopamine agonists: their role in the treatment of Parkinson's disease: *Journal of Neurology, Neurosurgery & Psychiatry*, 68:685-689.

Brown, P. & Marsden, C. 1998. What do the basal ganglia do? *The Lancet*, 351(9118):1801-1804.

Brunner, H.G., Nelen, M., Breakefield, X., Ropers, H. & Van Oost, B. 1993. Abnormal behavior associated with a point mutation in the structural gene for monoamine oxidase A. *Science,* 262(5133):578-580.

Burba, J. & Becking, G. 1969. Effect of the antioxidant nordihydroguaiaretic acid on the in vitro activity of catechol-o-methyl transferase. *Archives Internationales de Pharmacodynamie et de Therapie*, 180(2):323.

Burlingham, B.T. & Widlanski, T.S. 2003. An intuitive look at the relationship of Ki and IC50: a more general use for the Dixon plot. *Journal of Chemical Education*, 80(2):214.

Caccia, C., Maj, R., Calabresi, M., Maestroni, S., Faravelli, L., Curatolo, L., et al. 2006. Safinamide from molecular targets to a new anti-Parkinson drug. *Neurology*, 67(7 suppl 2):S18-S23.

Calabresi, P., Castrioto, A., Di Filippo, M. & Picconi, B. 2013. New experimental and clinical links between the hippocampus and the dopaminergic system in Parkinson's disease. *The Lancet Neurology*, 12(8):811-821.

Cannon, W.R., Singleton, S.F. & Benkovic, S.J. 1996. A perspective on biological catalysis. *Nature Structural and Molecular Biology*, 3(10):821.

Cardinal, R.N., Parkinson, J.A., Hall, J. & Everitt, B.J. 2002. Emotion and motivation: the role of the amygdala, ventral striatum, and prefrontal cortex. *Neuroscience & Biobehavioral Reviews,* 26(3):321-352.

Carlsson, A. 1959. The occurrence, distribution and physiological role of catecholamines in the nervous system. *Pharmacological Reviews*, 11(2):490-493.

Carlsson, A., Lindqvist, M. & Magnusson, T. 1957. 3, 4-Dihydroxyphenylalanine and 5-hydroxytryptophan as reserpine antagonists. *Nature*, 180(4596):1200.

Caspi, A., McClay, J., Moffitt, T.E., Mill, J., Martin, J., Craig, I.W., et al. 2002. Role of genotype in the cycle of violence in maltreated children. *Science*, 297(5582):851-854.

Cedarbaum, J.M., Leger, G. & Guttman, M. 1991. Reduction of circulating 3-O-methyldopa by inhibition of catechol-O-methyltransferase with OR-611 and OR-462 in cynomolgus monkeys:

implications for the treatment of Parkinson's disease. *Clinical Neuropharmacology*, 14(4):330-342.

Chan, P., DeLanney, L.E., Irwin, I., Langston, J.W. & Di Monte, D. 1991. Rapid ATP loss caused by 1-methyl-4-phenyl-1, 2, 3, 6-tetrahydropyridine in mouse brain. *Journal of Neurochemistry*, 57(1):348-351.

Chiba, K., Trevor, A. & Castagnoli Jr, N. 1984. Metabolism of the neurotoxic tertiary amine, MPTP, by brain monoamine oxidase. *Biochemical and Biophysical Research Communications*, 120(2):574-578.

Chondrogiorgi, M., Tatsioni, A., Reichmann, H. & Konitsiotis, S. 2014. Dopamine agonist monotherapy in Parkinson's disease and potential risk factors for dyskinesia: a meta-analysis of levodopa-controlled trials. *European Journal of Neurology*, 21(3):433-440.

Chuang, Y.C., Chuang, H.Y., Lin, T.K., Chang, C.C., Lu, C.H., Chang, W.N., et al. 2012. Effects of long-term antiepileptic drug monotherapy on vascular risk factors and atherosclerosis. *Epilepsia*, 53(1):120-128.

Clark, D. 2001. Prediction of intestinal absorption and blood-brain barrier penetration by computational methods. *Combinatorial Chemistry & High Throughput Screening*, 4(6):477-496.

Clark, D.E. 2003. In silico prediction of blood–brain barrier permeation. *Drug Discovery Today*, 8(20):927-933.

Collins, G., Sandler, M., Williams, E. & Youdim, M.B.H. 1970. Multiple Forms of Human Brain Monoamine Oxidase. *Nature*, 225:817–820.

Corsini, G., Del Zompo, M., Gessa, G. & Mangoni, A. 1979. Therapeutic efficacy of apomorphine combined with an extracerebral inhibitor of dopamine receptors in Parkinson's disease. *The Lancet*, 313(8123):954-956.

Creveling, C., Dalgard, N., Shimizu, H. & Daly, J. 1970. Catechol O-methyltransferase: III. m- and pO-methylation of catecholamines and their metabolites. *Molecular Pharmacology*, 6(6):691-696.

Dauer, W. & Przedborski, S. 2003. Parkinson's disease: mechanisms and models. *Neuron*, 39(6):889-909.

Davie, C.A. 2008. A review of Parkinson's disease. *British Medical Bulletin*, 86(1):109-127.

Davis, G.C., Williams, A.C., Markey, S.P., Ebert, M.H., Caine, E.D. & Reichert, C.M. 1979. Chronic parkinsonism secondary to intravenous injection of meperidine analogues. *Psychiatry research*, 1(3):249-254.

de Montellano, P.R.O. & Correia, M.A. 1995. Inhibition of cytochrome P450 enzymes. Cytochrome P450. *Springer*. p. 305-364.

Dean, P.M. 1988. Molecular foundations of drug-receptor interaction: Cambridge University Press Cambridge.

Delcambre, S., Nonnenmacher, Y. & Hiller, K. 2016. Dopamine metabolism and reactive oxygen species production. (*in* Mitochondrial Mechanisms of Degeneration and Repair in Parkinson's Disease. Springer International,p. 25-47).

DeLong, M.R. 1990. Primate models of movement disorders of basal ganglia origin. *Trends in neurosciences*, 13(7):281-285.

Dickson, D.W. 2018. Neuropathology of Parkinson disease. *Parkinsonism & Relatated Disorders*, 46(Suppl 1):S30-S33.

Diez, J.A. & Maderdrut, J.L. 1977. Development of multiple forms of mouse brain monoamine oxidase in vivo and in vitro. *Brain Research*, 128(1):187-192.

DiMauro, S. & Davidzon, G. 2005. Mitochondrial DNA and disease. *Annals of Medicine*, 37(3):222-232.

Doan, K.M.M., Humphreys, J.E., Webster, L.O., Wring, S.A., Shampine, L.J., Serabjit-Singh, C.J., et al. 2002. Passive permeability and P-glycoprotein-mediated efflux differentiate central nervous system (CNS) and non-CNS marketed drugs. *Journal of Pharmacology and Experimental Therapeutics*, 303(3):1029-1037.

Du, J.-J. & Chen, S.-D. 2017. Current nondopaminergic therapeutic options for motor symptoms of Parkinson's disease. *Chinese Medical Journal*, 130(15):1856.

Ebadi, M., Srinivasan, S.K. & Baxi, M.D. 1996. Oxidative stress and antioxidant therapy in Parkinson's disease. *Progress in Neurobiology*, 48(1):1-19.

Edmondson, D.E., Mattevi, A., Binda, C., Li, M. & Hubalek, F. 2004. Structure and mechanism of monoamine oxidase. *Currant Medicinal Chemistry*, 11(15):1983-1993.

Edwards, L.L., Quigley, E.M. & Pfeiffer, R.F. 1992. Gastrointestinal dysfunction in Parkinson's disease: frequency and pathophysiology. *Neurology*, 42(4):726-732.

Ehler, A., Benz, J., Schlatter, D. & Rudolph, M.G. 2014. Mapping the conformational space accessible to catechol-O-methyltransferase. *Acta Crystallographica Section D: Biological Crystallography*, 70(8):2163-2174.

Ekue, A., Boulanger, J.F., Morissette, M. & Di Paolo, T. 2002. Lack of Effect of Testosterone and Dihydrotestosterone Compared to 17β-Oestradiol in 1-Methyl-4-Phenyl-1, 2, 3, 6, Tetrahydropyridine-Mice. *Journal of Neuroendocrinology*, 14(9):731-736.

Ellingson, T., Duddempudi, S., Greenberg, B.D., Hooper, D. & Eisenhofer, G. 1999. Determination of differential activities of soluble and membrane-bound catechol-O-methyltransferase in tissues and erythrocytes. *Journal of Chromatography B: Biomedical Sciences and Applications*, 729(1-2):347-353.

Engelbrecht, I., Petzer, J.P. & Petzer, A. 2015. The synthesis and evaluation of sesamol and benzodioxane derivatives as inhibitors of monoamine oxidase. *Bioorganic & Medicinal Chemistry letters*, 25(9):1896-1900.

Engelbrecht, I., Petzer, J.P. & Petzer, A. 2018. Nitrocatechol Derivatives of Chalcone as Inhibitors of Monoamine Oxidase and Catechol-O-Methyltransferase. *Central Nervous System Agents Medicinal Chemistry,* 18(2):115-127.

Fagervall, I. & Ross, S.B. 1986. Inhibition of mono amine oxidase in monoaminergic neurones in the rat brain by irreversible inhibitors. *Biochemical Pharmacology*, 35(8):1381-1387.

Fersht, A. 1999. Structure and mechanism in protein science: a guide to enzyme catalysis and protein folding.New York: Macmillan.

Fišar, Z. 2016. Drugs related to monoamine oxidase activity. *Progress in Neuro-Psychopharmacology and Biological Psychiatry*, 69:112-124.

Fišar, Z., Hroudová, J. & Raboch, J. 2010. Inhibition of monoamine oxidase activity by antidepressants and mood stabilizers. *Neuroendocrinology Letters*, 31(5):645.

Fisher, E. 1894. The influence of configuration on enzyme activity.(Translated from German). *Chemische Berichte*, 27:2984-2993.

Florvall, L., Fagervall, I., Ask, A.L. & Ross, S.B. 1986. Selective monoamine oxidase inhibitors. 4. 4-Aminophenethylamine derivatives with neuron-selective action. *Journal of Medicinal Chemistry*, 29(11):2250-2256.

Fowler, C.J., Mantle, T.J. & Tipton, K.F. 1982. The nature of the inhibition of rat liver monoamine oxidase types A and B by the acetylenic inhibitors clorgyline, l-deprenyl and pargyline. *Biochemical Pharmacology*, 31(22):3555-3561.

Fraga, C.A.M. 2009. Drug hybridization strategies: before or after lead identification*? Expert Opinion on Drug Discovery*, 4(6):605-609.

Frank-Cannon, T.C., Alto, L.T., McAlpine, F.E. & Tansey, M.G. 2009. Does neuroinflammation fan the flame in neurodegenerative diseases? *Molecular Neurodegeneration*, 4(1):47.

Frank, M.G. 2006. The mystery of sleep function: current perspectives and future directions. *Reviews in the Neurosciences*, 17(4):375-392.

Fredriksson, A. & Archer, T. 1995. Synergistic interactions between COMT-/MAO-inhibitors and L-Dopa in MPTP-treated mice. *Journal of Neural Transmission*, 102(1):19-34.

Frentzel, D., Judanin, G., Borozdina, O., Klucken, J., Winkler, J. & Schlachetzki, J. 2017. Increase of Reproductive Life Span Delays Age of Onset of Parkinson's Disease. *Frontiers in Neurology,* 8:397.

Garcia-Viloca, M., Gao, J., Karplus, M. & Truhlar, D.G. 2004. How enzymes work: analysis by modern rate theory and computer simulations. *Science*, 303(5655):186-195.

Gaweska, H. & Fitzpatrick, P.F. 2011. Structures and mechanism of the monoamine oxidase family. *Biomolecular Concepts*, 2(5):365-377.

Gelb, D.J., Oliver, E. & Gilman, S. 1999. Diagnostic criteria for parkinson disease. *Archives of Neurology*, 56(1):33-39.

Giasson, B.I., Duda, J.E., Murray, I.V., Chen, Q., Souza, J.M., Hurtig, H.I., et al. 2000. Oxidative damage linked to neurodegeneration by selective α-synuclein nitration in synucleinopathy lesions. *Science*, 290(5493):985-989.

Gibb, W. & Lees, A. 1991. Anatomy, pigmentation, ventral and dorsal subpopulations of the substantia nigra, and differential cell death in Parkinson's disease. *Journal of Neurology, Neurosurgery & Psychiatry*, 54(5):388-396.

Gomes, M.N., Muratov, E.N., Pereira, M., Peixoto, J.C., Rosseto, L.P. & Cravo, P.V. 2017. Chalcone derivatives: promising starting points for drug design. *Molecules*, 22(8):1210.

Gonzalez-Usigli, H.A. 2017. Parkinson Disease. https://www.merckmanuals.com/professional/neurologic-disorders/movement-and-cerebellar-disorders/parkinson-disease: Merck Manual. Date of access: 28-2. 2017.

Gottwald, M.D., Bainbridge, J.L., Dowling, G.A., Aminoff, M.J. & Alldredge, B.K. 1997. New pharmacotherapy for Parkinson's disease. *Annals of Pharmacotherapy*, 31(10):1205-1217.

Group, P.S. 2000. Pramipexole vs levodopa as initial treatment for Parkinson disease: a randomized controlled trial. *Jama*, 284(15):1931-1938.

Guggenheim, M. 1913. Dioxyphenylalanin, eine neue Aminosäure aus Vicia faba. *Hoppe-Seyler´ s Zeitschrift für physiologische Chemie,* 88(4):276-284.

Guldberg, H.C. & Marsden, C.A. 1975. Catechol-O-methyl transferase: pharmacological aspects and physiological role. *Pharmacological Reviews*, 27(2):135-206.

Haaxma, C.A., Bloem, B.R., Borm, G.F., Oyen, W.J., Leenders, K.L., Eshuis, S., et al. 2007. Gender differences in Parkinson's disease. *Journal of Neurology, Neurosurgery & Psychiatry*, 78(8):819-824.

Haldane, J. 1930. Enzymes. London, Longmann and Green.

Hall, C.N., Klein-Flügge, M.C., Howarth, C. & Attwell, D. 2012. Oxidative phosphorylation, not glycolysis, powers presynaptic and postsynaptic mechanisms underlying brain information processing. *Journal of Neuroscience*, 32(26):8940-8951.

Halliwell, B. 1992. Reactive oxygen species and the central nervous system. *Journal of neurochemistry*, 59(5):1609-1623.

Harding, A.J., Stimson, E., Henderson, J.M. & Halliday, G.M. 2002. Clinical correlates of selective pathology in the amygdala of patients with Parkinson's disease. *Brain*, 125(11):2431-2445.

Henriot, S., Kuhn, C., Kettler, R. & Da Prada, M. 1994. Lazabemide (Ro 19-6327), a reversible and highly sensitive MAO-B inhibitor: preclinical and clinical findings. Amine Oxidases: Function and Dysfunction. *Springer*. p. 321-325).

Hollenberg, P.F. 2002. Characteristics and common properties of inhibitors, inducers, and activators of CYP enzymes. *Drug Metabolism Reviews*, 34(1-2):17-35.

Holloway, R., Shoulson, I., Fahn, S., Kieburtz, K., Lang, A. & Marek, K. 2004. Pramipexole vs levodopa as initial treatment for Parkinson disease: a 4-year randomized controlled trial. *Archives of Neurology*, 61(7):1044-1053.

Holtz, P., Heise, R. & Lüdtke, K. 1938. Fermentativer Abbau von l-dioxyphenylalanin (Dopa) durch Niere. *Naunyn-Schmiedebergs Archiv für Experimentelle Pathologie und Pharmakologie*, 191(1):87-118.

Hoover, J.E. & Strick, P.L. 1993. Multiple output channels in the basal ganglia. *Science*, 259(5096):819-821.

Hornykiewicz, O. 2002. L-DOPA: from a biologically inactive amino acid to a successful therapeutic agent. *Amino Acids*, 23(1-3):65-70.

Huh, M. & Friedhoff, A.J. 1979. Multiple molecular forms of catechol-O-methyltransferase. Evidence for two distinct forms, and their purification and physical characterization. *Journal of biological chemistry*, 254(2):299-308.

Jahng, J.W., Houpt, T.A., Wessel, T.C., Chen, K., Shih, J.C. & Joh, T.H. 1997. Localization of monoamine oxidase A and B mRNA in the rat brain by in situ hybridization. *Synapse*, 25(1):30-36.

Jellinger, K. 1987. Neuropathological substrates of Alzheimer's disease and Parkinson's disease. *Journal of Neural Transmission Supplementum*, 24:109-129.

Jenner, P. & Smith, L. 1993. Interaction of the COMT inhibitor entacapone with L-dopa in MPTP treated common marmosets. C*anadian Journal of Neurological Sciences*, 20(Suppl 4):S211.

Jones, D.P. 2006. Redefining oxidative stress. *Antioxidants & Redox Signaling*, 8(9-10):1865-1879.

Kaakkola, S. 2000. Clinical pharmacology, therapeutic use and potential of COMT inhibitors in Parkinson’s disease. *Drugs*, 59(6):1233-1250.

Kaakkola, S. 2010. Problems with the present inhibitors and a relevance of new and improved COMT inhibitors in Parkinson’s disease. *International Review of Neurobiology*. Elsevier. p. 207-225.

Kaakkola, S., Teräväinen, H., Ahtila, S., Rita, H. & Gordin, A. 1994. Effect of entacapone, a COMT inhibitor, on clinical disability and levodopa metabolism in parkinsonian patients. *Neurology*, 44(1):77-77.

Katzenschlager, R., Sampaio, C., Costa, J. & Lees, A. 2002. Anticholinergics for symptomatic management of Parkinson s disease. *Cochrane Database of Systematic Reviews(3)*.

Katzung, B.G., Masters, S.B. & Trevor, A.J. 2012. Basic and Clinical Pharmacology. 12th ed. USA: McGraw-Hill Education.

Kelder, J., Grootenhuis, P.D., Bayada, D.M., Delbressine, L.P. & Ploemen, J.-P. 1999. Polar molecular surface as a dominating determinant for oral absorption and brain penetration of drugs. *Pharmaceutical research*, 16(10):1514-1519.

Kilpatrick, B., Heller, M. & Arns, S. 2013. Chemoselective nitration of aromatic sulfonamides with tert-butyl nitrite. *Chemical Communications*, 49(5):514-516.

Kiray, M., Bagriyanik, H., Pekcetin, C., Ergur, B., Uysal, N., Ozyurt, D., et al. 2006. Deprenyl and the relationship between its effects on spatial memory, oxidant stress and hippocampal neurons in aged male rats. *Physiological Research*, 55(2):205.

Kish, S.J., Shannak, K.S., Rajput, A.H., Gilbert, J.J. & Hornykiewicz, O. 1984. Cerebellar norepinephrine in patients with Parkinson's disease and control subjects. *Archives of Neurology*, 41(6):612-614.

Kiss, L.E., Ferreira, H.S., Torrao, L., Bonifácio, M.J., Palma, P.N., Soares-da-Silva, P.C., Learmonth, D.A. 2010. Discovery of a long-acting, peripherally selective inhibitor of catechol-O-methyltransferase. *Journal of Medicinal Chemistry*, 53(8):3396-3411.

Kiss, L.s.E. & Soares-da-Silva, P. 2014. Medicinal chemistry of catechol O-methyltransferase (COMT) inhibitors and their therapeutic utility. *Journal of Medicinal Chemistry*, 57(21):8692-8717.

Knowles, J.R. 1991. Enzyme catalysis: not different, just better. *Nature*, 350(6314):121.

Kuhn, D.M., Arthur Jr, R.E., Thomas, D.M. & Elferink, L.A. 1999. Tyrosine hydroxylase is inactivated by catechol-quinones and converted to a redox-cycling quinoprotein: possible relevance to Parkinson's disease. *Journal of Neurochemistry*, 73(3):1309-1317.

Kuntz, I.D. 1992. Structure-Based Strategies for Drug Design and Discovery. *Science*, 257(5073):1078-1082.

Langston, J.W., Irwin, I., Langston, E.B. & Forno, L.S. 1984. 1-Methyl-4-phenylpyridinium ion (MPP+): identification of a metabolite of MPTP, a toxin selective to the substantia nigra. *Neuroscience Letters*, 48(1):87-92.

Learmonth, D.A., Kiss, L.E., Palma, P.N.L., Ferreria, H.D.S. & Silva, P.M.V.A.S.d. 2012. Nitrocatechol derivatives as COMT inhibitors . Patent number: US8168793B2.

Lee, E.S.Y., Chen, H., King, J. & Charlton, C. 2008. The role of 3-O-methyldopa in the side effects of L-dopa. *Neurochemical Research*, 33(3):401-411.

Legoabe, L.J., Petzer, A. & Petzer, J.P. 2014. α-Tetralone derivatives as inhibitors of monoamine oxidase. *Bioorganic & Medicinal Chemistry Letters*, 24(12):2758-2763.

Lerner, C., Masjost, B., Ruf, A., Gramlich, V., Jakob-Roetne, R., Zürcher, G., et al. 2003. Bisubstrate inhibitors for the enzyme catechol-O-methyltransferase (COMT): influence of inhibitor preorganisation and linker length between the two substrate moieties on binding affinity. *Organic & Biomolecular Chemistry*, 1(1):42-49.

Lewinsohn, R., Glover, V. & Sandler, M. 1980. Development of benzylamine oxidase and monoamine oxidase A and B in man. *Biochemical Pharmacology*, 29(9):1221-1230.

Lewitt, P. & Oertel, W.H. 1999. Parkinsons's Disease: The Treatment Options: CRC Press.

LeWitt, P.A. 2015. Levodopa therapy for Parkinson's disease: pharmacokinetics and pharmacodynamics. *Movement Disorders*, 30(1):64-72.

Liccione, J. & Azzaro, A.J. 1988. Different roles for type A and type B monoamine oxidase in regulating synaptic dopamine at D-1 and D-2 receptors associated with adenosine-3′, 5′-cyclic monophosphate (cyclic AMP) formation. *Naunyn-Schmiedeberg's Archives of Pharmacology*, 337(2):151-158.

Lin, J.H., Chen, I.-W., Chiba, M. & Nishime, J.A. 2000. Route-dependent nonlinear pharmacokinetics of a novel HIV protease inhibitor: involvement of enzyme inactivation. *Drug Metabolism and Disposition*, 28(4):460-466.

Lotta, T., Vidgren, J., Tilgmann, C., Ulmanen, I., Melen, K., Julkunen, I., et al. 1995. Kinetics of human soluble and membrane-bound catechol O-methyltransferase: a revised mechanism and description of the thermolabile variant of the enzyme. *Biochemistry*, 34(13):4202-4210.

Luque, J.M., Kwan, S.W., Abell, C.W., Prada, M.D. & Richards, J.G. 1995. Cellular expression of mRNAs encoding monoamine oxidases A and B in the rat central nervous system. *Journal of Comparative Neurology,* 363(4):665-680.

Lyytinen, J., Kaakkola, S., Ahtila, S., Tuomainen, P. & Teräväinen, H. 1997. Simultaneous MAO-B and COMT inhibition in l-dopa-treated patients with parkinson's disease. *Movement Disorders: Official Journal of the Movement Disorder Society*, 12(4):497-505.

Ma, J., Yoshimura, M., Yamashita, E., Nakagawa, A., Ito, A. & Tsukihara, T. 2004. Structure of rat monoamine oxidase A and its specific recognitions for substrates and inhibitors. *Journal of Molecular Biology*, 338(1):103-114.

Männistö, P.T., Tuomainen, P. & Tuominen, R.K. 1992. Different in vivo properties of three new inhibitors of catechol O-methyltransferase in the rat. *British Journal of Pharmacology*, 105(3):569-574.

Markey, S., Johannessen, J., Chiueh, C., Burns, R. & Herkenham, M. 1984. Intraneuronal generation of a pyridinium metabolite may cause drug-induced parkinsonism. *Nature*, 311(5985):464.

Marras, C., Beck, J., Bower, J., Roberts, E., Ritz, B. & Ross, G. 2018. Prevalence of Parkinson's disease across North America. *NPJ Parkinson's Disease*, 4(1):21.

Masson, G., Mestre, D. & Blin, O. 1993. Dopaminergic modulation of visual sensitivity in man. *Fundamental & Clinical Pharmacology*, 7(8):449-463.

McDonald, A.J. 1996. Glutamate and aspartate immunoreactive neurons of the rat basolateral amygdala: colocalization of excitatory amino acids and projections to the limbic circuit. *Journal of Comparative Neurology*, 365(3):367-379.

McGuire, S.O., Ling, Z.D., Lipton, J.W., Sortwell, C.E., Collier, T.J. & Carvey, P.M. 2001. Tumor necrosis factor α is toxic to embryonic mesencephalic dopamine neurons. *Experimental Neurology*, 169(2):219-230.

McRitchie, D., Cartwright, H. & Halliday, G. 1997. Specific A10 dopaminergic nuclei in the midbrain degenerate in Parkinson's disease. *Experimental Neurology*, 144(1):202-213.

Meiser, J., Weindl, D. & Hiller, K. 2013. Complexity of dopamine metabolism. C*ell Communication and Signaling*, 11(34):18.

Meyer, J.H., Ginovart, N., Boovariwala, A., Sagrati, S., Hussey, D., Garcia, A., et al. 2006. Elevated monoamine oxidase a levels in the brain: an explanation for the monoamine imbalance of major depression. *Archives of General Psychiatry*, 63(11):1209-1216.

Milne, G., Nicklaus, M. & Wang, S. 1998. Pharmacophores in drug design and discovery. *SAR and QSAR in Environmental Research*, 9(1-2):23-38.

Moore, R.Y. 2003. Organization of midbrain dopamine systems and the pathophysiology of Parkinson's disease. *Parkinsonism & Related Disorders*, 9:65-71.

Mostert, S., Petzer, A. & Petzer, J.P. 2015. Indanones As High-Potency Reversible Inhibitors of Monoamine Oxidase. *ChemMedChem*, 10(5):862-873.

Mucklow, J. 2000. Martindale: the complete drug reference. *British Journal of Clinical Pharmacology*, 49(6):613-613.

Muguet, D., Broussolle, E. & Chazot, G. 1995. Apomorphine in patients with Parkinson's disease. *Biomedicine & Pharmacotherapy*, 49(4):197-209.

Müller, T. 2008. Role of homocysteine in the treatment of Parkinson's disease. *Expert Review of Neurotherapeutics*, 8(6):957-967.

Müller, T. 2011. Motor complications, levodopa metabolism and progression of Parkinson's disease. *Expert Opinion on Drug Metabolism & Toxicology*, 7(7):847-855.

Müller, T. 2015. Catechol-O-methyltransferase inhibitors in Parkinson’s disease. *Drugs*, 75(2):157-174.

Murphy, M.P. 2009. How mitochondria produce reactive oxygen species. *Biochemical Journal*, 417(1):1-13.

Naoi, M., Maruyama, W., Youdim, M., Yu, P. & Boulton, A. 2003. Anti-apoptotic function of propargylamine inhibitors of type-B monoamine oxidase. *Inflammopharmacology*, 11(2):175-181.

Napolitano, A., Manini, P. & d'Ischia, M. 2011. Oxidation chemistry of catecholamines and neuronal degeneration: an update. *Current Medicinal Chemistry*, 18(12):1832-1845.

Napolitano, A., Pezzella, A. & Prota, G. 1999. New reaction pathways of dopamine under oxidative stress conditions: nonenzymatic iron-assisted conversion to norepinephrine and the neurotoxins 6-hydroxydopamine and 6, 7-dihydroxytetrahydroisoquinoline. *Chemical Research in Toxicology*, 12(11):1090-1097.

Nissinen, E., Lindén, I.-B., Schultz, E., Kaakkola, S., Männistö, P.T. & Pohto, P. 1988. Inhibition of catechol-O-methyltransferase activity by two novel disubstituted catechols in the rat. *European Journal of Pharmacology*, 153(2-3):263-269.

Nord, M., Zsigmond, P., Kullman, A., Årstrand, K. & Dizdar, N. 2010. The effect of peripheral enzyme inhibitors on levodopa concentrations in blood and CSF. *Movement Disorders*, 25(3):363-367.

Nord, M., Zsigmond, P., Kullman, A. & Dizdar, N. 2017. Levodopa Pharmacokinetics in Brain after Both Oral and Intravenous Levodopa in One Patient with Advanced Parkinson's Disease. *Advances in Parkinson's Disease*, 6(02):52.

Norinder, U. & Haeberlein, M. 2002. Computational approaches to the prediction of the blood–brain distribution. *Advanced Drug Delivery Reviews*, 54(3):291-313.

Nuno Palma, P., João Bonifácio, M., Isabel Loureiro, A. & Soares-da-Silva, P. 2012. Computation of the binding affinities of catechol-O-methyltransferase inhibitors: multisubstate relative free energy calculations. *Journal of Computational Chemistry*, 33(9):970-986.

Nutt, J., Woodward, W., Beckner, R., Stone, C., Berggren, K., Carter, J., et al. 1994. Effect of peripheral catechol-O-methyltransferase inhibition on the pharmacokinetics and pharmacodynamics of levodopa in parkinsonian patients. *Neurology*, 44(5):913-913.

Obeso, J.A., Rodriguez-Oroz, M.C., Rodriguez, M., Lanciego, J.L., Artieda, J., Gonzalo, N., et al. 2000. Pathophysiology of the basal ganglia in Parkinson's disease. *Trends in NEUROSCIENCES*, 23:S8-S19.

Ochiai, Y., Itoh, K., Sakurai, E., Adachi, M. & Tanaka, Y. 2006. Substrate selectivity of monoamine oxidase A, monoamine oxidase B, diamine oxidase, and semicarbazide-sensitive amine oxidase in COS-1 expression systems. *Biological and Pharmaceutical Bulletin*, 29(12):2362-2366.

Olanow, C.W., Watts, R.L. & Koller, W.C. 2001. An algorithm (decision tree) for the management of Parkinson's disease: Treatment Guidelines. *Neurology*, 56(suppl 5):S1-S88.

Oldfield, V., Keating, G.M. & Perry, C.M. 2007. Rasagiline. *Drugs*, 67(12):1725-1747.

Olson, E.J., Boeve, B.F. & Silber, M.H. 2000. Rapid eye movement sleep behaviour disorder: demographic, clinical and laboratory findings in 93 cases. *Brain*, 123(2):331-339.

Onofrj, M., Thomas, A., D'Andreamatteo, G., Iacono, D., Luciano, A., Di Rollo, A., et al. 2002. Incidence of RBD and hallucination in patients affected by Parkinson's disease: 8-year follow-up. *Neurological Sciences*, 23(2):s91-s94.

Pardridge, W.M. 2002. Drug and gene targeting to the brain with molecular Trojan horses. N*ature Reviews Drug Discovery*, 1(2):131.

Parker Jr, W.D., Boyson, S.J. & Parks, J.K. 1989. Abnormalities of the electron transport chain in idiopathic Parkinson's disease. *Annals of Neurology: Official Journal of the American Neurological Association and the Child Neurology Society*, 26(6):719-723.

Parkinson, J. 2002. An essay on the shaking palsy. *The Journal of Neuropsychiatry and Clinical Neurosciences*, 14(2):223-236.

Patel, M. 2016. Targeting oxidative stress in central nervous system disorders. *Trends in Pharmacological Sciences*, 37(9):768-778.

Pauling, L. 1948. Nature of forces between large molecules of biological interest. *Nature*, 36:58.

Paulus, W. & Jellinger, K. 1991. The neuropathologic basis of different clinical subgroups of Parkinson's disease. J*ournal of Neuropathology & Experimental Neurology*, 50(6):743-755.

Pham, D.Q. & Nogid, A. 2008. Rotigotine transdermal system for the treatment of Parkinson's disease. *Clinical Therapeutics*, 30(5):813-824.

Photos, A.S. & Server, V.C. Adobe®.

Pich, E.M. & Collo, G. 2015. Pharmacological targeting of dopamine D3 receptors: Possible clinical applications of selective drugs. *European Neuropsychopharmacology*, 25(9):1437-1447.

Polymeropoulos, M.H., Lavedan, C., Leroy, E., Ide, S.E., Dehejia, A., Dutra, A., et al. 1997. Mutation in the α-synuclein gene identified in families with Parkinson's disease. *Science*, 276(5321):2045-2047.

Ponsen, M.M., Stoffers, D., Booij, J., van Eck-Smit, B.L., Wolters, E.C. & Berendse, H.W. 2004. Idiopathic hyposmia as a preclinical sign of Parkinson's disease. *Annals of Neurology: Official Journal of the American Neurological Association and the Child Neurology Society*, 56(2):173-181.

Popa, V.T. 1984. Clinical pharmacology of adrenergic drugs. *Journal of Asthma*, 21(3):183-207.

Porst, H. & Buvat, J. 2008. Standard practice in sexual medicine. 1st ed. USA: John Wiley & Sons.

Porter, C., Watson, L., Titus, D., Totaro, J. & Byer, S. 1962. Inhibition of dopa decarboxylase by the hydrazino analog of α-methyldopa. *Biochemical Pharmacology*, 11(11):1067-1077.

Raab, W. & Gigee, W. 1951. Concentration and Distribution of "Encephalin" in the Brain of Humans, and Animals. *Proceedings of the Society for Experimental Biology and Medicine*, 76(1):97-100.

Radzicka, A. & Wolfenden, R. 1995. Transition state and multisubstrate analog inhibitors. (*in* Methods in enzymology. Elsevier. p. 284-312.)

Rascol, O., Brooks, D.J., Brunt, E.R., Korczyn, A.D., Poewe, W.H. & Stocchi, F. 1998. Ropinirole in the treatment of early Parkinson's disease: a 6-month interim report of a 5-year levodopa-controlled study. *Movement Disorders: Official Journal of the Movement Disorder Society*, 13(1):39-45.

Rascol, O., Brooks, D.J., Korczyn, A.D., De Deyn, P.P., Clarke, C.E. & Lang, A.E. 2000. A five-year study of the incidence of dyskinesia in patients with early Parkinson's disease who were treated with ropinirole or levodopa. N*ew England Journal of Medicine*, 342(20):1484-1491.

Rebrin, I., Geha, R.M., Chen, K. & Shih, J.C. 2001. Effects of carboxyl-terminal truncations on the activity and solubility of human monoamine oxidase B. *Journal of Biological Chemistry*, 276(31):29499-29506.

Reeve, A.K., Krishnan, K.J. & Turnbull, D. 2008. Mitochondrial DNA mutations in disease, aging, and neurodegeneration. *Annals of the New York Academy of Sciences*, 1147(1):21-29.

Rinne, U., Larsen, J., Siden, Å. & Worm-Petersen, J. 1998. Entacapone enhances the response to levodopa in parkinsonian patients with motor fluctuations. *Neurology*, 51(5):1309-1314.

Rinne, U. & Mölsä, P. 1979. Levodopa with benserazide or carbidopa in Parkinson disease. *Neurology*, 29(12):1584-1589.

Rocha, E.M., De Miranda, B. & Sanders, L.H. 2018. Alpha-synuclein: pathology, mitochondrial dysfunction and neuroinflammation in Parkinson's disease. *Neurobiology of Disease*, 109:249-257.

Rocha, J.-F., Falcão, A., Santos, A., Pinto, R., Lopes, N., Nunes, T., et al. 2014. Effect of opicapone and entacapone upon levodopa pharmacokinetics during three daily levodopa administrations. *European Journal of Clinical Pharmacology*, 70(9):1059-1071.

Rose, A.S., Bradley, A.R., Valasatava, Y., Duarte, J.M., Prlić, A. & Rose, P.W. 2018. NGL viewer: web-based molecular graphics for large complexes. *Bioinformatics*, 34(21):3755-3758.

Ruottinen, H. & Rinne, U. 1996. Entacapone prolongs levodopa response in a one month double blind study in parkinsonian patients with levodopa related fluctuations. *Journal of Neurology, neurosurgery & psychiatry*, 60(1):36-40.

Saraste, M. 1999. Oxidative phosphorylation at the fin de siecle. *Science*, 283(5407):1488-1493.

Saura, J., Bleuel, Z., Ulrich, J., Mendelowitsch, A., Chen, K. & Shih, J. 1996. Molecular neuroanatomy of human monoamine oxidases A and B revealed by quantitative enzyme radioautography and in situ hybridization histochemistry. *Neuroscience*, 70(3):755-774.

Schapira, A.H. 2002. Neuroprotection and dopamine agonists. *Neurology*, 58(suppl 1):S9-S18.

Schenkman, J.B., Sligar, S.G. & Cinti, D.L. 1981. Substrate interaction with cytochrome P-450. *Pharmacology & Therapeutics*, 12(1):43-71.

Schwartz, R.S., Halliday, G.M., Cordato, D.J. & Kril, J.J. 2012. Small-vessel disease in patients with Parkinson's disease: a clinicopathological study. *Movement disorders*, 27(12):1506-1512.

Segura-Aguilar, J., Paris, I., Muñoz, P., Ferrari, E., Zecca, L. & Zucca, F.A. 2014. Protective and toxic roles of dopamine in Parkinson's disease. *Journal of Neurochemistry*, 129(6):898-915.

Shih, J., Chen, K. & Ridd, M. 1999. Monoamine oxidase: from genes to behavior. *Annual Review of Neuroscience*, 22(1):197-217.

Shulman, L.M. 1999. Parkinson’s disease: The proper use of dopamine receptor agonists. *Current Treatment Options in Neurology*, 1(1):14-20.

Sian, J., Youdim, M., Riederer, P. & Gerlach, M. 1999. MPTP-induced parkinsonian syndrome. (*in* Basic Neurochemistry: Molecular, Cellular and Medical Aspects. Philidelphia: Lippencot-Raven)

Sies, H. 2015. Oxidative stress: a concept in redox biology and medicine. *Redox Biology*, 4:180-183.

Silverman, R.B. & Holladay, M.W. 2014. The organic chemistry of drug design and drug action. 2nd ed. USA: Academic press.

Smith, K.S., Smith, P.L., Heady, T.N., Trugman, J.M., Harman, W.D. & Macdonald, T.L. 2003. In vitro metabolism of tolcapone to reactive intermediates: relevance to tolcapone liver toxicity. *Chemical Research in Toxicology*, 16(2):123-128.

Son, S.Y., Ma, J., Kondou, Y., Yoshimura, M., Yamashita, E. & Tsukihara, T. 2008. Structure of human monoamine oxidase A at 2.2-Å resolution: the control of opening the entry for substrates/inhibitors. *Proceedings of the National Academy of Sciences*, 105(15):5739-5744.

Spencer, J.P., Jenner, P., Daniel, S.E., Lees, A.J., Marsden, D.C. & Halliwell, B. 1998. Conjugates of catecholamines with cysteine and GSH in Parkinson's disease: possible mechanisms of formation involving reactive oxygen species. *Journal of Neurochemistry*, 71(5):2112-2122.

Spillantini, M.G., Schmidt, M.L., Lee, V.M.-Y., Trojanowski, J.Q., Jakes, R. & Goedert, M. 1997. α-Synuclein in Lewy bodies. *Nature*, 388(6645):839.

Stacy, M. & Silver, D. 2008. Apomorphine for the acute treatment of “off” episodes in Parkinson's disease. *Parkinsonism & Related Disorders*, 14(2):85-92.

Standaert, D.G. & Roberson, E.D. 2015. Treatment of Central Nervous System Degenerative Disorders. (In Brunton, L.L., Chabner, B.A. & Knollmann, B.C., eds. Goodman & Gilman's: The Pharmacological Basis of Therapeutics, 12th ed. New York: McGraw-Hill Education.

Starkov, A.A. 2008. The role of mitochondria in reactive oxygen species metabolism and signaling. *Annals of the New York Academy of Sciences*, 1147(1):37-52.

Stein, R.L. 2011. Kinetics of enzyme action: essential principles for drug hunters. 1st ed. USA: John Wiley & Sons.

Stowe, R., Ives, N., Clarke, C., Ferreira, J., Hawker, R.J. & Shah, L.. 2008. Dopamine agonist therapy in early Parkinson's disease. *The Cochrane Database of Systemic Reviews,* 2:CD006564.

Sun, Y., Zhang, J., Yuan, Y., Yu, X., Shen, Y. & Xu, Q. 2012. Study of a possible role of the monoamine oxidase A (MAOA) gene in paranoid schizophrenia among a Chinese population. *American Journal of Medical Genetics Part B: Neuropsychiatric Genetics*, 159(1):104-111.

Takahasi, T., Yamashita, H., ZHANG, Y.-X. & NAKAMURA, S. 1996. Inhibitory effect of MK-801 on amantadine-induced dopamine release in the rat striatum. *Brain Research Bulletin*, 41(6):363-367.

Tenhunen, J., Salminen, M., Lundström, K., Kiviluoto, T., Savolainen, R. & Ulmanen, I. 1994. Genomic organization of the human catechol O-methyltransferase gene and its expression from two distinct promoters. *European Journal of Biochemistry*, 223(3):1049-1059.

Tipton, K.F., Boyce, S., O'Sullivan, J., Davey, G.P. & Healy, J. 2004. Monoamine oxidases: certainties and uncertainties. *Current Medicinal Chemistry*, 11(15):1965-1982.

Tohgi, H., Abe, T., Kikuchi, T., Takahashi, S. & Nozaki, Y. 1991. The significance of 3-O-methyldopa concentrations in the cerebrospinal fluid in the pathogenesis of wearing-off phenomenon in Parkinson's disease. *Neuroscience Letters*, 132(1):19-22.

Tong, J., Meyer, J.H., Furukawa, Y., Boileau, I., Chang, L.-J., Wilson, A.A., et al. 2013. Distribution of monoamine oxidase proteins in human brain: implications for brain imaging studies. J*ournal of Cerebral Blood Flow & Metabolism*, 33(6):863-871.

Transm, J.N. 1994. Amantadine and memantine are NMDA receptor antagonists with neuroprotective properties. *Journal of Neuronal Transmission*, 43:91-104.

Trifunovic, A. & Larsson, N.G. 2008. Mitochondrial dysfunction as a cause of ageing. *Journal of Internal Medicine*, 263(2):167-178.

Ul Haq, I., Lewitt, P.A. & Fernandez, H.H. 2007. Apomorphine therapy in Parkinson's disease: a review. *Expert Opinion on Pharmacotherapy*, 8(16):2799-2809.

van de Waterbeemd, H., Camenisch, G., Folkers, G., Chretien, J.R. & Raevsky, O.A. 1998. Estimation of blood-brain barrier crossing of drugs using molecular size and shape, and H-bonding descriptors. *Journal of Drug Targeting*, 6(2):151-165.

Vidgren, J., Svensson, L.A. & Liljas, A. 1994. Crystal structure of catechol O-methyltransferase. *Nature*, 368(6469):354.

Viegas-Junior, C., Danuello, A., da Silva Bolzani, V., Barreiro, E.J. & Fraga, C.A.M. 2007. Molecular hybridization: a useful tool in the design of new drug prototypes. *Current Medicinal Chemistry*, 14(17):1829-1852.

Vijayakumar, D. & Jankovic, J. 2016. Drug-induced dyskinesia, part 1: treatment of levodopa-induced dyskinesia. *Drugs*, 76(7):759-777.

Visanji, N.P., Fox, S.H., Johnston, T., Reyes, G., Millan, M.J. & Brotchie, J.M. 2009. Dopamine D3 receptor stimulation underlies the development of L-DOPA-induced dyskinesia in animal models of Parkinson's disease. *Neurobiology of Disease*, 35(2):184-192.

Wharton, C.W. 2013. Molecular enzymology. 1st ed. USA: Springer Science & Business Media.

Whitehead, R.E., Ferrer, J.V., Javitch, J.A. & Justice, J.B. 2001. Reaction of oxidized dopamine with endogenous cysteine residues in the human dopamine transporter. *Journal of Neurochemistry*, 76(4):1242-1251.

Winklhofer, K.F. & Haass, C. 2010. Mitochondrial dysfunction in Parkinson's disease. *Biochimica et Biophysica Acta*, 1802(1):29-44.

Yadav, R., Shukla, G., Goyal, V., Singh, S. & Behari, M. 2012. A case control study of women with Parkinson's disease and their fertility characteristics. *Journal of the Neurological Sciences*, 319(1-2):135-138.

Youdim, M., Finberg, J. & Tipton, K. 1988. Monoamine oxidase. (*in* Trendelenburg, U*., ed.* Catecholamines. USA:Springer. p. 119-192.)

Youdim, M.B. & Bakhle, Y. 2006. Monoamine oxidase: isoforms and inhibitors in Parkinson's disease and depressive illness. *British Journal of Pharmacology*, 147(S1).

Youdim, M.B., Edmondson, D. & Tipton, K.F. 2006. The therapeutic potential of monoamine oxidase inhibitors. *Nature Reviews Neuroscience*, 7(4):295.

Zeldowicz, L. & Huberman, J. 1973. Long-term therapy of Parkinson's disease with amantadine, alone and combined with levodopa. *Canadian Medical Association Journal*, 109(7):588.

Zhai, S., Tanimura, A., Graves, S.M., Shen, W. & Surmeier, D.J. 2018. Striatal synapses, circuits, and Parkinson's disease. *Current Opinion in Neurobiology*, 48:9-16.

Zhu, B.T., Ezell, E.L. & Liehr, J.G. 1994. Catechol-O-methyltransferase-catalyzed rapid O-methylation of mutagenic flavonoids. Metabolic inactivation as a possible reason for their lack of carcinogenicity in vivo. *Journal of Biological Chemistry*, 269(1):292-299.

CHAPTER 3 ARTICLE

3.1 Design, synthesis and biological evaluation of nitrocatechol bearing cyclic chalcones and related analogues as dual MAO/COMT inhibitors.

Mr. AD de Beer, Prof. LJ Legoabe, Prof. JP Petzer, Prof. A Petzer

Keywords:

Monoamine oxidase
Catechol-O-methyltransferase
Parkinson’s disease
Tetralone
Indanone
Dual inhibitors

3.2 Abstract:

Parkinson's disease (PD) is rapidly becoming the leading cause of geriatric disability in the world. This, coupled with an expanding range of aetiologies and theories, is the driving force for the development of new drug therapies. The use of monoamine oxidase (MAO) inhibitors in PD is well established. Since catechol-O-methyltransferase (COMT) inhibitors are also used for the treatment of PD, this study hybridised the moieties of known MAO inhibitors with the acidic nitrocatechol moiety used in commercial COMT inhibitors.

This approach led to the discovery of a bicyclic chalcone, compound **G**, with an IC_{50} value for the inhibition of MAO-B of 7.25 µM, and an IC_{50} value of the inhibition of COMT of 0.567 µM. The use of the chroma-4-one moiety as bicyclic system yielded the most potent MAO-B inhibition and selectivity over MAO-A. The indanone bicyclic system showed the best overall average IC_{50} value. The nitrocatechol chalcones showed good inhibition with the most potent inhibition value (IC_{50}) of 0.163 µM. This study shows that indanone-nitrocatechol hybrid compounds substituted with either the hydroxyl or methoxy groups on the 5-position of the indanone have potential in the future design of dual inhibitors of MAO-B and COMT.

In silico determination via SwissADME shows poor brain penetration but very high absorption from the gastrointestinal tract, which suggests that these compounds may act as peripheral COMT inhibitors for future development as antiparkinsonian drugs.

Keywords: MAO, COMT, Parkinson's disease, chalcone, nitrocatechol, hybrids.

3.3 Introduction

Parkinson's disease (PD) is described as a multi-system, hypokinetic neurodegenerative disorder with the progressive loss of dopamine neurons in the midbrain (Brady *et al.*, 2005). The loss of these dopaminergic neurons gives rise to the known clinical motor symptoms that are used to diagnose PD: resting tremor, stiffness, decreased movement and a loss of balance (Vijayakumar & Jankovic, 2016). For a definitive diagnosis, the following must be present, normally seen in post mortem examinations: intraneuronal inclusions – also known as Lewy bodies – and the loss of dopaminergic neurons in the midbrain and associated structures (Alexander, 2004). Non-motor symptoms such as depression, constipation, psychosis and dementia also aid in the diagnosis (Gelb *et al.*, 1999; Gonzalez-Usigli, 2017). There are several theories and hypotheses on the aetiology of PD which involves oxidative stress, environmental factors, genetic factors, mitochondrial dysfunction, neuroinflammation and gender difference (Alexander, 2004; Bourque *et al.*, 2015; Brady *et al.*, 2005; Dauer & Przedborski, 2003).

Levodopa (L-dopa) is used in PD because, unlike dopamine (DA), it is able to cross the blood-brain barrier (BBB) and can thus be converted to dopamine in the central nervous system (CNS). L-Dopa leads to elevated DA levels in the brain by supplementing endogenous DA levels. The conversion to DA is achieved via the enzyme amino acid decarboxylase (AADC) (Figure 3-1) while DA metabolism occurs via monoamine oxidase (MAO) and catechol-O-methyltransferase (COMT) (Meiser, 2013). Evidence further show that when L-dopa is metabolised peripherally by COMT, the metabolite, 3-O-methyldopa, may compete with L-dopa for active absorption through the BBB (Tohgi *et al.*, 1991).

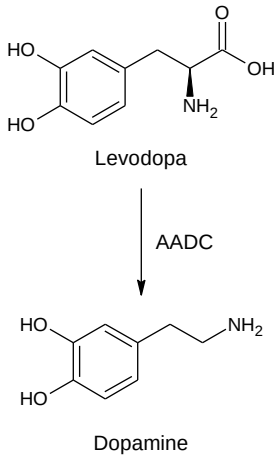

Figure 3-1: Metabolism of L-dopa by AADC

A peripheral AADC inhibitor such as carbidopa or benserazide (Figure 3-2) can reduce the extent of peripheral metabolism of L-dopa. This leads to a higher concentration of L-dopa that is available

to penetrate the brain and that is converted to DA. This is useful as the brain penetration by DA is very low compared to the ability of L-dopa to penetrate the brain (Aminoff, 2004). L-Dopa therapy is prone to an effect called “wearing-off”. “Wearing-off” is associated with a reduced availability of L-dopa to the brain at a specific dosage. This is due to an increased peripheral metabolism of L-dopa (Lee *et al.*, 2008; Nord *et al.*, 2010; Standaert & Roberson, 2015). “Wearing-off” is responsible for most of the challenges with L-dopa therapy such as induced dyskinesia and bradykinesia. For this reason, L-dopa is not used as monotherapy and an AADC inhibitor can dramatically reduce adverse effects associated with L-dopa (Mucklow, 2000). These adverse effects include gastrointestinal irritation, anorexia and orthostatic hypotension (Aminoff, 2004).

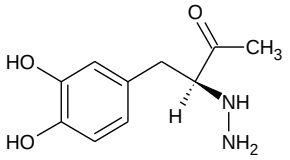

Carbidopa

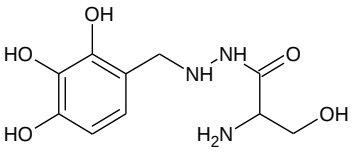

Benserazide

Figure 3-2: Structures of commercially used AADC inhibitors.

The combination of L-dopa with an AADC inhibitor is highly effective in raising DA levels in the brain. However, adverse neurological effects may occur with a sudden increase in central DA levels. Hence controlled dosage increments must be used to achieve a level appropriate for each individual patient (Nord *et al.*, 2017). While DA is increased in the brain by the use of L-dopa and an AADC inhibitor, MAO and COMT inhibitors may also be used as adjunct therapies. MAO and COMT inhibitors decrease the breakdown of striatal dopamine and increase the concentration of usable DA in the striatal cortex (Kaakkola, 2000; Youdim & Bakhle, 2006).

DA degradation catalysed by MAO produces potentially harmful products such as hydrogen peroxide and 3,4-dihydroxyacetaldehyde (DOPAL) (Carlsson *et al.*, 1957; Meiser, 2013; Tohgi *et al.*, 1991). Several reactive oxygen species (ROS) are produced in the complex metabolism of DA and these species may have a further degenerative effect on neurons (Segura-Aguilar *et al.*, 2014).

MAO is an enzyme mostly found on the outer membrane of the mitochondria, and catalyses the deamination of several neurotransmitters including noradrenaline, serotonin and dopamine (Son *et al.*, 2008). This reaction produces a corresponding aldehyde, hydrogen peroxide and either ammonia or a substituted amine (Youdim *et al.*, 2006). MAO is present as two isoforms, MAO-A and MAO-B, with different substrate and inhibitor specificities (Shih *et al.*, 1999; Tipton *et al.*, 2004). MAO-A inhibitors are used for the treatment of anxiety and depression (Aminoff, 2004), whereas MAO-B inhibitors are used for the treatment of PD (Collins *et al.*, 1970). MAO inhibitors are considered as useful drugs although adverse effects, especially with the use of irreversible inhibitors have been reported. The earliest known inhibitor of MAO was the tuberculosis drug, isoniazid. The related compound, iproniazid, became the first commercially used MAO inhibitor used in depressive illness. However, severe liver toxicity led to the removal of the drug from the market. It was postulated that the hydrazine structure of this drug is linked to the observed toxicity (Figure 3-2) (Fagervall & Ross, 1986; Youdim *et al.*, 1988; Youdim & Bakhle, 2006).

After the development of a non-hydrazine drug, namely tranylcypromine, a new adverse effect was noticed, the “cheese effect”. The “cheese effect” is a severe hypertensive reaction to an excess of tyramine in the system. The excess tyramine cannot be metabolised by MAO-A due to inhibition by tranylcypromine. Tyramine enhances the physiological response to the sympathomimetic effects of noradrenaline, and thus may induce severe hypertension, which may be fatal (Fišar, 2016; Gottwald *et al.*, 1997; Youdim & Bakhle, 2006). This effect is mainly seen in non-selective irreversible inhibitors (Liccione & Azzaro, 1988).

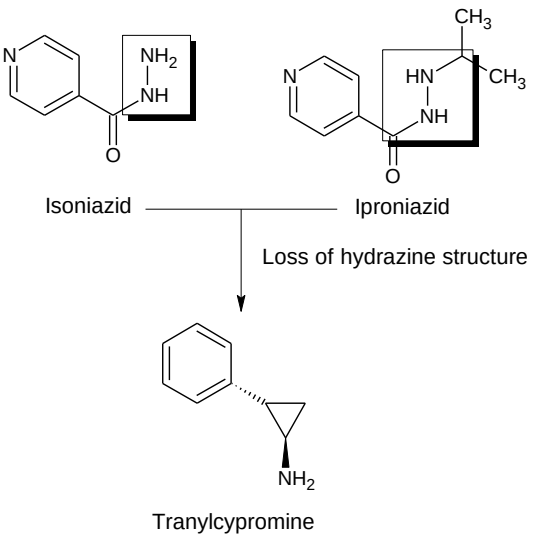

Figure 3-3: MAO inhibitors as discussed in text.

COMT is an intracellular enzyme that catalyses the transfer of an activated methyl group from S-adenosyl-L-methionine to one of the hydroxyl groups in a catechol neurotransmitter (Kaakkola,

2000; Vidgren *et al.*, 1994). The enzyme exists as two forms: a 221-residues soluble protein, mostly in the cytosol of the cells, and as a membrane-bound protein with 50 extra residues at the N-terminus (Backstrom *et al.*, 1989; Bai *et al.*, 2007; Huh & Friedhoff, 1979; Tenhunen *et al.*, 1994). The nitro-substituted catechol derivatives are well-known inhibitors of COMT, and these compounds represent the most potent COMT inhibitors (Backstrom *et al.*, 1989). The reaction of catechol breakdown can be inhibited by acidic nitrocatechol containing drugs including clinically used tolcapone and entacapone (Ehler *et al.*, 2014).

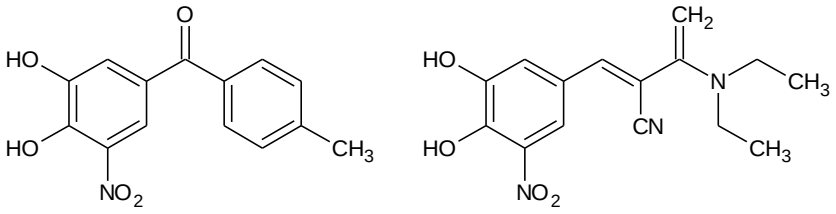

Tolcapone Entacapone

Figure 3-4: COMT inhibitors discussed in text.

3.3.1 Dual inhibition of COMT and MAO

In a study involving MPTP-treated mice, researchers investigated the synergistic effects of L-dopa with COMT and MAO inhibitors. Following treatment with both COMT and MAO inhibitors, the animal models showed decreased akinesia and an increase in overall movement compared to the control group. Decreased DA metabolism was observed in the autopsies performed post-experiment (Fredriksson & Archer, 1995). In a double blind, placebo controlled cross over study in 1997, further investigation of dual inhibition of both MAO and COMT was done by using selegiline as the MAO inhibitor and entacapone as the COMT inhibitor. The findings showed that the inhibition of both enzymes increased the half-life of L-dopa and decreased the amount of 3-OMD that forms, thus increasing the brain penetration of L-dopa. The use of dual inhibitors can possibly direct catechol metabolism down other pathways that can induce different side effects not associated with known side effect profiles of these compounds (Lyytinen *et al.*, 1997). A later study showed that motor symptoms improve with dual MAO-B/COMT inhibition, especially in the "wear-off" times of L-dopa therapy (Rinne & Mölsä, 1979; Ruottinen & Rinne, 1996).

3.3.2 Molecular hybridisation and lead structure

Selecting a structure to synthesise can be a daunting task, but by using approaches such as molecular hybridisation and lead discovery, one is able to hypothesise a possible combination of effective substituents that may be added to a pharmacophore to produce targeted activity (Viegas-Junior *et al.*, 2007). Lead discovery is the process of considering the natural occurring substrate

for the enzyme/receptor in question, and reducing it to the smallest active configuration, the *pharmacophore*, which is the minimum structural features needed for enzyme binding (Milne *et al.*, 1998). To assure the possibility of a good match, novel compounds must be structurally and chemically compliant to the natural substrate. In the case of MAO, DA is the natural substrate (Dean, 1988). Upon the identification of the lead pharmacophore, one can consider existing drugs and use the method of molecular hybridisation to proposed plausible bioactive derivatives. Two strategies exists: 1) the development of new ligands by the fusion of two pharmacophoric sub-structures, and this fusion leads to the forming of a new hybrid structure that maintain the characteristics of the pre-selected templates (Kuntz, 1992; Viegas-Junior *et al.*, 2007); 2) the use of two pharmacophoric entities and a linker to merge the entities as a new chemical compound (Fraga, 2009).

Chalcones are very interesting chemical scaffolds and are found in large array of structures with many possible uses. Although in theory chalcones can occur in either *E*- or *Z*-configuration, it was reported that *E*-configuration is favourable on a thermodynamic basis due to steric interaction between the aryl and carbonyl groups in case of the *Z*-isomers. Indeed, in previous studies it was found that most synthetic chalcones occur in that *E*-configuration (Chimenti *et al.,* 2009). With two aromatic rings, there is a large possible number of replaceable hydrogens that can be used to synthesise a large variety of derivatives (Gomes *et al.*, 2017).

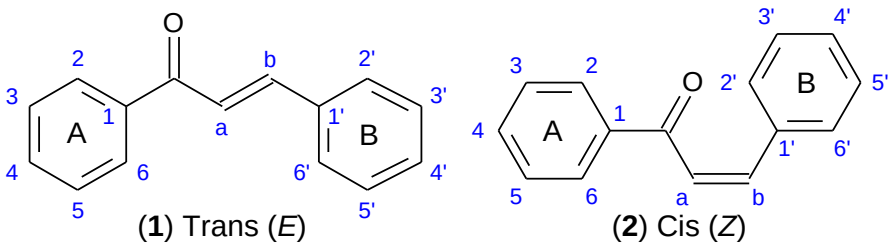

Figure 3-5: Structural representations of the chalcone scaffold (Gomes *et al.*, 2017).

Studies showed that α-tetralones are promising MAO-inhibitors with average IC_{50} values of 14.8 ± 2.12 µM for MAO-A and 18.6 ± 1.58 µM for MAO-B (Legoabe *et al.*, 2014). Furthermore, indanone analogues are also MAO inhibitors with average IC_{50} values of 64.7 ± 4.28 µM for MAO-A and 85.4 ± 5.82 µM for MAO-B (Medvedev *et al.*, 1995; Mostert *et al.*, 2015). Based on these reports, the present study uses the chalcone structure as lead to produce the corresponding ring-closed tetralone and indanone analogues.

Compounds bearing nitrocatechol moiety that have been associated with high potency COMT inhibition, and this activity is attributed to nitrocatechol moiety. (Kiss & Soares-da-Silva, 2014). In

addition, previous studies reported MAO inhibitors that bears the nitrocatechol (Tripathi *et al*., 2018), which suggest that if appropriately done its hybridisation with known MAO inhibitors will not lead to loss of activity for either enzyme target

Based on the aforementioned findings, we envisage that appropriate hybridising of ring-closed chalcone and nitrocatechol moieties will lead to compounds with dual MAO-B/COMT inhibitory properties as seen in Figure 3-6.

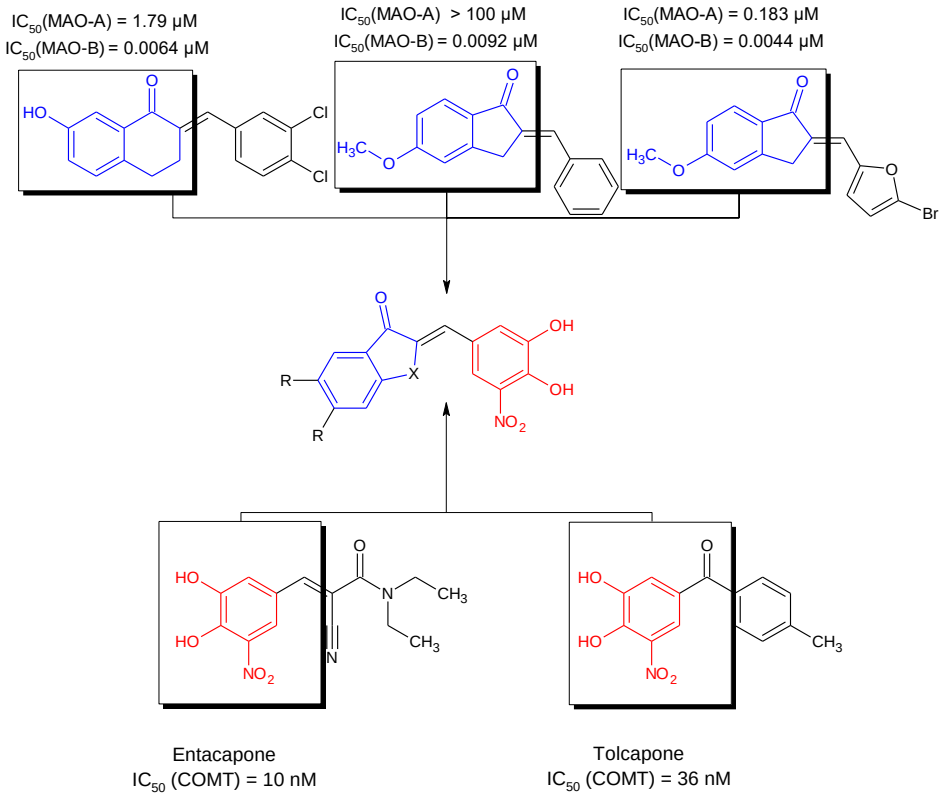

Figure 3-6: Design approach for dual-target-directed MAO and COMT inhibitors

3.4 Results and Discussion:

3.4.1 Chemistry

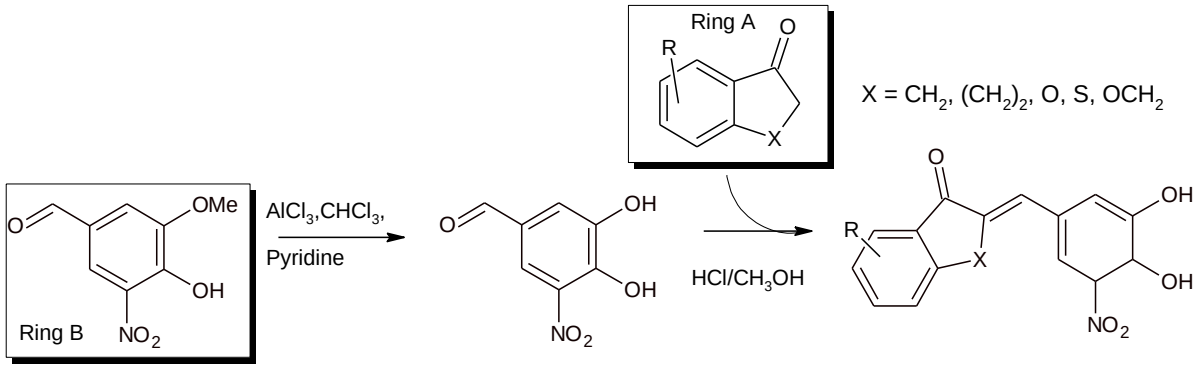

Figure 3-7: General synthesis route of chalcones A-T.

This study synthesised ring-closed tetralone and indanone analogues of chalcone in an attempt to discover dual-target-directed MAO and COMT inhibitors. As shown in Figure 3-7, the first step was to demethylate 5-nitrovanillin by treatment with a mixture of aluminium chloride in chloroform and pyridine. The aldehyde produced was isolated by ethyl acetate extraction and hot filtration with boiling toluene, and was subsequently combined with derivatives of indanone, tetralone or acetophenone to produce the corresponding chalcone. The chalcones were synthesised with the Claisen-Schmidt condensation in acidic conditions (32% HCl). The reactions were monitored by TLC using petroleum ether and ethyl acetate (1:1) as mobile phase. After 24-26 h reflux, the chalcone precipitated when treated with ice cold water. The yields that were obtained were good, ranging between 77 and 91%.

The collected final products were dried and characterised by NMR, MS and HPLC.

Table 3-1: Final compound characterisation.

Compound	**Molecular formula**	**HPLC Purity**	**MS (APCI-HRMS) (g.mol^{-1})**		
			Calc. (MH^+)	Found	ppm
A	$C_{16}H_{11}NO_5$	98.9%	298.0709	298.0734	8.39
B	$C_{18}H_{12}NO_7$	95%	358.0921	358.0924	0.84
C	$C_{17}H_{11}NO_7$	N.A.	342.0608	342.0611	0.87
D	$C_{16}H_{11}NO_6$	94.3%	328.0815	328.0823	2.44
E	$C_{15}H_9NO_7$	98.7%	316.0451	316.0450	-0.32
F	$C_{16}H_{11}NO_6$	99.7%	314.0659	314.0662	0.96
G	$C_{16}H_{11}NO_6$	99.5%	314.0659	314.0656	-0.96
H	$C_{16}H_{15}NO_6S$	100%	330.0438	330.0430	-2.42
I	$C_{17}H_{13}NO_5$	100%	312.0866	312.0884	5.77
J	$C_{19}H_{17}NO_7$	95.4%	372.1077	372.1073	-1.07
K	$C_{18}H_{15}NO_6$	99.5%	342.0972	342.0973	0.29
L	$C_{18}H_{15}NO_6$	98.8%	342.0972	342.0977	1.46
M	$C_{18}H_{15}NO_6$	100%	342.0972	342.0973	0.29
N	$C_{17}H_{14}N_2O_5$	98.3%	327.0975	327.0978	0.92
O	$C_{15}H_{11}NO_5$	96.5%	286.0709	286.0717	2.79
Q	$C_{15}H_{10}BrNO_5$	97.7%	363.9815	363.9805	-2.75

S	$C_{15}H_9BrFNO_5$	91%	381.972	338.022	N.A.
T	$C_{16}H_9BrN_2O_5$	N.A.	388.976	389.051	N.A.

As seen in table 3-1, the synthesised compounds were characterised by MS and the purity was determined by HPLC. A majority of the compounds showed purity > 91%. The purities of compounds **C** and **T** could not be determined since these compounds are too poorly soluble in methanol and acetonitrile. Both ethanol and acetone were considered, but stability studies were not considered in the scope of this study. All MS data correlate with the proposed structures of the synthesised compounds, with the exception to compound **S**. A possible explanation for this discrepancy could be due to inappropriate storage of the compound, which could lead to degradation, as a significant period of time elapsed between final synthesis and characterisation. For most compounds, the ppm values were <5 ppm, which indicate good agreement between the calculated and experimentally determined molecular weights.

The structures were also characterised by ^{1}H and ^{13}C NMR. DMSO-*d6* was used as NMR solvent. As example, the NMR data of compound **A** will briefly be discussed. In the NMR of compound **A** (figure 3-8), the vinilic hydrogen at C10 is represented by the signal at 7.42 ppm (s, 1H). Since the NMR spectrum shows the presence of only one isomer, it is postulated that this compound is in the *trans* conformation (Perjési *et al.,* 2004). The two protons on C1 are represented by the signal at 4.07 ppm (s, 2H). For compounds with a methoxy at C7, the C7 methoxy protons are represented by the signal at 3.82 ppm (s, 3H) while the C8 methoxy protons are represented by the signal at 3.90 ppm (s, 3H). The catechol hydrogens, on C13 and C14, shows as a broad signal at 10.69 ppm (s, 2H). The six aromatic protons are represented by signals at 7.51 – 7.46 (2H), 7.70 (2H) and 7.76 ppm (2H). These catechol hydrogens were used as reference for the integration of protons of the rest of the structure. The ^{13}C NMR spectrum shows the carbonyl carbon signal (C10) at 193.15 ppm, and the indanone carbon signal (C1) at 31.75 ppm. The aromatic and vinilic carbons are represented by 14 signals: 118.07, 120.23, 123.63, 125.51, 126.74, 127.79, 131.47, 134.26, 134.94, 137.23, 137.83, 142.99, 147.88 and 149.83 ppm.

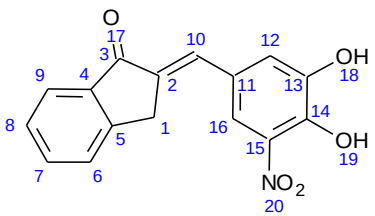

Figure 3-8: Compound A

For the unsubstituted tetralone derivative **I** (figure 3-9), the ^{1}H NMR shows the signals of the C1 and C2 hydrogens at 2.90 ppm (t, *J* = 6.2 Hz, 2H) and 3.03 ppm (t, *J* = 6.1 Hz, 2H), respectively. As expected these signals are two sets of triplets. The C12 vinilic proton is represented by the signal at 7.22 (s, 1H). The six aromatic protons are represented by signals at 7.39 - 7.32 (2H), 7.47 (1H), 7.54 (2H) and 7.90 ppm (1H). The catechol hydrogens are not found on the ^{1}H NMR spectrum, and likely overlap with the signals of water or DMSO-*d6*. The ^{13}C NMR spectrum shows the signals of C1 and C2 at 27.02 and 28.18 ppm, respectively. The carbonyl carbon of C5 is represented by the signal at 187.28, while the 14 aromatic and vinilic carbons are signals at: 117.15, 120.88, 126.14, 127.58, 127.87, 129.05, 133.14, 134.21, 134.65, 135.65, 137.68, 142.76, 143.85 and 148.00 ppm.

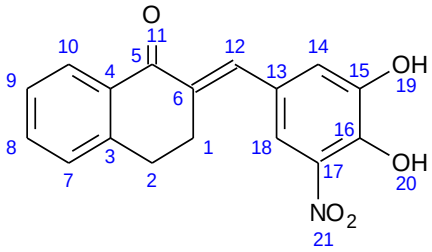

Figure 3-9: Compound I

3.4.1.1 MAO inhibition

The IC_{50} values for the inhibition of MAO-A and MAO-B were measured using the commercially available recombinant human enzymes. Kynuramine served as substrate for the measurement of enzyme catalytic rates for both isoforms of the MAO enzyme (Weissbach *et. al*., 1960). Kynuramine is oxidised by the MAOs to yield 4-hydroxyquinoline, which can conveniently be measured by fluorescence spectrophotometry.

The reaction shown in Figure 3-10 gives the reaction kynuramine undergo in the presence of MAO.

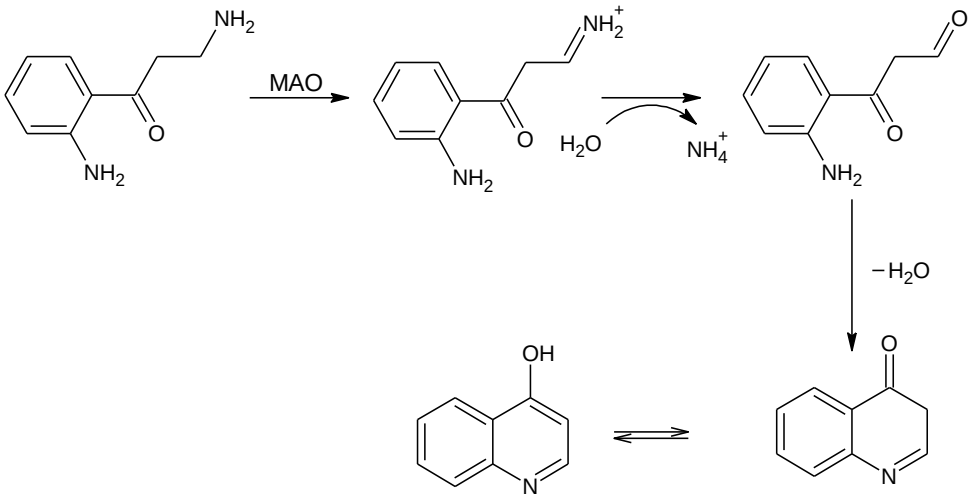

Figure 3-10: The formation of 4-hydroxyquinolone in the presence of MAO

The IC_{50} values of compounds **A**–**T** for the inhibition of MAO are shown in Table 3-2. As expected the chalcones exhibited MAO inhibitory activity although with low potencies. The IC_{50} values are > 30.34 µM for MAO-A, and > 7.25 µM for MAO-B.

Structure-activity relationships are important for novel compounds, and may explain certain aspects of the interaction of the molecules and the drug target. The indanone based chalcones (compounds **A**-**F**) showed relatively good inhibitory activity. Compound **B** showed a drastic reduction in activity for MAO-B (IC_{50} = 60.48 µM), and when compared to compound **D** (IC_{50} = 14.18 µM) showed that the monomethoxy substituent has the better activity. For the methylenedioxy compound, compound **C**, increased activity (IC_{50} = 24.2 µM) was observed, suggesting that dimethoxy substitution of compound **B** causes steric hindrance in the active site. The use of the monomethoxy in compound **D** was explored further in compound **F**, and resulted in a slight reduction in activity (IC_{50} = 15.04 µM) when the methoxy was substituted with a hydroxy group. This suggests that the active site of MAO-B is more lipophilic than polar. Compound **E** supports this hypothesis since the activity decreases further (IC_{50} = 17.34 µM) when the indanone is replaced by the benzofuranone. The activity of compound **A** (IC_{50} = 20.7 µM) shows that in general monosubstitution on the A-ring with either hydroxyl or methoxy increases MAO-B inhibition activity (compare **A** with **D** and **F**).

The tetralone derivatives (compound **G**-**N**) yielded of the more potent MAO-B inhibitors in the series, and in general the activity decreased as the molar mass increased. The most potent MAO inhibitor was found to be compound **G** with an IC_{50} value of 7.26 µM for MAO-B. Compound **G** also shows the highest degree of specificity towards MAO-B with an SI value of 6.33. Compound **G**, a chromanone derivative, thus exhibited the most potent MAO-B inhibition activity, which

suggests that the ether oxygen in in the ring system may be involved in productive interactions with the MAO-B active site. This is supported by the observation that replacement of the oxygen (compound **G**) by sulphur (compound **H**) led to significant decrease in MAO-B inhibition activity. When these results are compared to the unsubstituted compound **I**, it may be concluded that the addition of an oxygen in the tetralone ring can increase the MAO-B inhibition activity overall.

The second most potent MAO-B inhibitor was compound **L** with an IC_{50} of 7.83 µM. Compound **L**, which has a methoxy substituent at position 5 on the tetralone moiety, exhibited good inhibition activity (IC_{50} = 7.83 µM) against MAO-B. Substitution with a methoxy on position 7 (compound **M**) yielded slightly lower activity (IC_{50} = 11.0 µM), while substitution with a methoxy on position 6 (compound **K**) yielded a drastic reduction in activity (IC_{50} = 29.6 µM). Disubstitution with methoxy groups on positions 6 and 7 yielded compound **J**, which exhibited a further decrease in MAO-B inhibition activity (IC_{50} = 45.9 µM) compared to the corresponding monosubstituted analogues. Substitution of the methoxy group for an amine group (compound **N**) also slightly enhanced MAO-B inhibition (compare with **K**).

The open-chained chalcones (compounds **O**-**T**) showed overall reduction in MAO-B inhibition potency. The use of two halogen substituents in compound **S** resulted in the most potent MAO-B inhibition activity with an IC_{50} value of 16.3 µM. Compound **O** shows that unsubstituted chalcones has low potency, and by adding electron withdrawing groups on the unsaturated (enone) system (compounds **Q**, **T** and **S**) an increase in activity was observed, with all three compounds possessing a bromine on the enone system.

While the goal of this study was to discover dual-target-directed COMT/MAO-B inhibitors, the study compounds were also evaluated as MAO-A inhibitors. The results show that only compounds **B, E** and **J** are selective towards MAO-A. The most potent inhibition of MAO-A was achieved with compound **D** with an IC_{50} = 29.4 µM. Overall the compounds showed less potent MAO-A inhibition compared to MAO-B inhibition, which may be expected since chalcones are known to be MAO-B specific inhibitors. The use of the highly polar nitrocatechol group may further limit MAO-A inhibition. The weak inhibition of MAO-A observed with some compounds could, however, be useful in alleviating non-motor symptoms of PD such as depression. Since the MAO-B inhibitory properties would treat the motor symptoms, compounds such as **D** that inhibit both MAO-A and MAO-B (although weakly) may possess multiple mechanisms relevant to PD.

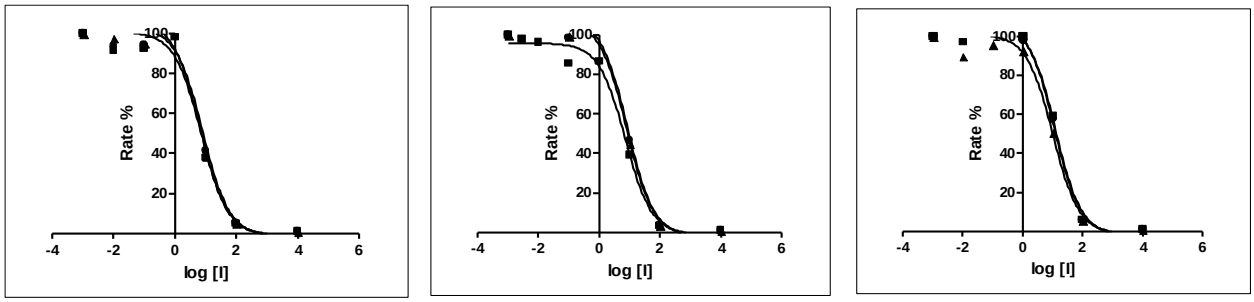

Compound **G** Compound **L** Compound **H**

Figure 3-11: Sigmoidal inhibitory plots for MAO-B inhibition by compounds G, L and H.

3.4.1.2 COMT inhibition

COMT activity was measured using esculetin (6,7-dihydroxycoumarin) as substrate. The reaction that takes place between COMT and esculetin is presented in Figure 3-12. Esculetin is methylated when the hydroxyl groups binds with the Mg^{2+} of COMT and an activated methyl group is transferred from S-adenosyl-L-methionine (SAM). SAM is subsequently converted to s-adenosyl-L-homocysteine (SAH), while esculetin is converted to scopoletin. The formation of scopoletin may be monitored by fluorescence spectrophotometry (Müller, 2008). In the enzyme SAM (5 mM) is added to aid in the forward reaction and ensure the enzyme's natural SAM is not depleted.

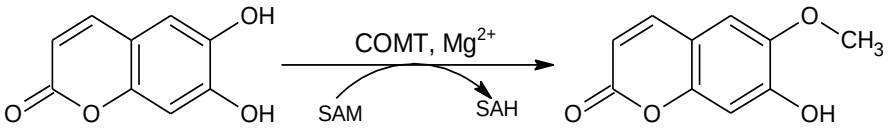

Figure 3-12: The formation of scopoletin from esculetin via COMT

In this study tolcapone was used as reference COMT inhibitor, and exhibits IC_{50} value of 0.26 µM for the inhibition of COMT (Engelbrecht *et al.*, 2018). The indanone derivatives (compounds **A**-**F**) showed similar inhibitory activities, with compound **F** being the least potent with an IC_{50} value of 0.37 µM. Compound **C** showed the best activity with an IC_{50} value of 0.162 µM, while compound **D** (IC_{50} = 0.166 µM) and compound **E** (IC_{50} = 0.188 µM) were also potent COMT inhibitors. These compounds are structurally related and have either a hydroxy or methoxy group on the 5-position. Compound **B**, with dimethoxy substitution also is a potent inhibitor, but with lower activity compared to the other compounds in the indanone class.

For the tetralone derivatives, (compounds **G**-**N**), *meta* substitution with a methoxy group, as seen with compound **L** yields enhanced COMT inhibition, whereas substitution in the *para* and *ortho* positions yields lower inhibition activity as seen with compounds **K** and **M**. The addition of an amino group on the 5-position resulted in a drastic decrease of activity (compound **N** with an IC_{50} value of 1.92 µM). Compounds **G** and **H**, also showed drastic reduction in activity, indicating that the addition of either an oxygen or sulphur group within the tetralone ring has a negative effect on COMT inhibition.

It is noteworthy that the indanone compound **A** is a more potent COMT inhibitor compared to tetralone compound **I**, showing that without ring substitution, the indanone scaffolds has better COMT inhibition activity than the tetralone derived compounds. The unsubstituted open chain chalcone, compound **O**, showed a further decrease in activity with an IC_{50} value of 0.897 µM, indicating that either the lack of the bicyclic system or the change in molecular weight can result in different COMT inhibition values.

The open chain chalcones in general were the least active COMT inhibitors with compound **T** showing the best activity at 0.41 µM. The relatively good potency of **T** may be due to the addition of the nitrile group as an electron withdrawing group. The addition of a halogen in the enone system showed little to no change in COMT inhibition activity (compounds **Q** and **S**).

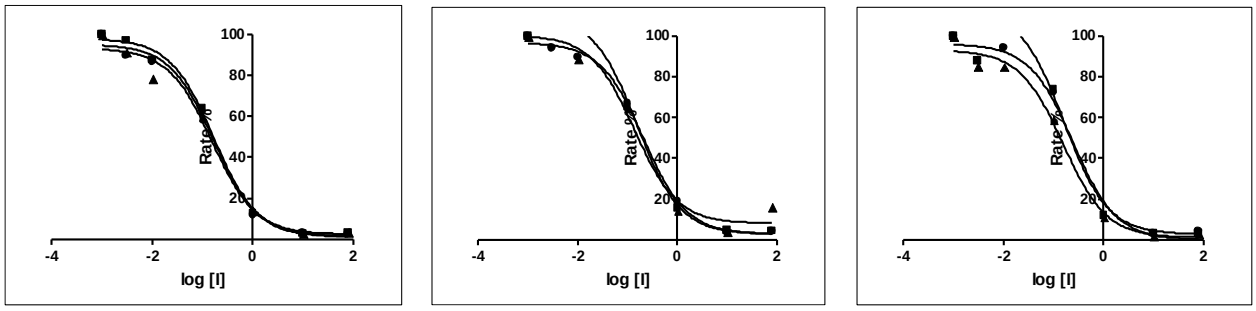

Compound **C** Compound **D** Compound **E**

Figure 3-13: Sigmoidal inhibitory plots for COMT inhibition by compounds C, D and E.

Table 3-2: IC_{50} Values (μM) for the inhibition of MAO and COMT by indanone and tetralone derivatives.

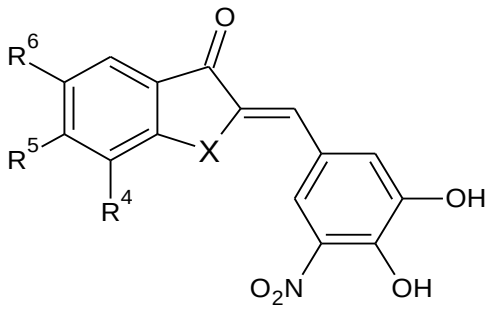

Compound	X	R^4	R^5	R^6	IC_{50} (μM)[a]			SI[b]
					MAO-A	MAO-B	COMT	
Toloxatone					3.92[C]	-	-	-
Lazabemide					-	0.091[C]	-	-
Tolcapone					-	-	0.26[D]	-
A	$-CH_2-$	-H	-H	-H	34. 3 ± 3.19	20.7 ± 0.96	0.21 ± 0.06	1.66
B	$-CH_2-$	-H	$-OCH_3$	$-OCH_3$	37.4 ± 0.247	60.5 ± 4.74	0.21 ± 0.03	0.62
C	$-CH_2-$	-H	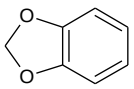		47.0 ± 6.43	24.2 ± 3.56	0.16 ± 0.007	1.94
D	$-CH_2-$	-H	$-OCH_3$	-H	29.4 ± 2.42	14.2 ± 2.73	0.167 ± 0.04	2.08
E	-O-	-H	-OH	-H	41.8 ± 5.72	17.3 ± 0.98	0.19 ± 0.05	0.27
F	$-CH_2-$	-H	-OH	-H	32.7 ± 1.26	15.0 ± 0.39	0.38 ± 0.072	2.17
G	$-OCH_2-$	-H	-H	-H	46.0 ± 5.26	7.26 ± 0.65	0.57 ± 0.05	6.3
H	$-SCH_2-$	-H	-H	-H	32.5 ± 3.37	11.2 ± 1.10	1.69 ± 0.29	2.9
I	$-(CH_2)_2-$	-H	-H	-H	42.3 ± 2.71	15.4 ± 0.64	0.46 ± 0.06	2.75
J	$-(CH_2)_2-$	-H	$-OCH_3$	$-OCH_3$	37.9 ± 1.09	45.9 ± 1.93	0.37 ± 0.07	0.83

K	-$(CH_2)_2$-	-H	-OCH_3	-H	36.6 ± 3.38	29.6 ± 2.31	0.79 ± 0.07	1.24
L	-$(CH_2)_2$-	-OCH_3	-H	-H	37.4 ± 0.98	7.83 ± 0.63	0.42 ± 0.18	4.78
M	-$(CH_2)_2$-	-H	-H	-OCH_3	30.3 ± 1.93	11.0 ± 0.31	0.71 ± 0.09	2.75
N	-$(CH_2)_2$-	-H	-NH_2	-H	53.1 ± 3.19	27.6 ± 1.45	0.24 ± 0.05	1.92

[A]All values expressed as mean ± SD of triplicate determinations.
[B]Selectivity Index [SI = IC_{50}(MAO-A)/IC_{50}(MAO-B)].
[C]Taken from (Petzer *et al.*, 2014)
[D]Taken from (Engelbrecht *et al*, 2018).

Table 3-3: IC_{50} Values (µM) for the inhibition of MAO and COMT by the open chain and α-substituted chalcones.

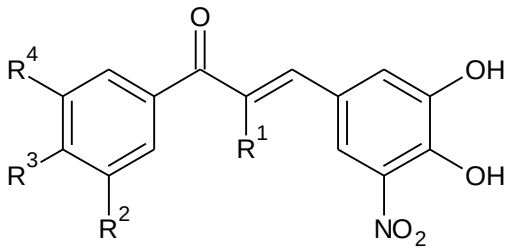

Compound	**R^1**	**R^2**	**R^3**	**R^4**	**IC_{50} (µM)[a]**			**SI[b]**
					MAO-A	MAO-B	COMT	
O	-H	-H	-H	-H	42.5 ± 3.35	39.8 ± 4.93	0.89 ± 0.25	1.1
Q	-Br	-H	-H	-H	48.6 ± 0.66	18.0 ± 4.01	0.91 ± 0.14	2.7
S	-Br	-H	-F	-H	49.9 ± 3.26	16.3 ± 1.13	0.59 ± 0.06	3.1
T	-Br	-NC	-H	-H	42.0 ± 2.58	28.5 ± 1.85	0.41 ± 0.03	1.5

[A]All values expressed as mean ± SD of triplicate determinations.
[B]Selectivity Index [SI = IC_{50}(MAO-A)/IC_{50}(MAO-B)].

3.4.2 Physicochemical properties and *in silico* brain penetration

Central nervous system CNS treatment is the second largest area of pharmacotherapy next to cardiovascular disease (Silva *et al*., 2015). The main route CNS drugs take to enter the brain is through the BBB. The BBB consists of the microcapillary blood vessels that are in close proximity to brain cells that carry oxygen and nutrients to brain cells, and waste products from the brain. The total area of the BBB is estimated to be over 12 m^2 and the length to be over 400 miles (±

625 km) (Pardridge, 2001). The BBB is composed of endothelial cells that form a single cell lining on the inner surface of the capillaries (Allt & Lawrenson, 2001). The endothelial layer has several mechanisms that either hinder or promote diffusion of the CNS drugs into the brain including transcellular passive diffusion, efflux and influx as well as paracellular transport (Pardridge, 2005).

Transcellular passive diffusion is the normal Brownian movement observed when the drug moves from a high concentration to a low concentration over a selective permeable membrane (Fischer *et al*., 1998). Passive diffusion is mostly limited by the physiochemical characteristics of the molecule in question. There is a general correlation between the structure of the molecule and the rate of passive diffusion. The most important structural features that determine BBB permeability are the number of hydrogen bonds, lipophilicity, polar surface area (PSA), molecular weight (MW) and acidity.

There exists a set of rules that may be used to evaluate the possibility of BBB penetration. Pardridge suggested the following (Pardridge, 1998):

- Hydrogen bonds (total) < 8 – 10
- MW < 400 – 500
- No acids
- Spranklin suggests H-bond donors < 2 and H-bond receptors < 6 (Maurer *et al*., 2005).

Another set of rules were compiled by Clark (2001) and Lobell *et. al.* (2003):

- Nitrogen + Oxygen < 6
- PSA < 60 – 70 $Å^2$
- MW < 450
- LogD between 1 – 3
- cLogP – (N + O) > 0

These are only guidelines, as there are molecules that do not abide by these rules, but are still active in the CNS (Bodor & Buchwald, 2003).

Influx and efflux are the active uptake or elimination of drugs, respectively. Influx is determined by a drug's structure and substrates for uptake transport are usually amino acid, peptides or glucose transporters. Efflux is the removal of drugs in the endothelial lining, before brain penetration can take place. This occurs via a P-glycoprotein system (Pgp) (Maurer *et al*., 2005). These Pgp-efflux transporters use ATP to transport a wide array of lipid-soluble compounds from

the CNS back into the capillary space. These transporters protect the brain tissue from potentially neurotoxic molecules, either endogenous or xenobiotic in nature, and detoxify the brain (Dallas et al., 2006).

Paracellular transport is the passive transport of molecule through spaces known as tight junctions that runs between the endothelial cells (Begley *et al*., 2008). The brain endothelial cells lack the abundance of tight junctions, thus transport via this route is limited (Graff & Pollack, 2004). Evidence suggests that in neurodegenerative disease with a prevalence of neuroinflammation, these tight junctions become more abundant due to inflammation processes in the brain, and can contribute to the permeation of toxins and drugs into the brain (Alexander, 2004; Patel, 2016; Sies, 2015).

3.4.2.1 Brain penetration *in silico* methods

Drug discovery is a time consuming and resource demanding process. Large amounts of synthesised and designed molecules must be tested against various parameters to ensure patient safety and therapeutic effectiveness. The use of *in silico* methods are inexpensive and time saving as they need less input to run and no added cost. These computer models uses parameters set up by various researchers to determine key physiochemical characteristics and to predict the ADME (absorption, distribution, metabolism and excretion) profile (Tian *et al*., 2015). However, most computational methods focus on one specific property, whereas the SwissADME tool, provided by the Swiss Institute of Informatics, is a free platform used to evaluate compounds against wide variety of parameters. These include ligand-based virtual screening, biotarget prediction, molecular docking, bio-isosteric design, molecular mechanics, ADME and pharmacokinetics (Cheng *et al*., 2012; Daina *et al*., 2014; Daina & Zoete, 2016; Gfeller *et al*., 2014; Grosdidier *et al*., 2011; Pires *et al*., 2015; Wirth *et al*., 2012; Zoete *et al*., 2011; Zoete *et al*., 2016).

The SwissADME tool was applied in this study to predict the brain penetration of several nitrocatechol compounds that were investigated in this study.

Brain penetration in SwissADME was calculated by the following guidelines: Chemical structure and certain physiochemical attributes are used to produce a bioavailability radar, which uses lipophilicity (Arnott & Planey, 2012; Pliška *et al*., 1996), size, polarity, solubility (Ali *et al*., 2012; Delaney, 2004), flexibility and saturation to produce a plot which shows whether a compound is considered drug-like (Lovering *et al*., 2009; Ritchie *et al*., 2011). These, coupled with attributes such as molecular weight, molecular refractivity and polar surface area (calculated as the topographic polar surface area, with sulphur and phosphorous seen as polar groups) are used to

predict biological barrier permeation, specifically gastrointestinal absorption and brain permeation (Ertl *et al*., 2000; Daina & Zoete, 2016). The chalcones of this study show negative *in silico* brain penetration (Table 3-4), primarily because of the higher tPSA (> 80 $Å^2$). This is unfavourable since the biological main targets of of this study, COMT and MAO-B, are located in the brain. The molecules, however, show good absorption form the gastrointestinal tract, and no rule exceptions with respect to the rules of Lipinski.

Table 3-4: Selected physicochemical properties of chalcones A-T

Molecule	MW	tPSA	Gastrointestinal absorption	CLogP	BBB penetration	Lipinski violations
A	297.26	103.35	High	2.22	No	0
B	357.31	121.81	High	2.07	No	0
C	341.27	121.81	High	1.9	No	0
D	327.29	112.58	High	2.08	No	0
E	315.23	132.81	High	1.49	No	0
F	313.26	123.58	High	1.84	No	0
G	313.26	112.58	High	1.78	No	0
H	329.33	128.65	High	2.33	No	0
I	311.29	103.35	High	2.46	No	0
J	371.34	121.81	High	2.46	No	0
K	341.31	112.58	High	2.25	No	0
L	341.31	112.58	High	2.37	No	0
M	341.31	112.58	High	2.38	No	0
N	326.3	129.37	High	1.89	No	0
O	285.25	103.35	High	1.89	No	0

Q	364.15	103.35	High	2.36	No	0
S	382.14	103.35	High	2.57	No	0
T	389.16	127.14	High	2.06	No	0

3.5 Conclusion

In this study, nitrocatechol containing chalcone derivatives were synthesised and evaluated as inhibitors of the MAO and COMT enzymes. Among the compounds, **G** and **L** exhibited promising inhibition properties. Compound **G** showed an IC_{50} value for the inhibition of MAO-B of 7.25 µM (with a selectivity index of 6.3 for MAO-B) and an IC_{50} value for the inhibition of COMT of 0.567 µM. The 6-methoxy substituted tetralone derivative (compound **L**) exhibited an IC_{50} value for the inhibition of MAO-B of 7.83 µM, and an IC_{50} value or the inhibition of COMT of 0.421 µM. These findings suggest that dual inhibition of two different, unrelated enzymes may be achieved. The compounds synthesised in this study show that dual inhibition of MAO-B and COMT is possible.

Computer modelling may provide some much needed insight into the mechanism of binding of inhibitors to the active sites of both enzymes. It may be hypothesised that hydrophobic residues located towards the outside the COMT active site may interact with the ring system not bearing the nitrocatechol moiety (i.e. ring A), and in this way alter the binding strength or duration. By employing hydrophobic interactions, it is postulated that the inhibitor side chains may be employed to better the binding in the active site.

As seen with compounds **G** and **L**, dual inhibition of MAO-B and COMT may be possible. Since the IC_{50} values for COMT and MAO-B differ to a large degree (2 orders of magnitude), these compounds will have to be optimised further in order to have clinical value. Inhibition activity levels (IC_{50} values) towards both enzymes should be similar to prepare stable dosages at later stages of development. This coupled with the high tPSA, which in turn limits the penetration into the brain, show that further optimisation will be necessary to discover compounds that may be advanced to the clinical phases.

3.6 Experimental Section

3.6.1 Chemicals and Instrumentation

All starting materials were obtained from Sigma-Aldrich, and were used “as is” without further purification. Carbon (^{13}C) and proton (^{1}H) NMR spectra were recorded on a Bruker Advance III 600 spectrometer at frequencies of 600 MHz and 151 MHz, respectively. DMSO-*d*6 served as

solvent for all compounds. Multiplicities are given as s (singlet), d (doublet), dd (doublet of doublets), ddd (doublet of doublet of doublets), t (triplet) and m (multiplet) (Annexure A). Silica gel 60 (Merck) with UV254 fluorescent indicator was used for the thin layer chromatography (TLC). High resolution mass spectra (HRMS) were recorded with a Bruker micrOTOF-Q II mass spectrometer in atmospheric pressure chemical ionisation (APCI) mode (Annexure B). Purity of the synthesised compounds were determined by high performance liquid chromatography (HPLC). Analyses were carried out with an Agilent 11000 HPLC system equipped with a quaternary pump and an Agilent 1100 series diode detector. HPLC grade acetonitrile (Merck) and Milli-Q water (Millipore) were used as mobile phase. The initial ratio was 30:70, the acetonitrile was increased linearly to 85% over 5 min. The flow rate was 1 mL/min. A Venusil XBP C18 column (4.60 x 150 mm, 5 µm) was used for the separation. Each run lasted 15 min and a period of 5 min was allowed as equilibrium between runs. 10 µL of test compound solution was injected to the system, and the eluent was monitored at wavelengths of 210, 230, 254 and 280 nm. The test compounds were dissolved in methanol and acetonitrile (50:50).

3.6.2 General Synthesis

Synthesis of the 3,4-dihydroxy-5-nitrobenzaldehyde intermediate

To a dry round bottom flask, 5-nitrovanillin (5 g, 25.4 mmol) and aluminium trichloride (3.72 g, 27.9 mmol) was placed and 50 mL chloroform was added. The mixture was cooled to 0 ˚C in an ice bath, and pyridine (9.01 mL, 111 mmol) was added dropwise. The flask was removed from the ice bath and the reaction mixture was refluxed in an atmosphere of nitrogen for 24 hours. The chloroform was removed under reduced pressure, and the crude product was quenched with a 100 mL aqueous hydrochloric acid (HCl) (20%) for one hour at room temperature. The water phase was extracted with three portions of ethyl acetate (50 mL). The combined organic phases were dried with anhydrous $MgSO_4$ for 30 min. The ethyl acetate was removed under reduced pressure and the crude was hot filtered with toluene (50 mL) to produce yellow crystals (Walz & Sundberg, 2000).

*Synthesis of the target chalcones (Compounds **A**–**T**)*

3,4-Dihydroxy-5-nitrobenzaldehyde (200 mg, 1.092 mmol) and 1.092 mmol of the appropriate indanone, tetralone or acetophenone were dissolved in a mixture of 6 mL HCl (32%) and 4 mL methanol, and heated under reflux for 24–26 hours. The progress of the reactions was monitored with silica gel TLC with petroleum ether: ethyl acetate (1:1) as mobile phase. Upon completion, the reaction was quenched with addition of ice water (50 mL) and the products precipitated. The precipitated material was collected by filtration and dried at 60 ˚C for 48 hours before further

analysis. Compound **B** and **T** were purified by recrystallisation from ethanol and acetonitrile, respectively.

3.6.3 Physical characterisation of the synthesised compounds

(2*E*)-2-(3,4-Dihydroxy-5-nitrobenzylidene)-2,3-dihydro-1*H*-inden-1-one (A)

A yield of 79.6% of a bright yellow powder was obtained. ^{1}H NMR (600 MHz, DMSO-*d*6) δ 4.07 (s, 2H), 7.42 (s, 1H), 7.51 – 7.46 (m, 2H), 7.70 (ddd, *J* = 14.7, 10.6, 4.2 Hz, 2H), 7.76 (dd, *J* = 10.1, 4.8 Hz, 2H), 10.69 (s, 2H). ^{13}C NMR (151 MHz, DMSO-*d*6) δ 31.75, 118.07, 120.23, 123.63, 125.51, 126.74, 127.79, 131.47, 134.26, 134.94, 137.23, 137.83, 142.99, 147.88, 149.83, 193.15. APCI-HRMS *m/z*: calc. for $C_{16}H_{11}NO_5$ (MH^+), 298.070, found 298.073. Purity (HPLC – 254 nm): 98.9%.

(2*E*)-2-(3,4-Dihydroxy-5-nitrobenzylidene)-5,6-dimethoxy-2,3-dihydro-1*H*-inden-1-one (B)

The crude was recrystallised from ethanol to produce a yield of 87.6% of a yellow powder. H NMR (600 MHz, DMSO-*d6*) δ 3.82 (s, 3H), 3.90 (s, 3H), 3.93 (s, 2H), 7.20 (d, *J* = 12.0 Hz, 2H), 7.29 (s, 1H), 7.44 (s, 1H), 7.71 (s, 1H). ^{13}C NMR (151 MHz, DMSO-*d6*) δ 31.83, 56.10, 56.47, 104.95, 108.55, 117.79, 120.91, 126.16, 130.02, 130.36, 135.59, 138.14, 143.19, 145.31, 148.29, 149.81, 155.75, 192.07. APCI-HRMS *m/z*: calc. for $C_{18}H_{12}NO_7$ (MH^+), 358.092, found 358.092. Purity (HPLC – 254 nm): 95%.

(6*E*)-6-(3,4-Dihydroxy-5-nitrobenzylidene)-6,7-dihydro-5*H*-indeno[5,6-*d*][1,3]dioxol-5-one (C)

A yield of 88.1% of a dark yellow powder was obtained. ^{1}H NMR (600 MHz, DMSO-*d6*) δ 3.94 (s, 2H), 6.19 (s, 2H), 6.19 (s, 2H), 7.17 (s, 1H), 7.19 (s, 1H), 7.29 (s, 1H), 7.44 (s, 1H), 7.71 (s, 1H), 10.63 (s, 1H). APCI-HRMS *m/z*: calc. for $C_{17}H_{11}NO_7$ (MH^+), 342.060, found 342.060.

(2*E*)-2-(3,4-Dihydroxy-5-nitrobenzylidene)-5-methoxy-2,3-dihydro-1*H*-inden-1-one (D)

A yield of 84.15% of a dark orange powder was obtained. ^{1}H NMR (600 MHz, DMSO-*d6*) δ 7.74 – 7.67 (m, 2H), 7.44 (s, 1H), 7.30 (s, 1H), 7.17 (s, 1H), 7.01 (d, *J* = 8.5 Hz, 1H), 3.99 (s, 2H), 3.88 (s, 3H). ^{13}C NMR (151 MHz, DMSO-*d6*) δ 31.81, 55.84, 110.24, 115.43, 117.53, 120.41, 125.46, 125.68, 130.06, 130.51, 134.90, 137.74, 142.79, 147.86, 152.71, 164.96, 191.38. APCI-HRMS *m/z*: calc. for $C_{16}H_{11}NO_6$ (MH^+), 328.081, found 328.081. Purity (HPLC – 254 nm): 94.3%.

(2*Z*)-2-(3,4-Dihydroxy-5-nitrobenzylidene)-6-hydroxy-1-benzofuran-3(2*H*)-one (E)

A yield of 89.4 % of a brownish orange powder was obtained. ^{1}H NMR (600 MHz, DMSO-*d6*) δ 6.760-06.96 (m, 6H), 7.62 (d, *J* = 8.4 Hz, 2H), 7.75 (d, *J* = 2.0 Hz, 2H), 7.90 (d, *J* = 1.9 Hz, 2H), 10.68 (s, 3H), 11.26 (s, 2H). ^{13}C NMR (151 MHz, DMSO-*d6*) δ 98.46, 109.40, 112.86, 113.20, 118.45, 120.57, 122.73, 126.11, 137.69, 143.02, 146.97, 147.83, 166.59, 167.73, 181.22. APCI-HRMS *m/z*: calc. for $C_{15}H_9NO_7$ (MH^+), 316.045, found 316.045. Purity (HPLC – 254 nm): 98.7%

(2*E*)-2-(3,4-Dihydroxy-5-nitrobenzylidene)-5-hydroxy-2,3-dihydro-1*H*-inden-1-one (F)

A yield of 84.7% of a mustard yellow powder was obtained. ^{1}H NMR (600 MHz, DMSO-*d6*) δ 3.96 (s, 1H), 6.86 (dd, *J* = 8.4, 2.1 Hz, 1H), 6.96 (d, *J* = 1.7 Hz, 1H), 7.28 (s, 1H), 7.46 (d, *J* = 2.0 Hz, 1H), 7.63 (d, *J* = 8.4 Hz, 1H), 7.70 (d, *J* = 2.0 Hz, 1H),10.66 (s, 2H). ^{13}C NMR (151 MHz, DMSO-*d6*) δ 31.62, 112.00, 116.25, 117.56, 120.17, 125.82, 125.87, 129.29, 120.60, 135.20, 137087, 142.60, 147.84, 152.86, 163.99, 191.23. APCI-HRMS *m/z*: calc. for $C_{16}H_{11}NO_6$ (MH^+), 314.065, found 314.066. Purity (HPLC – 254 nm): 99.7%.

(3*E*)-3-(3,4-Dihydroxy-5-nitrobenzylidene)-2,3-dihydro-4*H*-chromen-4-one (G)

A yield of 78.2% of an orange yellow powder was obtained. ^{1}H NMR (600 MHz, DMSO-*d6*) δ 5.36 (s, 2H), 7.03 (d, *J* = 8.1 Hz, 1H), 7.20 - 7.06 (m, 2H), 7.41 (s, 1H), 7.58 (d, *J* = 8.4 Hz, 2H), 7.91 - 7.76 (m, 1H) .^{13}C NMR (151 MHz, DMSO-*d6*) δ 67.51, 117.65, 118.22, 120.64, 121.67, 122.36, 124.54, 127.55, 130.56, 135.36, 136.63, 137.79, 143.26, 147.98, 160.85, 181.30. APCI-HRMS *m/z*: calc. for $C_{16}H_{11}NO_6$ (MH^+), 314.065, found 314.065. Purity (HPLC – 254 nm): 99.5%.

(3*Z*)-3-(3,4-Dihydroxy-5-nitrobenzylidene)-2,3-dihydro-4*H*-thiochromen-4-one (H)

A yield of 90.6% of an orange powder was obtained. ^{1}H NMR (600 MHz, DMSO-*d6*) δ 4.22 (s, 2H), 7.20 (s, 1H),7.31 (t, *J* = 7.6 Hz, 1H), 7.39 (d, *J* = 7.9 Hz, 1H), 7.49 (t, *J* = 10.5 Hz, 3H), 8.02 (d, *J* 7.9 Hz, 1H). ^{13}C NMR (151 MHz, DMSO-*d6*) δ 28.78, 117.11, 120.45, 125.20, 126.41, 128.37, 130.21, 132.15, 132.93, 133.96, 135.55, 137.92, 140.97, 142.94, 48.17, 185.43. APCI-HRMS *m/z*: calc. for $C_{16}H_{11}NO_5S$ (MH^+), 330.043, found 330.043. Purity (HPLC): 100%.

(2*E*)-2-(3,4-Dihydroxy-5-nitrobenzylidene)-3,4-dihydronaphthalen-1(2*H*)-one (I)

A yield of 89.54% of an orange powder was obtained. ^{1}H NMR (600 MHz, DMSO-*d6*) δ 2.90 (t, *J* = 6.2 Hz, 2H), 3.03 (t, *J* = 6.1 Hz, 2H), 7.22 (s, 1H), 7.39 - 7.32 (m, 2H), 7.47 (s, 1H), 7.54 (dd, *J* = 14.0, 6.3 Hz, 2H), 7.90 (d, *J* = 7.8 Hz, 1H). ^{13}C NMR (151 MHz, DMSO-*d6*) δ 27.07, 28.18, 117.15, 120.88, 126.14, 127.58, 127.87, 129.05, 133.14, 134.21, 134.65, 135.65, 137.68, 142.76, 143.85, 148.00, 187.28. APCI-HRMS *m/z*: calc. for $C_{17}H_{13}NO_5$ (MH^+), 312.086, found 312.086. . Purity (HPLC – 254 nm): 100%.

(2*E*)-2-(3,4-Dihydroxy-5-nitrobenzylidene)-6,7-dimethoxy-3,4-dihydronaphthalen-1(2*H*)-one (J)

A yield of 85.88% of a bright yellow powder was obtained. ^{1}H NMR (600 MHz, DMSO-*d6*) δ 2.86 (t, *J* = 6.0 Hz, 2H), 3.01 (d, *J* = 5.7 Hz, 2H), 3.77 (s, 3H), 3.83 (s, 3H), 6.90 (s, 1H), 7.21 (s, 1H), 7.39 (s, 1H), 7.46 (d, *J* = 2.2 Hz, 2H). ^{13}C NMR (151 MHz, DMSO-*d6*) δ 27.20, 27.79, 55.80, 56.16, 109.22, 110.97, 116.79, 120.67, 125.86, 126.21, 133.54, 135.60, 137.64, 138.79, 142.35, 147.84, 148.19, 153.86, 185.64. APCI-HRMS *m/z*: calc. for $C_{19}H_{17}NO_7$ (MH^+), 372.107, found 372.107. Purity (HPLC – 254 nm): 95.4%.

(2*E*)-2-(3,4-Dihydroxy-5-nitrobenzylidene)-6-methoxy-3,4-dihydronaphthalen-1(2*H*)-one (K)

A yield of 77.86% of a bright orange powder was obtained. ^{1}H NMR (600 MHz, DMSO-*d6*) δ 2.92 (t, *J* = 6.4 Hz, 2H), 3.05 (t, *J* = 6.0 Hz, 2H), 3.84 (s, 3H), 6.90 (d, *J* = 2.1 Hz, 1H), 6.94 (dd, *J* = 8.7, 2.4 Hz, 1H), 7.23 (d, *J* = 1.7 Hz, 1H), 7.53 – 7.47 (m, 2H), 7.91 (d, *J* = 8.7 Hz, 1H), 10.53 (s, 2H). ^{13}C NMR (151 MHz, DMSO-*d6*) δ 26.69, 28.20, 55.60, 112.34, 113.81, 116.61, 120.37, 125.89, 126.27, 129.95, 133.39, 135.33, 137.49, 141.98, 145.97, 147.54, 163.34, 185.20. APCI-HRMS *m/z*: calc. for $C_{18}H_{15}NO_6$ (MH^+), 342.097, found 342.097. Purity (HPLC – 254 nm): 99.5%.

(2*E*)-2-(3,4-Dihydroxy-5-nitrobenzylidene)-5-methoxy-3,4-dihydronaphthalen-1(2*H*)-one (L)

A yield of 82.8% of a dusty yellow powder was obtained. ^{1}H NMR (600 MHz, DMSO-*d6*) δ 2.08 (s, 3H), 2.86 (t, *J* = 6.5 Hz, 2H), 3.05 (t, *J* = 5.9 Hz, 2H), 3.84 (s, 3H), 7.26 – 7.24 (m, 2H), 7.37 (t, *J* = 8.0 Hz, 1H), 7.50 (d, *J* = 1.7 Hz, 1H), 7.53 (s, 1H), 7.57 (d, *J* = 7.8 Hz, 1H), 10.55 (s, 2H). ^{13}C NMR (151 MHz, DMSO-*d6*) δ 20.88, 25.91, 30.73, 55.84, 115.08, 116.80, 119.02, 120.30, 125.70, 127.44, 131.66, 133.69, 133.97, 134.93, 137.51, 142.12, 147.56, 156.10, 186.61. APCI-HRMS *m/z*: calc. for $C_{18}H_{15}NO_6$ (MH^+), 342.097, found 342.097. Purity (HPLC – 254 nm): 98.8%.

(2*E*)-2-(3,4-Dihydroxy-5-nitrobenzylidene)-7-methoxy-3,4-dihydronaphthalen-1(2*H*)-one (M)

A yield of 87.1% of a yellow powder was obtained. ^{1}H NMR (600 MHz, DMSO-*d6*) δ 2.08(s, 2H), 2.88 (t, *J* = 6.4 Hz, 2H), 3.05 (t, *J* = 5.8 Hz, 2H), 3.80 (s. 3H), 7.17 (dd, *J* = 8.4, 208 Hz, 1H), 7.25 (d, *J* = 1.8 Hz, 1H), 7.30 (d, *J* = 8.4, 1H), 7.42 (d, *J* = 2.8 Hz, 1H), 7.51 (d, *J* = 1.8 Hz, 1H), 7.56 (s, 1H), 10.55 (s, 2H). ^{13}C NMR (151 MHz, DMSO-*d6*) δ 26.83, 26.96 30.72, 55.33, 110.16, 116.81, 120.33, 120.91, 125.70, 129.94, 133.67, 134.23, 135.04, 135.81, 137.49, 142.13, 147.55, 158.22, 186.33. APCI-HRMS *m/z*: calc. for $C_{18}H_{15}NO_6$ (MH^+), 342.097, found 342.097. Purity (HPLC – 254 nm): 100%.

(2*E*)-6-Amino-2-(3,4-dihydroxy-5-nitrobenzylidene)-3,4-dihydronaphthalen-1(2*H*)-one (N)

A yield of 78.6% of a reddish orange powder. ^{1}H NMR (600 MHz, DMSO-*d6*) δ 2.77 (t, *J*, = 6.4 Hz, 6H), 2.98 (t, *J* = 5.9 Hz, 6H). 6.46 (s, 3H), 6.60 (dd, *J* = 8.5, 1.8 Hz, 3H), 7.23 (d, *J* = 1.9Hz, 3H), 7.46 – 7.39 (m, 6H), 7.50 (d, *J* = 1.9 Hz, 1H), 7.73 (d, *J* = 8.5 Hz, 3H), 7.97 (d, *J*= 1.9 Hz, 1H), 9.80 (s, 1H). ^{13}C NMR (151 MHz, DMSO-*d6*) δ 26.75, 28.31, 115.83, 116.28, 119.66, 120.39, 126.23, 127.01, 130.10, 123.04, 136.12, 137.51, 141.67, 145.50, 147.52, 148.36, 184.13, 190.65. APCI-HRMS *m/z*: calc. for $C_{17}H_{14}N_2O_5$ (MH^+), 327.097, found 327.097. Purity (HPLC – 254 nm): 98.3%.

(2*E*)-3-(3,4-Dihydroxy-5-nitrophenyl)-1-phenylprop-2-en-1-one (O)

A yield of 72% of a bright yellow powder was obtained. ^{1}H NMR (600 MHz, DMSO-*d6*) δ 2.08 (s, 3H), 7.56 (dd, *J* = 15.4, 7.7 Hz, 12H), 7.66 (dd, *J* = 14.8, 6.1 Hz, 8H), 7.82 (d, *J* = 15.5, 4H), 7.96 (s, 4H), 8.15 (d, *J* = 7.7 Hz, 8H), 10.60 (s, 8H). ^{13}C NMR (151 MHz, DMSO-*d6*) δ 30.73, 116.04, 118.97, 121.51, 125.56, 128.57, 128.82, 133.18, 137.61, 137.89, 142.61, 143.55, 147.86, 188.95. APCI-HRMS *m/z*: calc. for $C_{15}H_{11}NO_5$ (MH^+), 286.070, found 286.071. Purity (HPLC – 254 nm): 96.5%.

(2*Z*)-2-Bromo-3-(3,4-dihydroxy-5-nitrophenyl)-1-phenylprop-2-en-1-one (Q)

A yield of 77.6% of a dull yellow powder was obtained. ^{1}H NMR (600 MHz, DMSO-*d6*) δ 7.53 (s, 1H), 7.66 (d, *J* = 15.5 Hz, 1H), 7.79 (t, *J* = 11.2 Hz, 3H), 7.96 (s, 1H), 8.09 (d, *J* = 8.4 Hz, 2H), 10.59 (s, 2H). 13C NMR (151 MHz, DMSO-*d6*) δ 116.14, 118.99, 121.13, 125.40, 127.13, 130.58, 131.85, 136.58, 137.87, 143.12, 143.70, 147.85, 188.07. APCI-HRMS *m/z*: calc. for $C_{15}H_{10}BrNO_5$ (MH^+), 363.981, found 363.981. Purity (HPLC – 254 nm): 97.7%.

(2*Z*)-2-Bromo-3-(3,4-dihydroxy-5-nitrophenyl)-1-(4-fluorophenyl)prop-2-en-1-one (S)

A yield 76%, of a yellow powder was obtained, after the crude was extracted with 3x50mL ethyl acetate and then the solvent was removed under reduced pressure. ^{1}H NMR (600 MHz, DMSO-*d6*) δ 2.08 (s, 2H), 7.17 (d, *J* = 16.0 Hz, 1H), 7.44 (s, 1H), 7.68 (d, *J* = 16.0 Hz, 2H), 7.80 (s, 1H), 8.10 (s, 1H), 10.59 (s, 2H). APCI-HRMS *m/z*: calc. for $C_{15}H_9BrFNO_5$ (MH^+), 381.972, found 338.022. Purity (HPLC – 254 nm): 91%

(2*Z*)-2-Bromo-3-(3,4-dihydroxy-5-nitrophenyl)-1-(4-isocyanophenyl)prop-2-en-1-one (T)

The crude was recrystallised from acetonitrile to produce a yield of 21.4% of a dull yellow powder. ^{1}H NMR (600 MHz, DMSO-*d6*) δ 7.17 (d, *J* = 16.0 Hz, 1H), 7.40 (dd, *J* = 24.3, 15.8 Hz, 2H), 7.56 (s, 1H), 7.68 (d, *J* = 16.0 Hz, 1H), 7.89 – 7.77 (m, 2H), 7.93 (s, 1H), 10.69 (s, 1H). APCI-HRMS *m/z*: calc. for $C_{16}H_9BrN_2O_5$ (MH^+), 388.976, found 389.051.

3.6.4 Protocol for the determination of IC_{50} values for the inhibition of MAO

All enzyme reactions were carried out in white polypropylene 96-well microtiter plates to a final volume of 200 µL. The reactions contained potassium phosphate buffer (100 mM, pH 7.4, made isotonic with 20.1 mM KCl), kynuramine (50 µM) and the test inhibitors at seven different concentration levels namely 0; 0.003; 0.01; 0.1; 1; 10 and 100 µM. Stock solutions of the inhibitors were prepared in dimethyl sulfoxide (DMSO) and added to reactions to yield a final concentration of 4% (v/v) DMSO. Control reactions were carried out in the absence of an inhibitor that also contained 4% DMSO.

The reactions were incubated for 30 minutes at 37 ˚C and were subsequently initiated with the addition of MAO-A and MAO-B to yield a final enzyme concentration of 0.0075 mg protein/mL and 0.015 mg protein/mL for MAO-A and MAO-B, respectively. The reactions were incubated for a further 20 minutes at 37 ˚C, and were subsequently terminated by the addition of 80 µL NaOH (2 N). The concentration of 4-hydrozxyquinoline generated by MAO was measured by fluorescence spectrophotometry at an excitation wavelength of 310 nm and an emission wavelength of 400 nm. Refer to Figure 3-10.

To quantitate 4-hydroxyquinoline, a linear calibration curve was constructed with authentic 4-hydroxyquinoline (0.047–1.50 µM). In order to confirm that the test compounds do not fluoresce or quench the fluorescence of 4-hydroxyquinoline, control samples were included in the assay. These control samples (200 µL) contained 4-hydroxyquinoline (1.50 µM), the test compound (100 µM) and 80 µL NaOH. By employing the calibration curve, the enzyme catalytic rates were determined and sigmoidal plots of rate versus the logarithm of the concentration of the test inhibitor were constructed. These kinetic data were fitted to the one site competition model incorporated into the Prism 5 Software Package (GraphPad) and the corresponding IC_{50} values of the test compounds were estimated. The IC_{50} values were determined in triplicate and expressed as mean ± standard deviation (SD) as seen in Table 3-1 and Table 3-2 (Engelbrecht *et al.*, 2015; Engelbrecht *et al.*, 2018; Mostert *et al.*, 2015; Petzer *et al.*, 2014).

3.6.5 Protocol for the determination of IC_{50} values for the inhibition of COMT

To determine whether the synthesised compounds are inhibitors of COMT, the method described in literature (Borchardt, 1974) was used.

This protocol uses esculetin (6,7-dihydroxycoumarin) as substrate for COMT. After the test inhibitor is incubated with esculetin and COMT, fluorescence spectrophotometry was used to quantify the enzymatic product, scopoletin. Sigmoidal dose-response curves of COMT activity versus the logarithm of inhibitor concentration (Log[I]) were constructed using the Prism 5.0

software package (GraphPad), and the IC_{50} values were determined in triplicate and expressed as mean ± standard deviation (SD). As enzyme source, the soluble fraction obtained from homogenates of rat liver tissue was used.

The rat liver tissue was obtained under category 0 ethical approval (AnimCare). Sprague Dawley rats were bred, supplied and housed at the Vivarium of the Preclinical Drug Development Platform at the Potchefstroom campus of the North-West University (NWU) (SAVC reg no. FR15/13458; SANAS GLP compliance no. G0019). Experiments were approved by the AnimCare animal research ethics committee (NHREC reg. number AREC-130913-015) at the NWU. All animals were maintained and procedures performed in accordance with the code of ethics in research, training and testing of drugs in South Africa, and complied with national legislation. Ethical approval for the collection and use of animal tissue was obtained from the Research Ethics Committee, NWU. Ethics approval number: **NWU-00564-19-S5**. The liver tissue was prepared as reported in literature (Hirano *et al*., 2005; Zhu *et al*., 1994).

Frozen liver tissue was washed with ice cold saline, cut into smaller pieces and homogenised in three volumes sodium phosphate buffer (25 mM, pH 7.8, containing 0.5 mM dithiothreitol) for 2 min with a polytron homogeniser. The homogenate was centrifuged at 100,000 × g for 30 min at 4 °C, and the supernatant was stored as soluble COMT at –86 °C. Protein determination was carried out by the method of Bradford (Bradford, 1970). The enzyme reactions were prepared in potassium phosphate buffer (100 mM, pH 7.4) and contained esculetin, S-adenosyl-L-methionine as co-factor, magnesium chloride, L-cysteine, the test inhibitor (0.003–80 µM) and COMT. All reactions were carried out in 96-well microtiter plates (black) to a volume of 200 µl, and stock solutions of the test inhibitors were prepared in DMSO and added to the reactions to yield a final DMSO concentration of 4%. After addition and mixing of the reagents, the 96-well plate was placed in the oven to pre-incubate at 37 °C for 15 min. The reactions were initiated with the addition of the enzyme and the fluorescence intensities were recorded continuously (λ_{ex} 355, λ_{em} 460 nm) for 500 s (8.3 min) using a SpectraMax® iD3 instrument (Molecular Devices). From plots of fluorescence intensity versus time, the slopes were recorded and used to construct sigmoidal dose-response curves of slope versus Log[I]. For this purpose, the Prism 5.0 software package (GraphPad) was used. IC_{50} values were determined in triplicate from the sigmoidal plots, and expressed as mean ± SD

.

3.7 Bibliography

References

Alexander, G. 2004. Biology of Parkinson's disease: pathogenesis and pathophysiology of a multisystem neurodegenerative disorder. *State of the Art*, 6(3): 259.

Allt, G. & Lawrenson, J. 2001. Pericytes: cell biology and pathology. *Cells Tissues Organs*, 169(1):1-11.

Ali, J., Camilleri, P., Brown, M.B., Hutt, A.J. & Kirton, S.B. 2012. Revisiting the general solubility equation: in silico prediction of aqueous solubility incorporating the effect of topographical polar surface area. *Journal of Chemical Information and Modelling*, 52(2):420-428.

Aminoff, M. 2004. Pharmacologic Management of Parkinsonism & Other Movement Katzung Pharmacology Katzung, Basic and Clinical Pharmacology: Lang Medical Books, McGraw-Hill, New York, NY, USA.

Arnott, J.A. & Planey, S.L. 2012. The influence of lipophilicity in drug discovery and design. *Expert Opinion on Drug Discovery*, 7(10):863-875.

Backstrom, R., Honkanen, E., Pippuri, A., Kairisalo, P., Pystynen, J., Heinola, K., et al. 1989. Synthesis of some novel potent and selective catechol O-methyltransferase inhibitors. *Journal of Medicinal Chemistry*, 32(4):841-846.

Bai, H.W., Shim, J.Y., Yu, J. & Zhu, B.T. 2007. Biochemical and molecular modeling studies of the O-methylation of various endogenous and exogenous catechol substrates catalyzed by recombinant human soluble and membrane-bound catechol-O-methyltransferases. *Chemical Research in Toxicology*, 20(10):1409-1425.

Begley, D.J., Pontikis, C.C & Scarpa, M. 2008. Lysosomal storage diseases and the blood-brain barrier. *Current Pharmaceutical design*, 14(16): 1566-1580.

Bodor, N. & Buchwald, P. 2003. Brain-targeted drug delivery. *American Journal of Drug Delivery*, 1(1): 13-26.

Bourque, M., Morissette, M. & Di Paolo, T. 2015. Neuroprotection in Parkinsonian-treated mice via estrogen receptor α activation requires G protein-coupled estrogen receptor 1. *Neuropharmacology*, 95:343-352.

Borchardt, R.T. 1974. A rapid spectrophotometric assay for catechol-O-methyltransferase. *Analytical Biochemistry*, 58(2):382-389.

Bradford, M.M. 1970. A rapid and sensitive method for the quantitation of microgram quantities of protein utilizing the principle of protein-dye binding. *Analytical Biochemistry*. 72: 248-254.

Brady, S., Siegel, G., Albers, R. & Price, D. 2005. Inherited and Neurodegenerative Diseases. In Technology. *Basic Neurochemistry: Molecular, Cellular and Medical Aspects* 1:766 - 778.

Carlsson, A., Lindqvist, M. & Magnusson, T. 1957. 3, 4-Dihydroxyphenylalanine and 5-hydroxytryptophan as reserpine antagonists. *Nature*, 180(4596):1200.

Cheng, F., Li, W., Zhou, Y., Shen, J., Wu, Z., Liu, G., et al. 2012. admetSAR: a comprehensive source and free tool for assessment of chemical ADMET properties: ACS Publications.

Chimenti, F., Fioravanti, R., Bolasco, A., Chimenti, P., Secci, D., Rossi, F., Yanez, M., Orallo, F., Ortuso, F. & Alcaro, S. 2009. Chalcones: a valid scaffold for monoamine oxidases inhibitors. *Journal of Medicinal Chemistry*, 52(9):2818-2824.

Clark, D. 2001. Prediction of intestinal absorption and blood-brain barrier penetration by computational methods. *Combinatorial Chemistry & High Throughput Screening*, 4(6): 477-496.

Collins, G., Sandler, M., Williams, E. & Youdim, M.B.H. 1970. Multiple forms of human brain mitochondrial monoamine oxidase. *Nature*, 225:817–820.

Daina, A., Michielin, O. & Zoete, V. 2014. iLOGP: a simple, robust, and efficient description of n-octanol/water partition coefficient for drug design using the GB/SA approach. *Journal of Chemical Information and Modeling,* 54(12):3284-3301.

Daina, A. & Zoete, V. 2016. A boiled-egg to predict gastrointestinal absorption and brain penetration of small molecules. *ChemMedChem*, 11(11):1117-1121.

Dallas, S., Miller, D.S. & Bendayan, R. 2006. Multidrug resistance-associated proteins: expression and function in the central nervous system. *Pharmacological Reviews*, 58(2): 140-161.

Dauer, W. & Przedborski, S. 2003. Parkinson's disease: mechanisms and models. *Neuron*, 39(6):889-909.

Dean, P.M. 1988. Molecular foundations of drug-receptor interaction: Cambridge University Press Cambridge.

Delaney, J.S. 2004. ESOL: estimating aqueous solubility directly from molecular structure. *Journal of chemical information and computer sciences*, 44(3):1000-1005.

Ehler, A., Benz, J., Schlatter, D. & Rudolph, M.G. 2014. Mapping the conformational space accessible to catechol-O-methyltransferase. *Acta Crystallographica Section D: Biological Crystallography*, 70(8):2163-2174.

Engelbrecht, I., Petzer, J.P. & Petzer, A. 2015. The synthesis and evaluation of sesamol and benzodioxane derivatives as inhibitors of monoamine oxidase. *Bioorganic & Medicinal Chemistry letters*, 25(9):1896-1900.

Engelbrecht, I., Petzer, J.P. & Petzer, A. 2018. Nitrocatechol Derivatives of Chalcone as Inhibitors of Monoamine Oxidase and Catechol-O-Methyltransferase. *Central Nervous System Agents Medicinal Chemistry,* 18(2):115-127

Ertl, P., Rohde, B. & Selzer, P. 2000. Fast calculation of molecular polar surface area as a sum of fragment-based contributions and its application to the prediction of drug transport properties. *Journal of Medicinal Chemistry*, 43(20):3714-3717.

Fagervall, I. & S.B. Ross. 1986. Inhibition of mono amine oxidase in monoaminergic neurones in the rat brain by irreversible inhibitors. *Biochemical Pharmacology*, **35**(8):1381-1387.

Fišar, Z. 2016. Drugs related to monoamine oxidase activity. *Progress in Neuro-Psychopharmacology and Biological psycHiatry*, 69:112-124.

Fischer, H., Gottschlich, R. & Seelig, A. 1998. Blood-brain barrier permeation: molecular parameters governing passive diffusion. *The Journal of Membrane Biology*, 165(3): 201-211.

Fraga, C.A.M. 2009. Drug hybridization strategies: before or after lead identification? *Expert Opinion on Drug Discovery*, 4(6):605-609.

Fredriksson, A. & Archer, T. 1995. Synergistic interactions between COMT-/MAO-inhibitors and L-Dopa in MPTP-treated mice. *Journal of Neural Transmission*, 102(1):19-34.

Gelb, D.J., Oliver, E. & Gilman, S. 1999. Diagnostic criteria for parkinson disease. *Archives of Neurology*, 56(1):33-39.

Gfeller, D., Grosdidier, A., Wirth, M., Daina, A., Michielin, O. & Zoete, V. 2014. SwissTargetPrediction: a web server for target prediction of bioactive small molecules. *Nucleic Acids Research,* 42(W1):W32-W38.

Gomes, M.N., Muratov, E.N., Pereira, M., Peixoto, J.C., Rosseto, L.P. & Cravo, P.V. 2017. Chalcone derivatives: promising starting points for drug design. *Molecules*, 22(8):1210.

Gonzalez-Usigli, H.A. 2017. Parkinson Disease. https://www.merckmanuals.com/professional/neurologic-disorders/movement-and-cerebellar-disorders/parkinson-disease: Merck Manual. Date of access: 28-2-2017.

Gottwald, M.D., Bainbridge, J.L., Dowling, G.A., Aminoff, M.J., Alldredge, B.K. 1997. New pharmacotherapy for Parkinson's disease*. Annals of Pharmacotherapy*, 31(10):1205-1217.

Graff, C.L. & Pollack, G.E. 2004. (Section B: Integrated function of drug transporters in vivo) drug transport at the blood-brain barrier and the choroid plexus. *Current Drug Metabolism*, 5(1): 95-108.

Grosdidier, A., Zoete, V. & Michielin, O. 2011. SwissDock, a protein-small molecule docking web service based on EADock DSS. *Nucleic Acids Research*, 39(suppl-2):W270-W277.

Hirano, Y., Tsunoda, M., Funatsu, T. & Imai, K. 2005. Rapid assay for catechol-O-methyltransferase activity by high-performance liquid chromatography-fluorescence detection. *Journal of Chromatography B*. 819:41-46.

Huh, M. & Friedhoff, A.J. 1979. Multiple molecular forms of catechol-O-methyltransferase. Evidence for two distinct forms, and their purification and physical characterization. *Journal of Biological Chemistry*, 254(2):299-308.

Kaakkola, S. 2000. Clinical pharmacology, therapeutic use and potential of COMT inhibitors in Parkinson’s disease. *Drugs*, 59(6):1233-1250.

Kiss, L.S.E. & Soares-da-Silva, P. 2014. Medicinal chemistry of catechol O-methyltransferase (COMT) inhibitors and their therapeutic utility. *Journal of Medicinal Chemistry*, 57(21):8692-8717.

Kuntz, I.D. 1992. Structure-Based Strategies for Drug Design and Discovery. *Science*, 257(5073):1078-1082.

Lee, E.S.Y., Chen, H., King, J. & Charlton, C. 2008. The role of 3-O-methyldopa in the side effects of L-dopa. *Neurochemical Research*, 33(3):401-411.

Legoabe, L.J., Petzer, A. & Petzer, J.P. 2014. α-Tetralone derivatives as inhibitors of monoamine oxidase. *Bioorganic & Medicinal Chemistry Letters*, 24(12):2758-2763.

Liccione, J. & A.J. Azzaro. 1988. Different roles for type A and type B monoamine oxidase in regulating synaptic dopamine at D-1 and D-2 receptors associated with adenosine-3′, 5′-cyclic monophosphate (cyclic AMP) formation. *Naunyn-Schmiedeberg's Archives of Pharmacology*, 337(2):151-158.

Lobell, M., Molnár, L. & Keserü, G.M. 2003. Recent advances in the prediction of blood–brain partitioning from molecular structure. *Journal of Pharmaceutical Sciences*, 92(2): 360-370.

Lovering, F., Bikker, J. & Humblet, C. 2009. Escape from flatland: increasing saturation as an approach to improving clinical success. *Journal of Medicinal Chemistry*, 52(21):6752-6756.

Lyytinen, J., Kaakkola, S., Ahtila, S., Tuomainen, P. & Teräväinen, H. 1997. Simultaneous MAO-B and COMT inhibition in l-dopa-treated patients with parkinson's disease. *Movement Disorders: Official Journal of the Movement Disorder Society*, 12(4):497-505.

Maurer, T.S., DeBartolo, D.B., Tess, D.A. & Scott, D.O. 2005. Relationship between exposure and nonspecific binding of thirty-three central nervous system drugs in mice. *Drug Metabolism and Disposition*, 33(1):175-181.

Medvedev, A., Ivanov, A., Kamyshanskaya, N., Kirkel, A., Moskvitina, T. & Gorkin, V. 1995. Interaction of indole derivatives with monoamine oxidase A and B. Studies on the structure-inhibitory activity relationship. *Biochemistry and Molecular Biology International*, 36(1):113-122.

Meiser, J., Weindl, D., Hiller, K. 2013. Complexity of dopamine metabolism. *Cell Communication and Signaling*, 11(34):18.

Milne, G., Nicklaus, M. & Wang, S. 1998. Pharmacophores in drug design and discovery. *SAR and QSAR in Environmental Research*, 9(1-2):23-38.

Mostert, S., Petzer, A. & Petzer, J.P. 2015. Indanones As High-Potency Reversible Inhibitors of Monoamine Oxidase. *ChemMedChem*, 10(5):862-873.

Mucklow, J. 2000. Martindale: the complete drug reference. *British Journal of Clinical Pharmacology*, 49(6):613-613.

Müller, T. 2008. Role of homocysteine in the treatment of Parkinson's disease. *Expert Review of Neurotherapeutics*, 8(6):957-967.

Nord, M., Zsigmond, P., Kullman, A., Årstrand, K. & Dizdar, N. 2010. The effect of peripheral enzyme inhibitors on levodopa concentrations in blood and CSF. *Movement Disorders*, 25(3):363-367.

Pardridge, W.M. 1998. CNS drug design based on principles of blood-brain barrier transport. *Journal of Neurochemistry*, 70(5):1781-1792.

Pardridge, W.M. 2001. BBB-Genomics: creating new openings for brain-drug targeting. 2001, *Elsevier Current Trends.*

Pardridge, W.M. 2005. The blood-brain barrier: bottleneck in brain drug development. *NeuroRx*, 2(1):3-14.

Patel, M. 2016. Targeting oxidative stress in central nervous system disorders. *Trends in Pharmacological Sciences*, 37(9):768-778.

Perjési, P., Perjéssy, A., Kolehmainen, E., Ősz, E., Samaliková, M., Linnanto, J., et al. 2004. E-2-Benzylidenebenzocycloalkanones III. Studies on transmission of substituent effects on IR carbonyl stretching frequencies and 13C NMR chemical shifts of E-2-(X-benzylidene)-1-indanones. Comparison with the IR data of E-2-(X-benzylidene)-1-indanones,-tetralones, and-benzosuberones. *Journal of Molecular Structure*, 697(1-3):41-47.

Petzer, A., Harvey, B.H., Wegener, G. & Petzer, J.P. 2012. Azure B, a metabolite of methylene blue, is a high-potency, reversible inhibitor of monoamine oxidase. *Toxicology and Applied Pharmacology*. 258(3):403-409.

Petzer, A., Grobler, P., Bergh, J.J. and Petzer, J.P., 2014. Inhibition of monoamine oxidase by selected phenylalkylcaffeine analogues. *Journal of Pharmacy and Pharmacology*, 66(5), pp.677-687.

Pires, D.E., Blundell, T.L. & Ascher, D.B. 2015. pkCSM: predicting small-molecule pharmacokinetic and toxicity properties using graph-based signatures. *Journal of Medicinal chemistry*, 58(9):4066-4072.

Pliška, V., Testa, B. & van de Waterbeemd, H. 1996. Lipophilicity: The empirical tool and the fundamental objective: an introduction. *Lipophilicity in Drug Action and Toxicology*: 1-6.

Ritchie, T.J., Ertl, P. & Lewis, R. 2011. The graphical representation of ADME-related molecule properties for medicinal chemists. *Drug Discovery Today*, 16(1-2):65-72.

Rinne, U. & Mölsä, P. 1979. Levodopa with benserazide or carbidopa in Parkinson disease. *Neurology*, 29(12):1584-1589.

Rinne, U., Larsen, J., Siden, Å. & Worm-Petersen, J. 1998. Entacapone enhances the response to levodopa in parkinsonian patients with motor fluctuations. *Neurology*, 51(5):1309-1314.

Ruottinen, H. & Rinne, U. 1996. Entacapone prolongs levodopa response in a one month double blind study in parkinsonian patients with levodopa related fluctuations. *Journal of Neurology, neurosurgery & psychiatry*, 60(1):36-40.

Segura-Aguilar, J., Paris, I., Muñoz, P., Ferrari, E., Zecca, L. & Zucca, F.A. 2014. Protective and toxic roles of dopamine in Parkinson's disease. *Journal of Neurochemistry*, 129(6):898-915.

Shih, J., K. Chen, and M. Ridd, Monoamine oxidase: from genes to behavior. *Annual Review of Neuroscience*, 1999. **22**(1): p. 197-217.

Sies, H. 2015. Oxidative stress: a concept in redox biology and medicine. *Redox Biology*, 4:180-183.

Silva, B.M., Rodrigues, J.J., de la Torre Díez, I., López-Coronado, M. & Saleem, K. 2015. Mobile-health: A review of current state in 2015. *Journal of Biomedical Informatics*, 56:265-272.

Son, S.Y., Ma, J., Kondou, Y., Yoshimura, M., Yamashita, E. & Tsukihara, T. 2008. Structure of human monoamine oxidase A at 2.2-Å resolution: the control of opening the entry for substrates/inhibitors. *Proceedings of the National Academy of Sciences*, 105(15):5739-5744.

Standaert, D.G. & Roberson, E.D. 2015. Treatment of Central Nervous System Degenerative Disorders. (In Brunton, L.L., Chabner, B.A. & Knollmann, B.C., eds. Goodman & Gilman's: The Pharmacological Basis of Therapeutics, 12th ed. New York: McGraw-Hill Education.

Tenhunen, J., Salminen, M., Lundström, K., Kiviluoto, T., Savolainen, R. & Ulmanen, I. 1994. Genomic organization of the human catechol O-methyltransferase gene and its expression from two distinct promoters. *European Journal of Biochemistry*, 223(3):1049-1059.

Tian, S., Wang, J., Li, Y., Li, D., Xu, L. & Hou, T. 2015. The application of in silico drug-likeness predictions in pharmaceutical research. *Advanced Drug Delivery Reviews*, 86:2-10.

Tipton, K.F., Boyce, S., O'Sullivan, J., Davey, G.P. & Healy, J. 2004. Monoamine oxidases: certainties and uncertainties. *Current Medicinal Chemistry*, 11(15):1965-1982.

Tohgi, H., Abe, T., Kikuchi, T., Takahashi, S. & Nozaki, Y. 1991. The significance of 3-O-methyldopa concentrations in the cerebrospinal fluid in the pathogenesis of wearing-off phenomenon in Parkinson's disease. *Neuroscience Letters*, 132(1):19-22.

Tripathi, A.C., Upadhyay, S., Paliwal, S. & Saraf, S.K. 2018. Privileged scaffolds as MAO inhibitors: Retrospect and prospects. *European Journal of Medicinal Chemistry*, 10(145):445-497.

Vidgren, J., Svensson, L.A. & Liljas, A. 1994. Crystal structure of catechol O-methyltransferase. *Nature*, 368(6469):354.

Viegas-Junior, C., Danuello, A., da Silva Bolzani, V., Barreiro, E.J. & Fraga, C.A.M. 2007. Molecular hybridization: a useful tool in the design of new drug prototypes. *Current Medicinal Chemistry*, 14(17):1829-1852.

Vijayakumar, D. & Jankovic, J. 2016. Drug-induced dyskinesia, part 1: treatment of levodopa-induced dyskinesia. *Drugs*, 76(7):759-777.

Walz, A.J. & Sundberg, R.J. 2000. Synthesis of 8-Methoxy-1-methyl-1 H-benzo [de][1, 6] naphthyridin-9-ol (Isoaaptamine) and Analogues. *The Journal of Organic Chemistry*, 65(23):8001-8010.

Weissbach, H., Smith, T.E., Daly, J.W., Witkop, B. & Udenfriend, S. 1960. A rapid spectrophotometric assay of monoamine oxidase based on the rate of disappearance of kynuramine. *Journal of Biological Chemistry*, 235(2):1160-1163.

Wirth, M., Zoete, V., Michielin, O. & Sauer, W.H. 2012. SwissBioisostere: a database of molecular replacements for ligand design. *Nucleic Acids Research*, 41(D1):D1137-D1143.

Youdim, M., Finberg, J. & Tipton, K. 1988. Monoamine oxidase. (*in* Trendelenburg, U*., ed.* Catecholamines. USA:Springer, 119-192.)

Youdim, M.B., Edmondson, D. & Tipton, K.F. 2006. The therapeutic potential of monoamine oxidase inhibitors. *Nature Reviews Neuroscience*, 7(4):295.

Youdim, M.B. & Bakhle, Y. 2006. Monoamine oxidase: isoforms and inhibitors in Parkinson's disease and depressive illness. *British Journal of Pharmacology*, 147(S1).

Zhu, B.T., Ezell, E.L. & Liehr, J.G. 1994. Catechol-O-methyltransferase-catalyzed rapid O-methylation of mutagenic flavonoids. Metabolic inactivation as a possible reason for their lack of carcinogenicity in vivo. *Journal of Biological Chemistry*, 269(1):292-299.

Zoete, V., Cuendet, M.A., Grosdidier, A. & Michielin, O. 2011. SwissParam: a fast force field generation tool for small organic molecules. *Journal of Computational Chemistry*, 32(11):2359-2368.

Zoete, V., Daina, A., Bovigny, C. & Michielin, O. 2016. SwissSimilarity: a web tool for low to ultra high throughput ligand-based virtual screening: ACS Publications.

CHAPTER 4 CONCLUSIONS

4.1 Final remarks

In this study, the main goal to design and synthesise bicyclic nitrocatechol chalcone derivatives, were achieved. By following a hybridisation approach, dual-target-directed inhibitors of MAO and COMT were designed. By using Claisen-Schmidt condensation in an acidic environment, the chalcones were produced in poor (21%) to high (>75%) yields.

Three series of chalcone derivatives were thus synthesised and included tetralone, indanone and open-chain chalcone derivatives. The general structures of these series are given in Tables 3-1 and Table 3-2. The results of the MAO inhibition studies showed that the potencies of the compounds are average to poor, ranging between 7.2 to 60.5 µM for MAO-B, and 29.43 to 53.07 µM for MAO-A. Most compounds showed selectivity towards MAO-B, except compounds **J**, **B** and **E**. Selectivity towards MAO-B is advantageous since MAO-B is the target for reducing dopamine metabolism in PD. Thus the side effects of MAO-A can be avoided as all the compounds showed lower potency towards the MAO-A isoform. MOA-B activity can be increased by decreasing polarity of the molecules, as seen in the difference in activity between compounds **D** and **F**. In this case, substitution of the hydroxy group on the 6-position with a methoxy group resulted in an increase in activity.

In contrast, the compounds proved to be potent COMT inhibitors with IC_{50} values ranging from 0.162 to 1.69 µM. This is due to the use of the nitrocatechol moiety, which is present in potent COMT inhibitors. Compounds **A**–**E** and **N** showed more potent inhibition than the reference drugs tolcapone (0.26 µM) and entacapone (0.25 µM). Compound **H**, a thiochromanone, showed the lowest activity, possibly due a loss of polar interaction with COMT. The indanone compounds proved to be higher potency COMT inhibitors compared to the tetralones, and either a methoxy or hydroxy at the 5-position of the bicyclic system are suitable for COMT inhibition.

It may be concluded that some of the compounds investigated in this study exhibit dual inhibition of MAO-B and COMT, thus the hypothesis of designing dual inhibitors by hybridisation of active moieties is possible. Due to potent COMT inhibition and average MAO-B inhibition values expressed by compounds **G** and **L**, it can be postulated that these molecules can conserve endogenous dopamine levels and show promise as therapies in PD.

However, when the physicochemical properties are taken into account, these compounds showed in *in silico* simulations that the brain penetration is very low. The tPSA of the compounds are too high to be properly absorbed though the BBB. This will lead to a very low concentration in the

CNS and the targeted enzymes will not be reached. COMT in the periphery will, however, be adequately inhibited, thus increasing the amount of unaltered or non-metabolised L-dopa from conventional PD therapy. The absorption of these compounds from the gastrointestinal tract may be good, as seen by the CLogP values of 1–3. The potential use of these compounds in conjunction with an AADC inhibitor can show promise in the future, as both of these therapies will inhibit the peripheral metabolism of L-dopa.

Certain assays that could have been included in this study is the ORAC (oxygen radical absorbance capacity), FRAP (ferric oxidation/reduction) and TBARS (thioburbituric acid-reactive substances) assays (Greeff *et al*., 2012). These assays test for antioxidant potency, and since neurodegenerative disease such as PD are associated with oxidative stress and oxidative damage, this could show a possible third mechanism of action for the chalcones in this study.

Other possible nitrocatechol derivatives of chalcone may also be synthesised to be evaluated for inhibitory action future studies. These are 6,7-dihydroxy-5-nitro-3,4-dihydronaphthalen-1(2*H*)-one or 5,6-dihydroxy-4-nitro-2,3-dihydro-1*H*-inden-1-one derivatives. In this case, the nitrocatechol moiety is part of the bicyclic scaffold as seen in figure 4-1. This would be an investigational study that may attempt to enhance MAO-B inhibition.

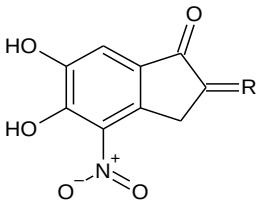

5,6-dihydroxy-4-nitro-2,3-dihydro-1*H*-inden-1-one

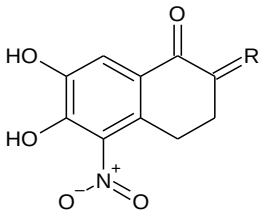

6,7-dihydroxy-5-nitro-3,4-dihydronaphthalen-1(2*H*)-one

Figure 4-1: Nitrocatechol derivatives to be investigated in future studies.

The success is this study may be attributed to hybridisation, a now acceptable method of drug design. The conclusions of this study can be used in future studies to design more potent dual inhibitors of COMT and MAO-B.

4.2 Future dual inhibitors of COMT and MAO-B

The use of the catechol moiety can be problematic since it is a moiety shared with many endogenous neurotransmitters. This can be overcome by replacing the moiety used for COMT inhibition. The large tPSA may be reduced by replacing the nitrocatechol for *N*-heterocyclic pyridinones as reported in literature (Zhao *et. al.,* 2016). Literature has shown that derivatives of N-heterocyclic pyridinones has potent COMT inhibition properties when tested against the

membrane-bound COMT isoform. Compound **1a** this has an IC_{50} value of 40 nM for the inhibition of COMT, followed by **1b** with an IC_{50} of 35 nM (Zhao *et al*., 2016). The pharmacophore of this series is the 3-hydroxy-4-pyridinone system.

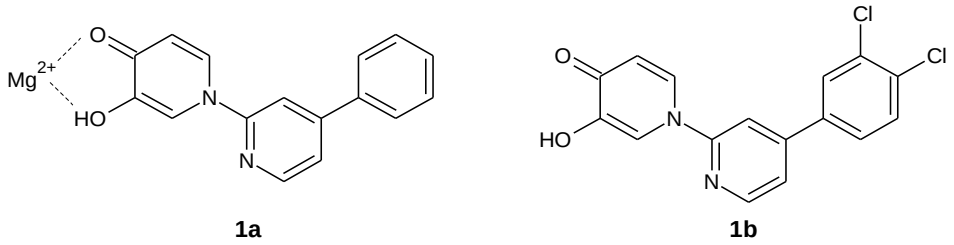

1a **1b**

Figure 4-2: Structures discussed in text (Zhao *et al*., 2016).

Literature reports that bicyclic systems are often good potency MAO-B inhibitors (Section 3.3.5, Figure 3-5). In a study by Meiring *et al.* (2013), a series of 3,4-dihydro-2(1*H*)-quinolinone derivatives were synthesised and evaluated as human MAO inhibitors. This study showed that substitution of 3,4-dihydro-2(1*H*)-quinolinone with the benzoyloxy moiety produced potent inhibitors (IC_{50} values of 0.0062 µM [**2a**] and 0.0029 µM [**2b**], respectively), which are all selective for MAO-B (selectivity index of 2751). Both inhibitors showed reversible inhibition in dialysis studies. The study concluded that the bromine substituent on the benzyloxy ring is more potent than the chlorine substituent, and that placement of the benzyloxy moiety on the C7 position resulted in better overall inhibition compared to the C6 position (Meiring *et al*., 2013)

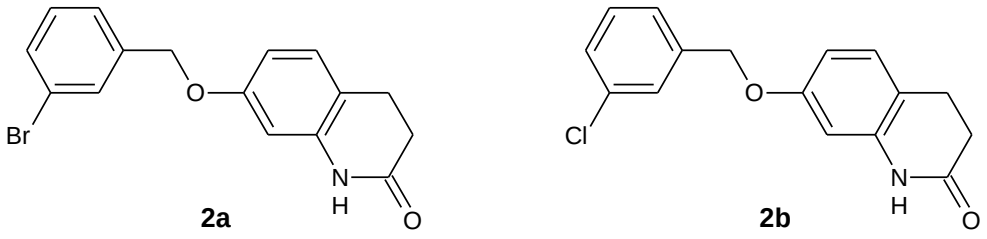

2a **2b**

Figure 4-3: Structures of 3,4-dihydro-2(1*H*)-quinolinone derivatives discussed in the text (Meiring *et al*., 2013).

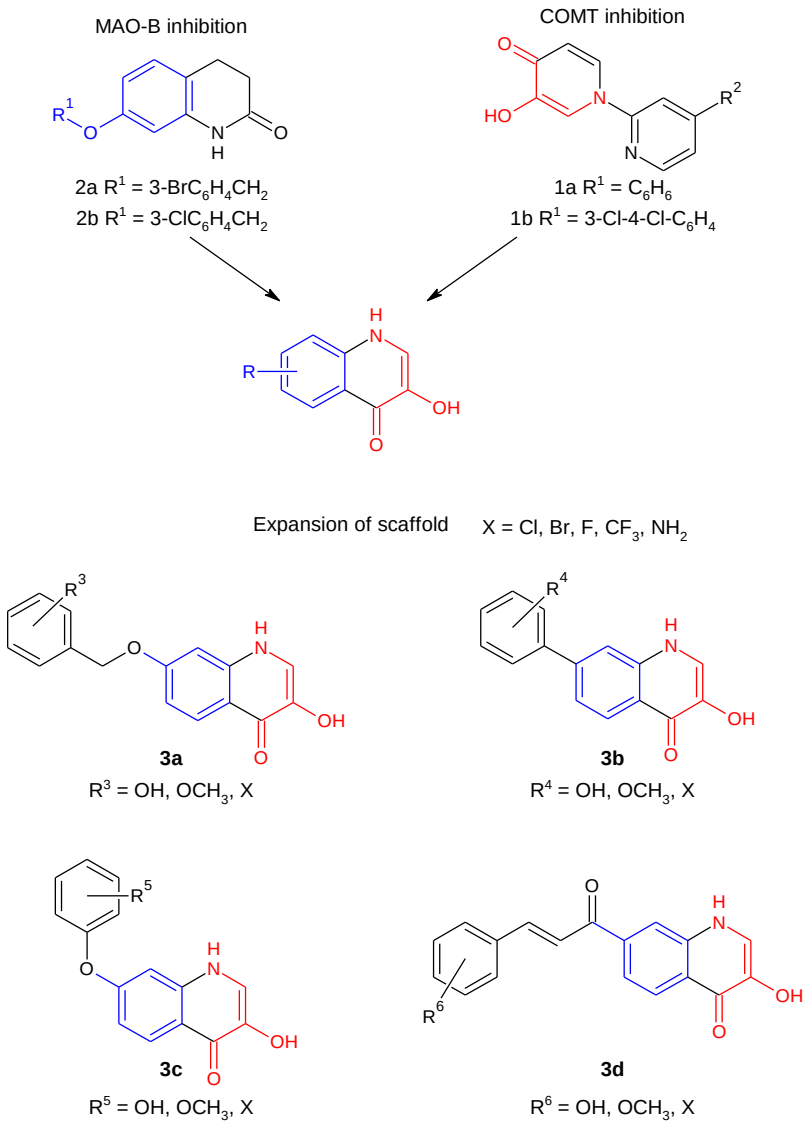

Figure 4-4: Hybridisation strategy for the 3-hydroxyquinolin-4(1*H*)-one derivatives as dual MAO and COMT inhibitors.

With these two studies in mind, a new hybrid structure can be proposed that combines the quinolinone scaffold with the N-heterocyclic pyridinone moiety as seen in Figure 4-4. These new hybrid compounds can be substituted with hydroxy- and methoxy-containing benzyloxy substituents (**3a**), phenyl substituents (**3b**), phenoxy substituents (**3c**) or the beta-styryl ketone (**3d**). Phenyl or phenyloxy derivatives can mimic the chalcone structure, while the hybrid compounds substituted with beta-styryl ketone will closely resemble the structure of chalcone (Duarte *et. al.,* 2007).

Oxidative stress is described as an imbalance between pro-oxidants (reactive oxygen species) and anti-oxidants (Patel, 2016). This leads to many secondary complications, many of which further increases oxidative stress, such as neuroinflammation, increased macrophage activation and permeation of mitochondrial cell walls (Berman & Hastings, 1999; Blesa *et al*., 2015; Ebadi *et al*., 1996; Meiser *et al.*, 2013). A previous study showed the potential of 4-quinolones and related flavones as antioxidants (**4a**–**b**), and the results indicated that substitution with hydrogen donating substituents increases antioxidant effect, as shown with assays for ORAC (oxygen radical absorbance capacity), FRAP (ferric oxidation/reduction) and TBARS (thioburbituric acid-reactive substances) (Greeff *et al*., 2012). The proposed hybrid derivatives **3a**–**d** show similarity in structures to these 4-quinolones, which suggest that **3a**–**d** may possess antioxidant activities. This would further increase their relevance to the treatment of PD

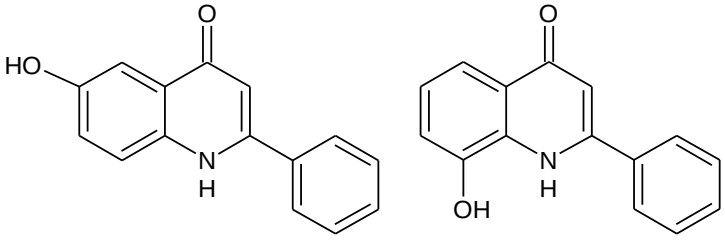

4a **4b**

Figure 4-5: 2-Phenylquinolin-4(1*H*)-one derivatives that showed antioxidant activity in a previous study (Greeff *et al*., 2012).

REFERENCES:

Berman, S.B. & Hastings, T.G. 1999. Dopamine oxidation alters mitochondrial respiration and induces permeability transition in brain mitochondria: implications for Parkinson's disease. *Journal of Neurochemistry*, 73(3):1127-1137.

Blesa, J., Trigo-Damas, I., Quiroga-Varela, A. & Jackson-Lewis, V.R. 2015. Oxidative stress and Parkinson's disease. *Frontiers in Neuroanatomy*, 9:91.

Duarte, C.D., Barreiro, E.J. & Fraga, C.A. 2007. Privileged structures: a useful concept for the rational design of new lead drug candidates. *Mini Reviews in Medicinal Chemistry*, 7(11):1108-1119.

Ebadi, M., Srinivasan, S.K. & Baxi, M.D. 1996. Oxidative stress and antioxidant therapy in Parkinson's disease. *Progress in Neurobiology*, 48(1):1-19.

Greeff, J., Joubert, J., Malan, S.F. & van Dyk, S. 2012. Antioxidant properties of 4-quinolones and structurally related flavones. *Bioorganic & Medicinal Chemistry*, 20(2):809-818.

Meiring, L., Petzer, J.P. & Petzer, A. 2013. Inhibition of monoamine oxidase by 3, 4-dihydro-2 (1H)-quinolinone derivatives. *Bioorganic & Medicinal Chemistry Letters*, 23(20):5498-5502.

Meiser, J., Weindl, D., Hiller, K. 2013. Complexity of dopamine metabolism. *Cell Communication and Signaling*, 11(34):18.

Patel, M. 2016. Targeting oxidative stress in central nervous system disorders. *Trends in Pharmacological Sciences*, 37(9):768-778.

Zhao, Z., Harrison, S.T., Schubert, J.W., Sanders, J.M., Polsky-Fisher, S., Zhang, N.R*., et al.* 2016. Synthesis and optimization of N-heterocyclic pyridinones as catechol-O-methyltransferase (COMT) inhibitors. *Bioorganic & Medicinal Chemistry Letters*, 26(12):2952-2956.

ANNEXURE A ^{1}H AND ^{13}C NMR SPECTRA

(2*E*)-2-(3,4-Dihydroxy-5-nitrobenzylidene)-2,3-dihydro-1*H*-inden-1-one (A) [^{1}H NMR]

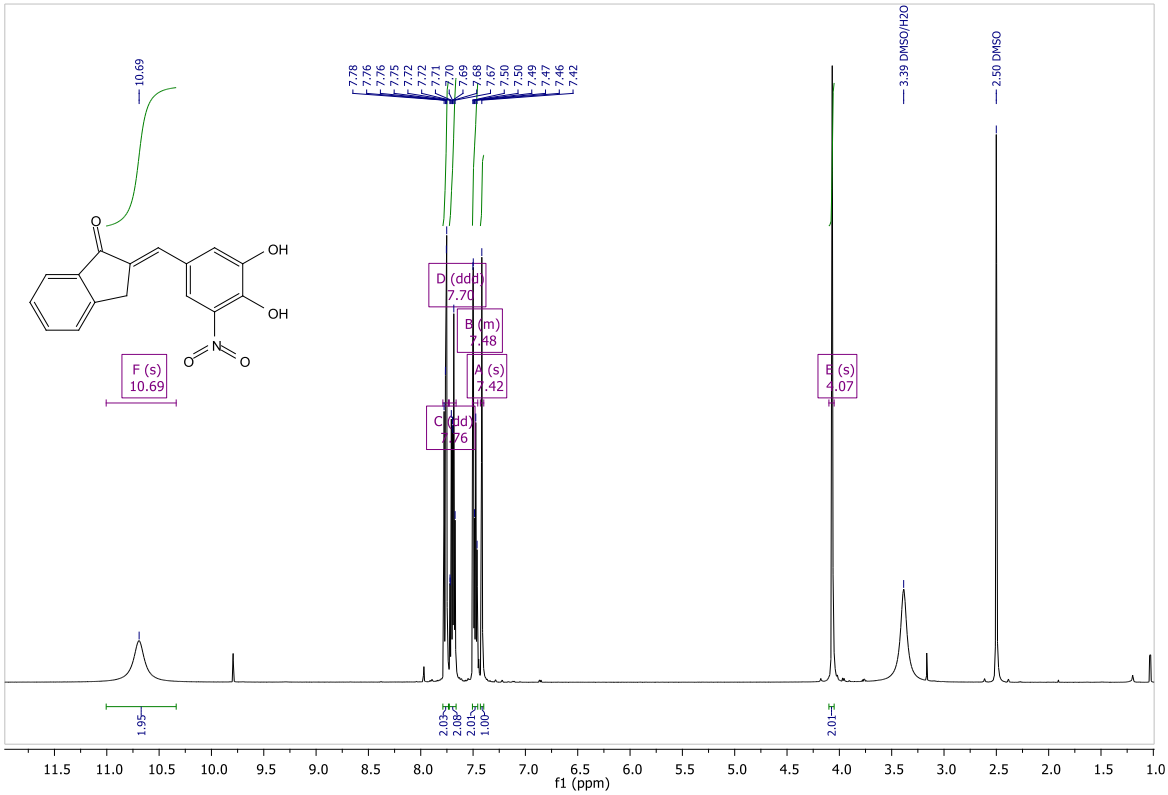

(2*E*)-2-(3,4-Dihydroxy-5-nitrobenzylidene)-2,3-dihydro-1*H*-inden-1-one (A) [^{13}C NMR]

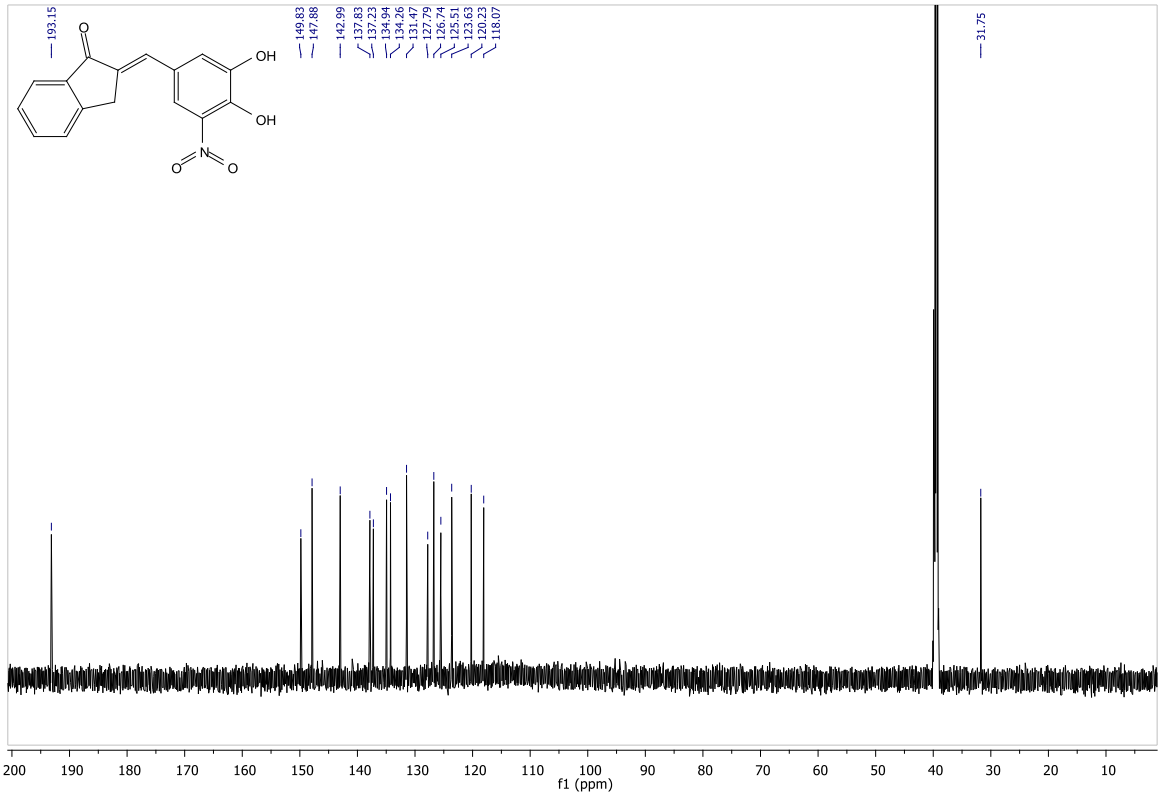

(2*E*)-2-(3,4-Dihydroxy-5-nitrobenzylidene)-5,6-dimethoxy-2,3-dihydro-1*H*-inden-1-one (B) [^{1}H NMR]

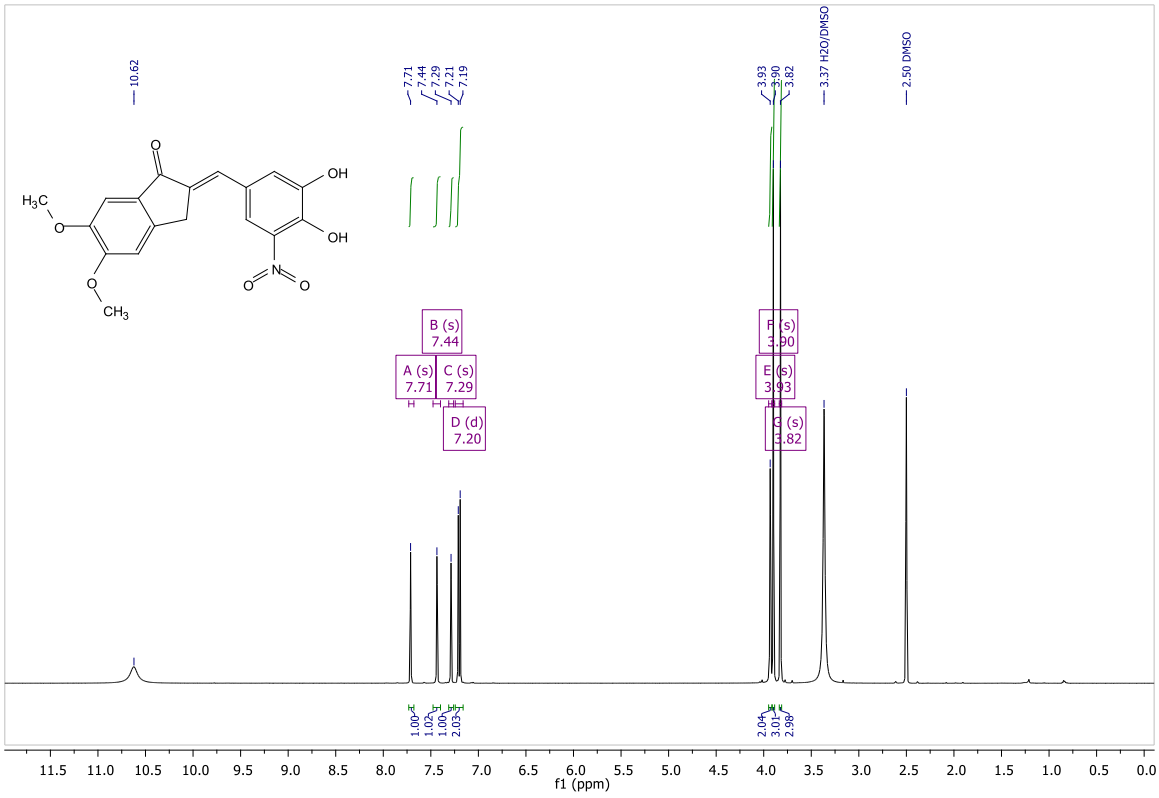

(2*E*)-2-(3,4-Dihydroxy-5-nitrobenzylidene)-5,6-dimethoxy-2,3-dihydro-1*H*-inden-1-one (B) [^{13}C NMR]

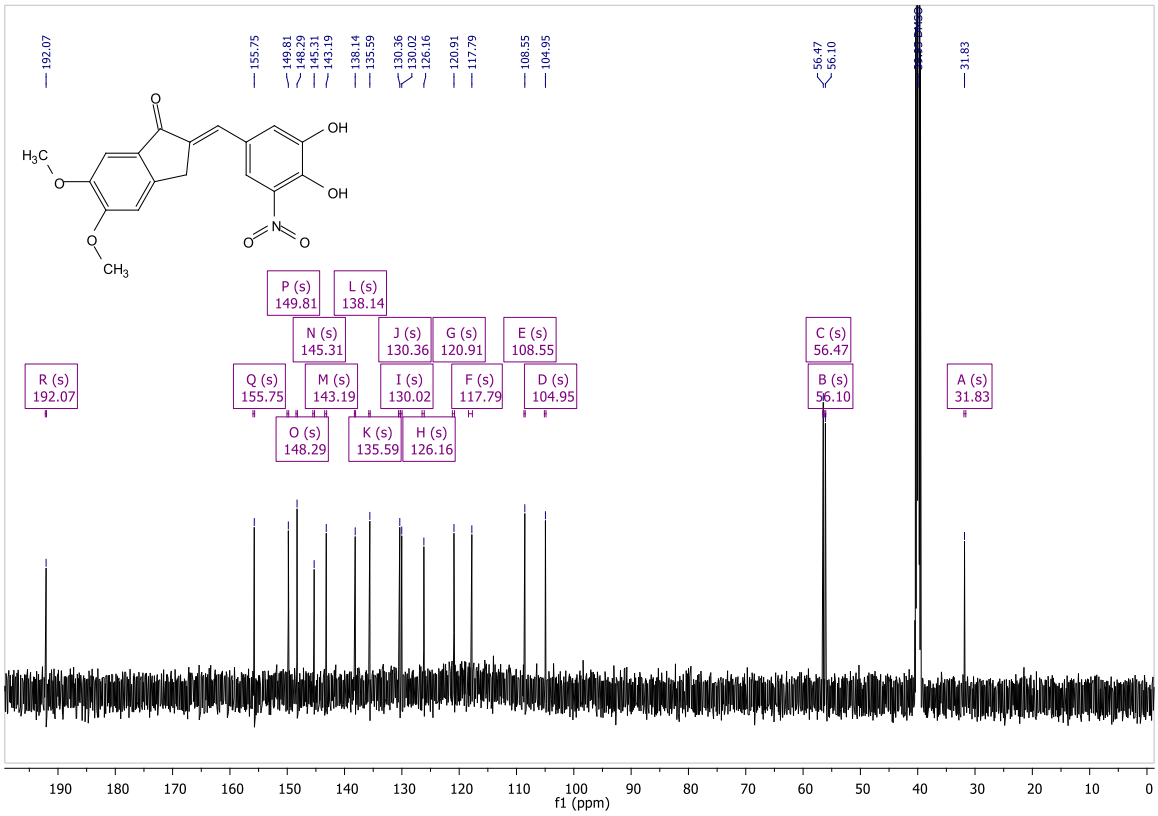

(6*E*)-6-(3,4-Dihydroxy-5-nitrobenzylidene)-6,7-dihydro-5*H*-indeno[5,6-*d*][1,3]dioxol-5-one (C) [^{1}H NMR]

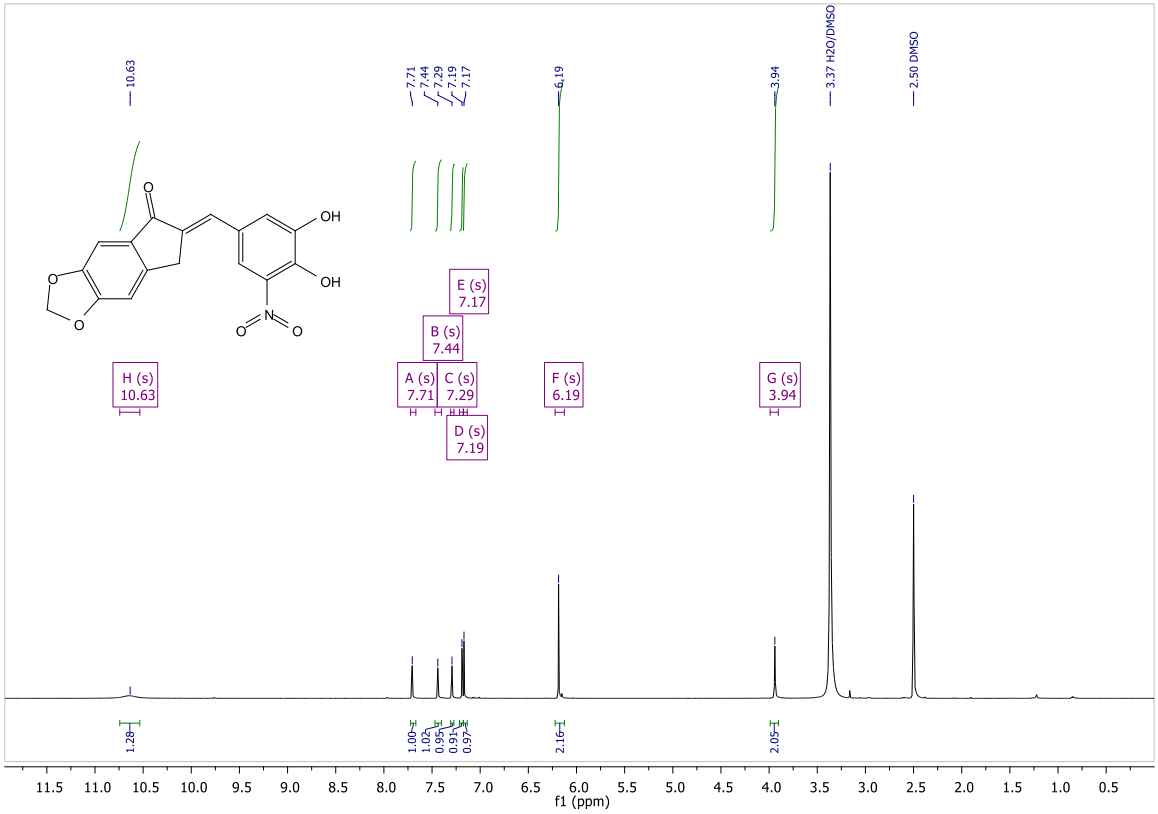

(2*E*)-2-(3,4-Dihydroxy-5-nitrobenzylidene)-5-methoxy-2,3-dihydro-1*H*-inden-1-one (D) [^{1}H NMR]

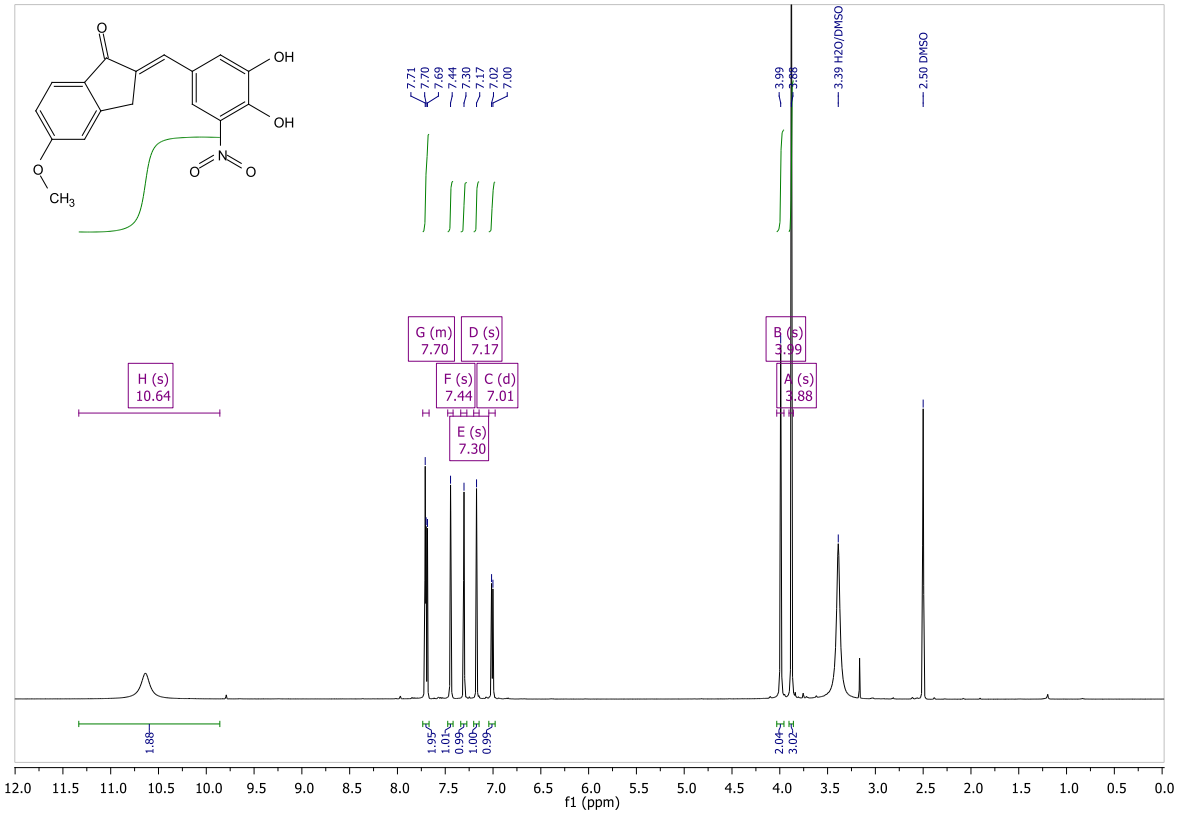

(2*E*)-2-(3,4-Dihydroxy-5-nitrobenzylidene)-5-methoxy-2,3-dihydro-1*H*-inden-1-one (D) [^{13}C NMR]

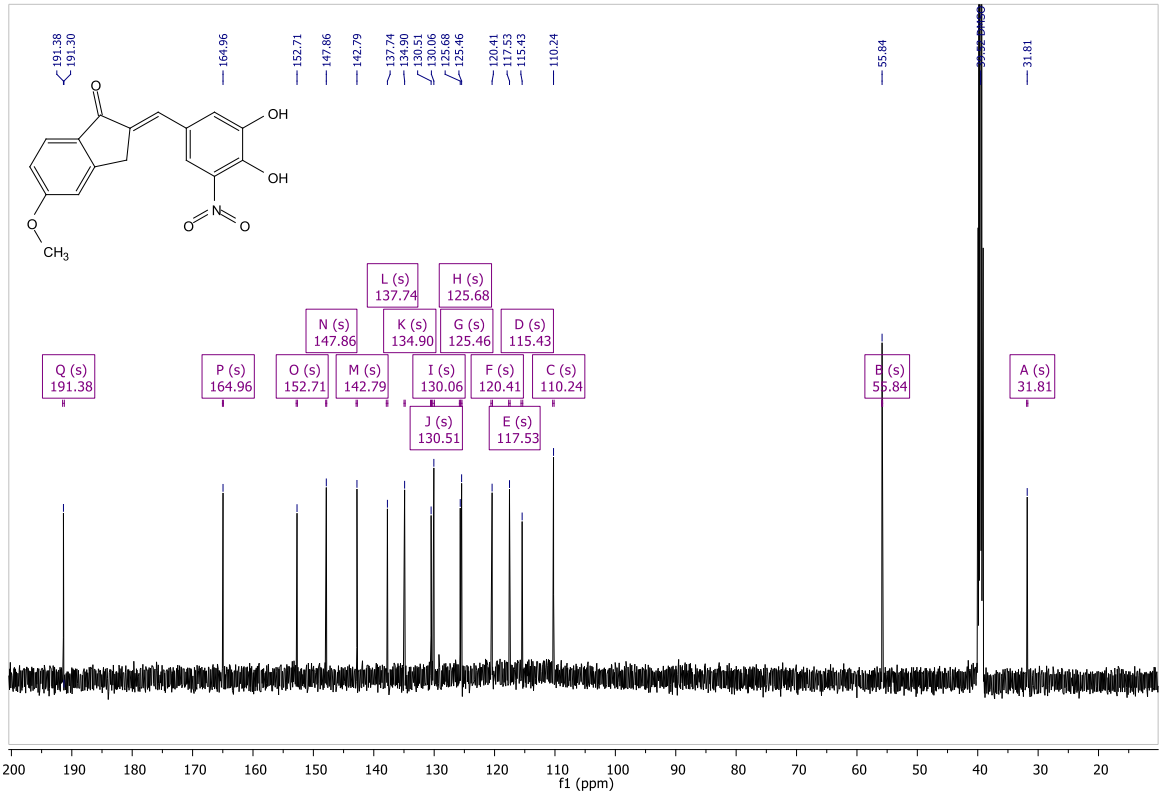

(2*Z*)-2-(3,4-Dihydroxy-5-nitrobenzylidene)-6-hydroxy-1-benzofuran-3(2*H*)-one (E) [^{1}H NMR]

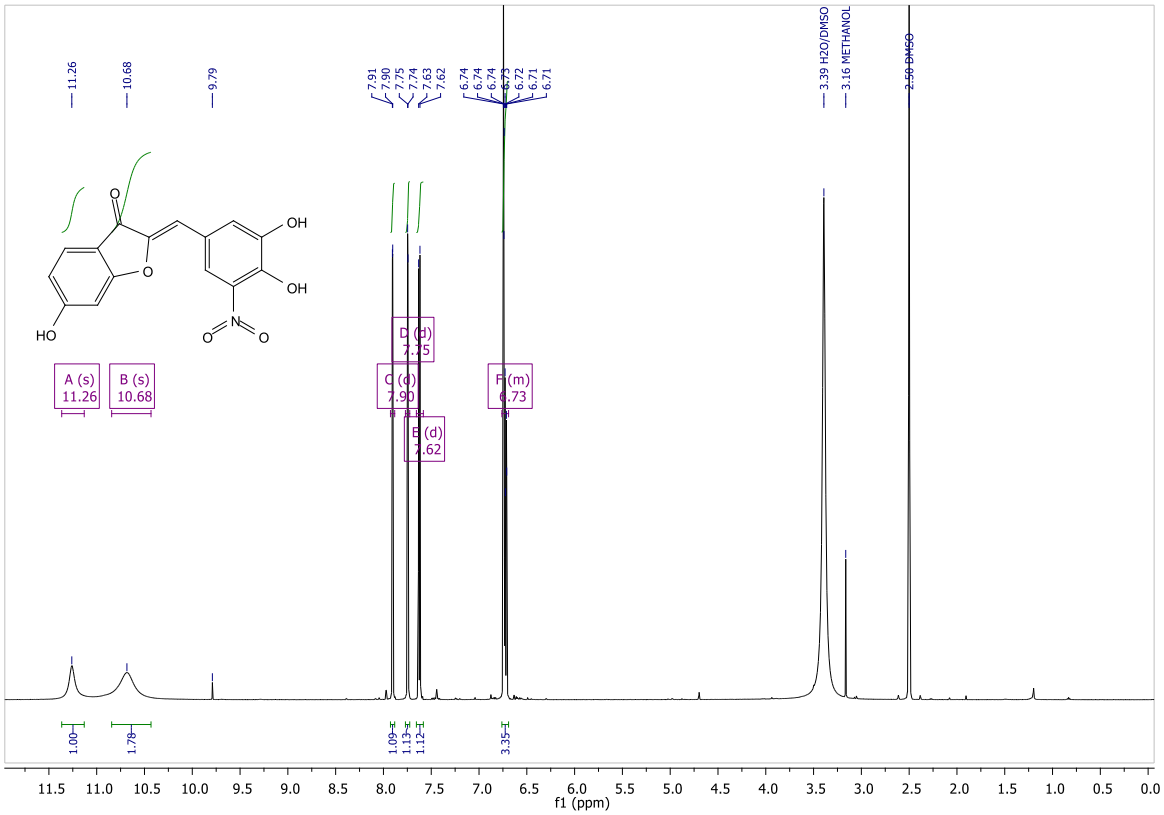

(2*Z*)-2-(3,4-Dihydroxy-5-nitrobenzylidene)-6-hydroxy-1-benzofuran-3(2*H*)-one (E) [^{13}C NMR]

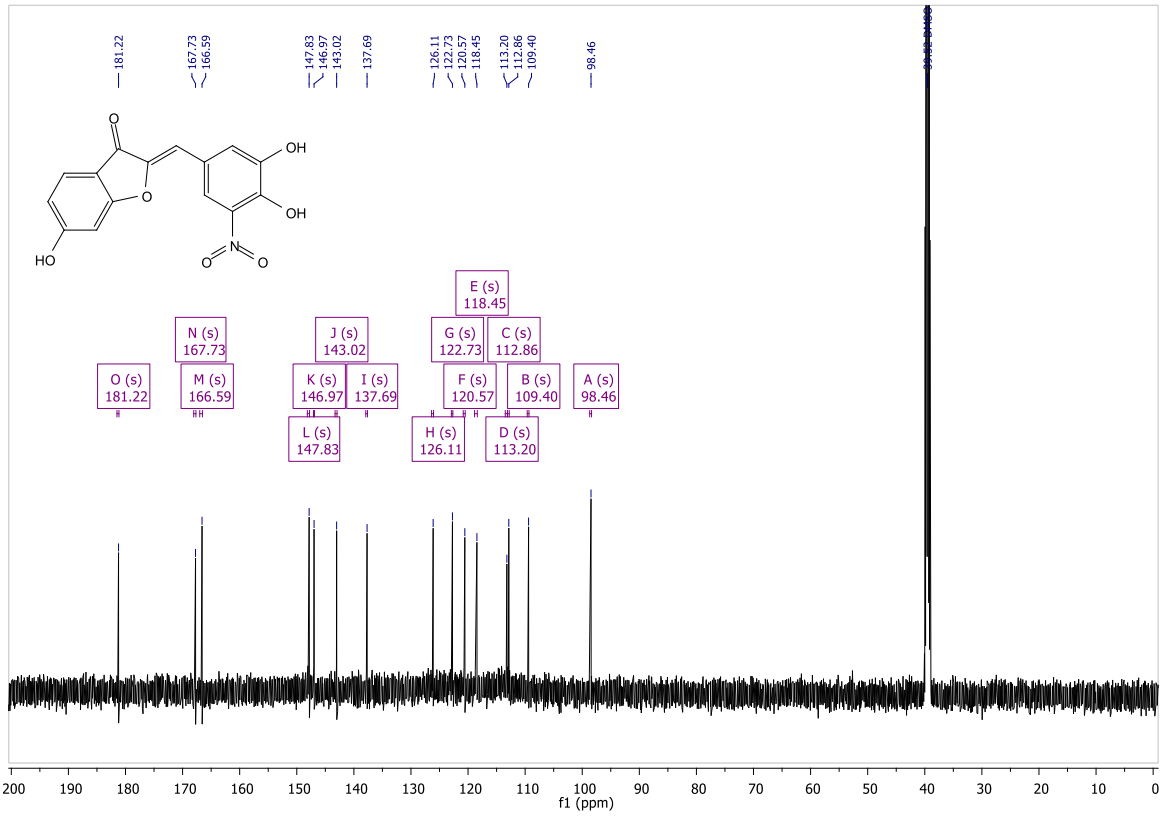

(2*E*)-2-(3,4-Dihydroxy-5-nitrobenzylidene)-5-hydroxy-2,3-dihydro-1*H*-inden-1-one (F) [^{1}H NMR]

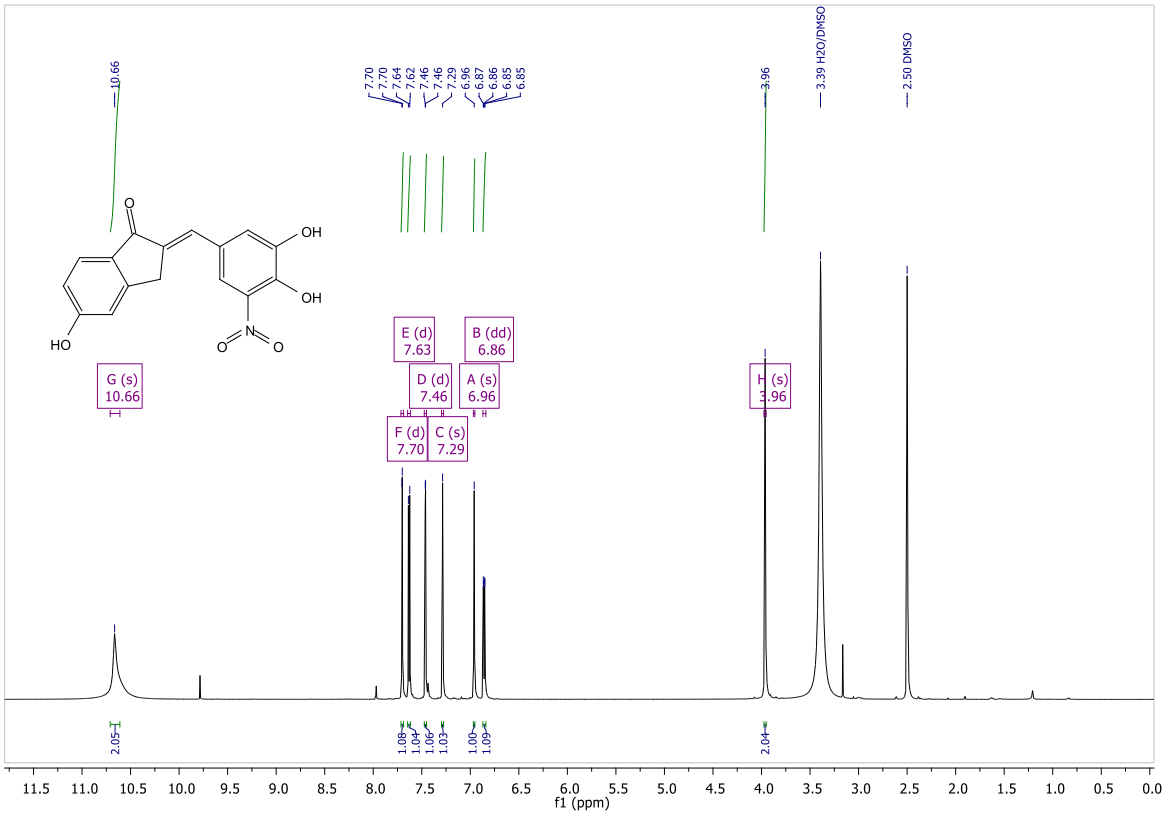

(2*E*)-2-(3,4-Dihydroxy-5-nitrobenzylidene)-5-hydroxy-2,3-dihydro-1*H*-inden-1-one (F) [^{13}C NMR]

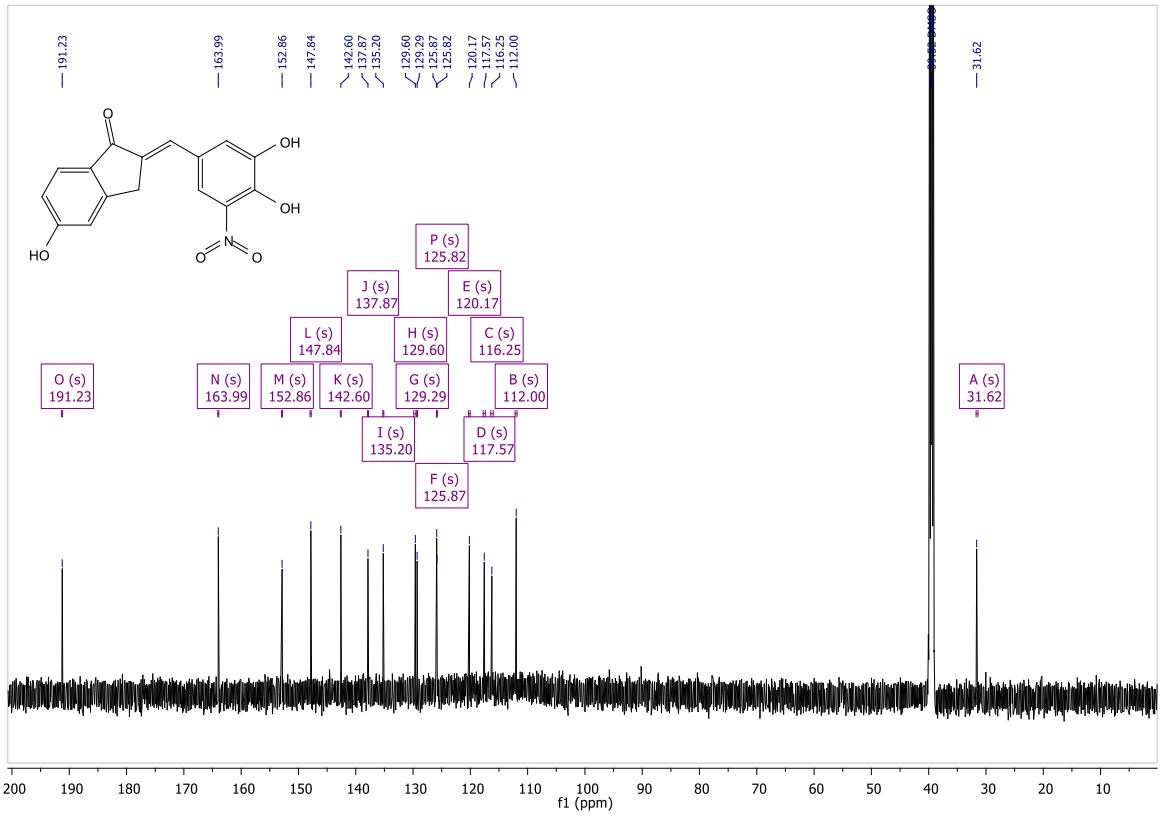

(3*E*)-3-(3,4-Dihydroxy-5-nitrobenzylidene)-2,3-dihydro-4*H*-chromen-4-one (G) [^{1}H NMR]

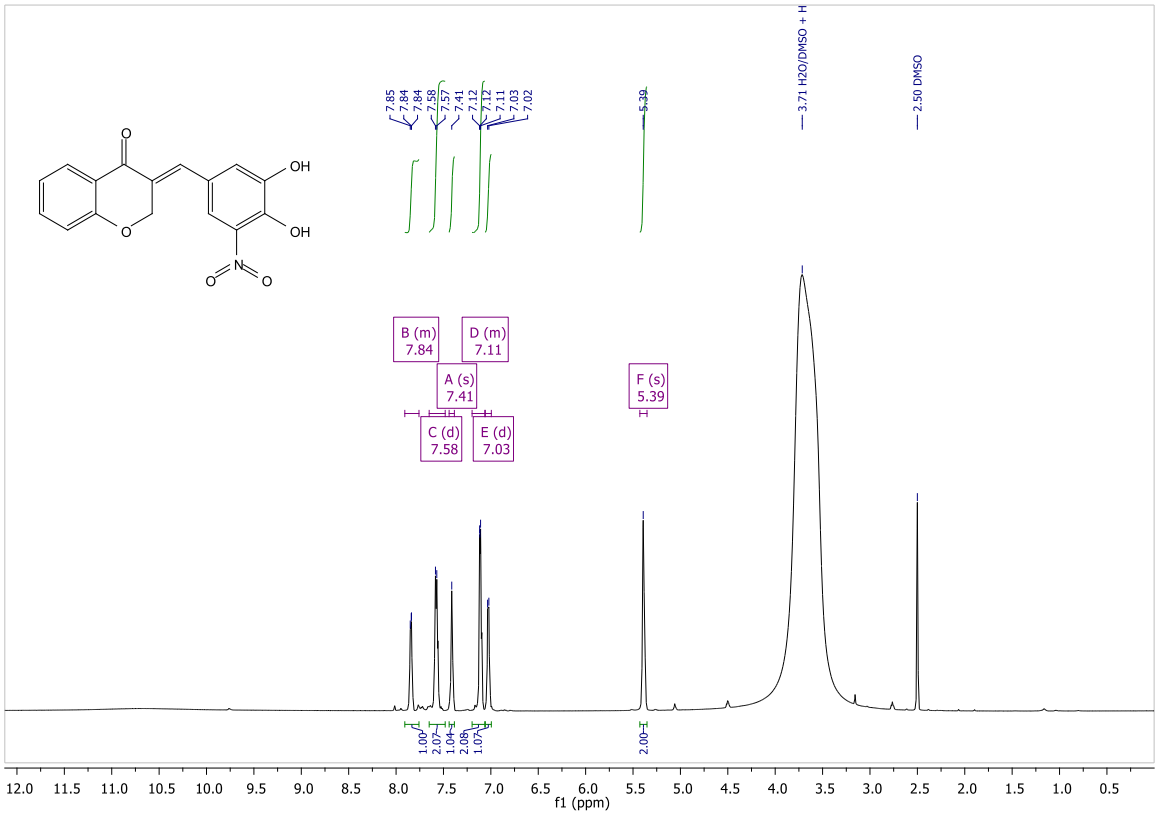

(3*E*)-3-(3,4-Dihydroxy-5-nitrobenzylidene)-2,3-dihydro-4*H*-chromen-4-one (G) [^{13}C NMR]

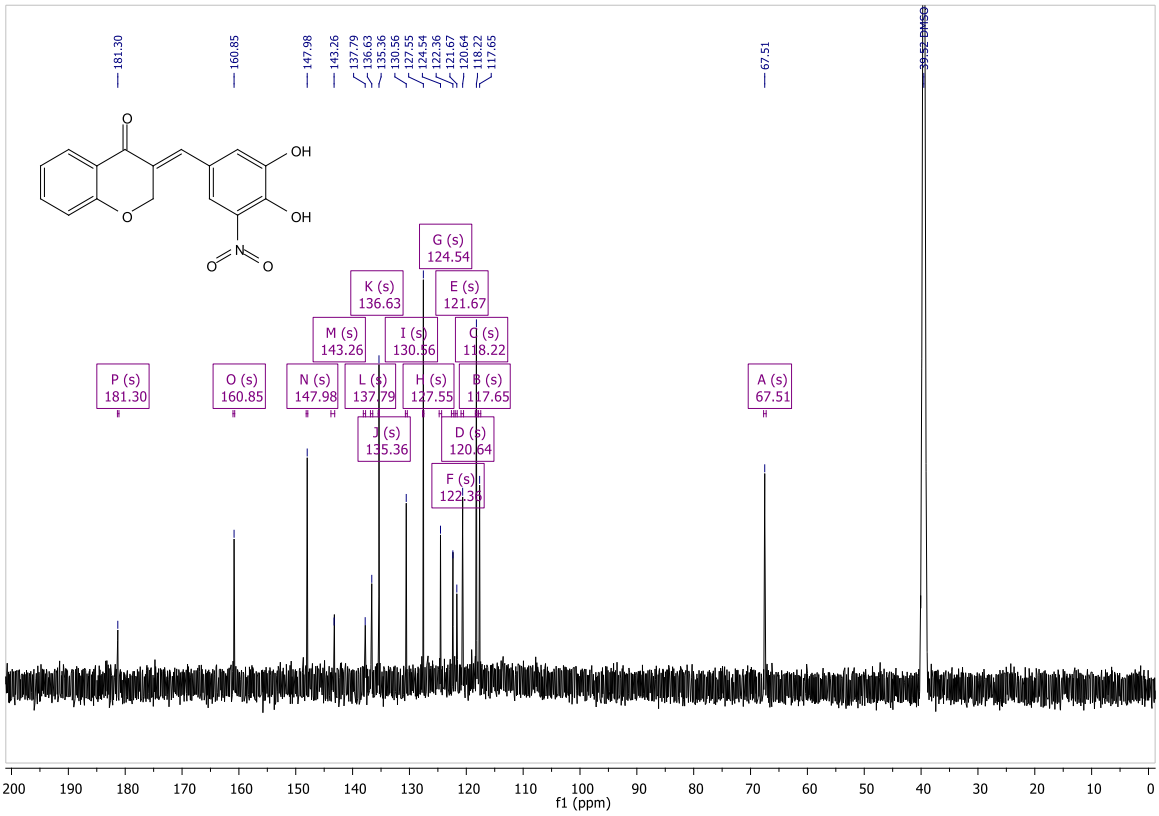

(3*Z*)-3-(3,4-Dihydroxy-5-nitrobenzylidene)-2,3-dihydro-4*H*-thiochromen-4-one (H) [^{1}H NMR]

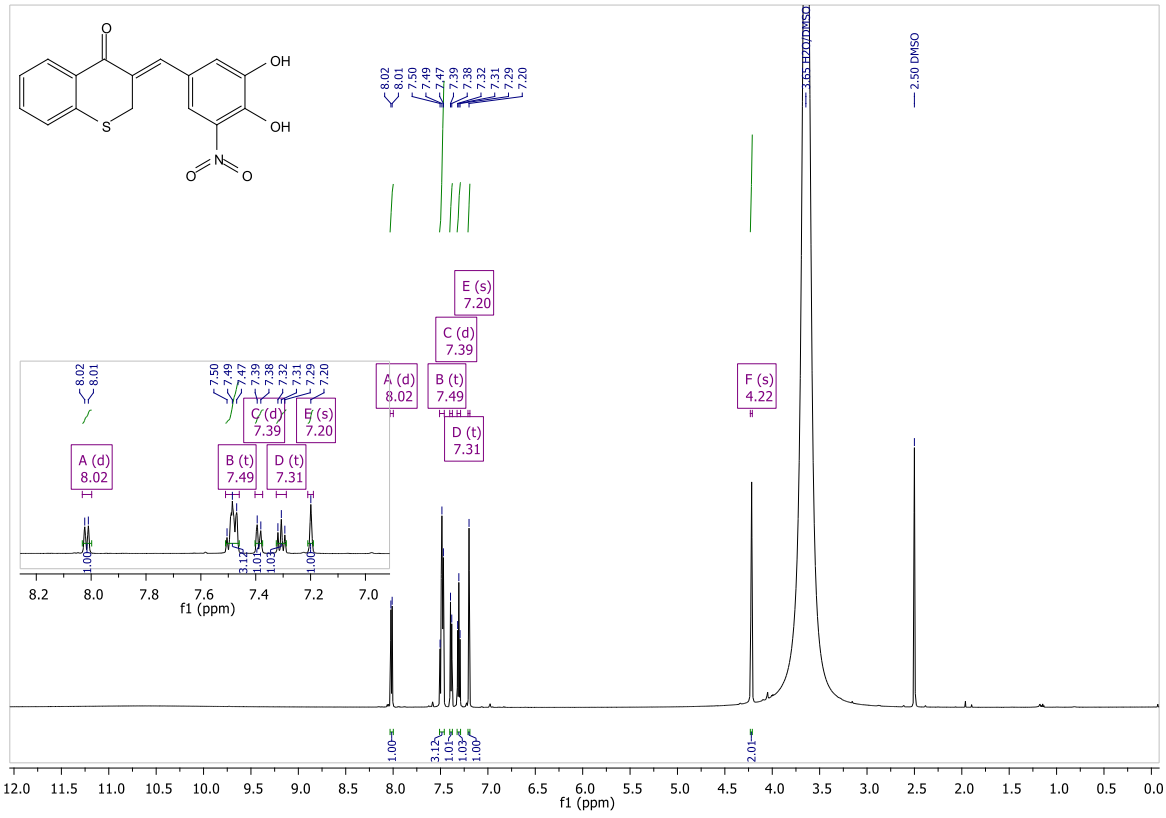

(3*Z*)-3-(3,4-Dihydroxy-5-nitrobenzylidene)-2,3-dihydro-4*H*-thiochromen-4-one (H) [^{13}C NMR]

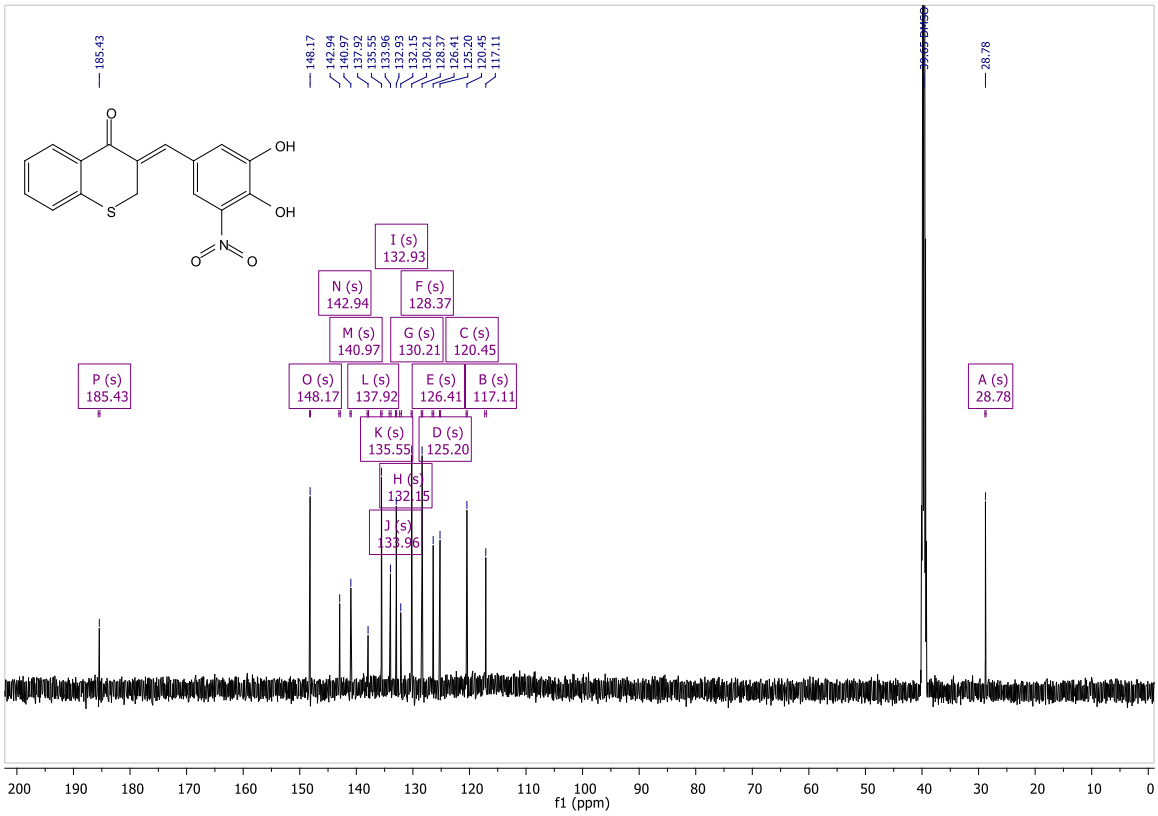

(2*E*)-2-(3,4-Dihydroxy-5-nitrobenzylidene)-3,4-dihydronaphthalen-1(2*H*)-one (I) [^{1}H NMR]

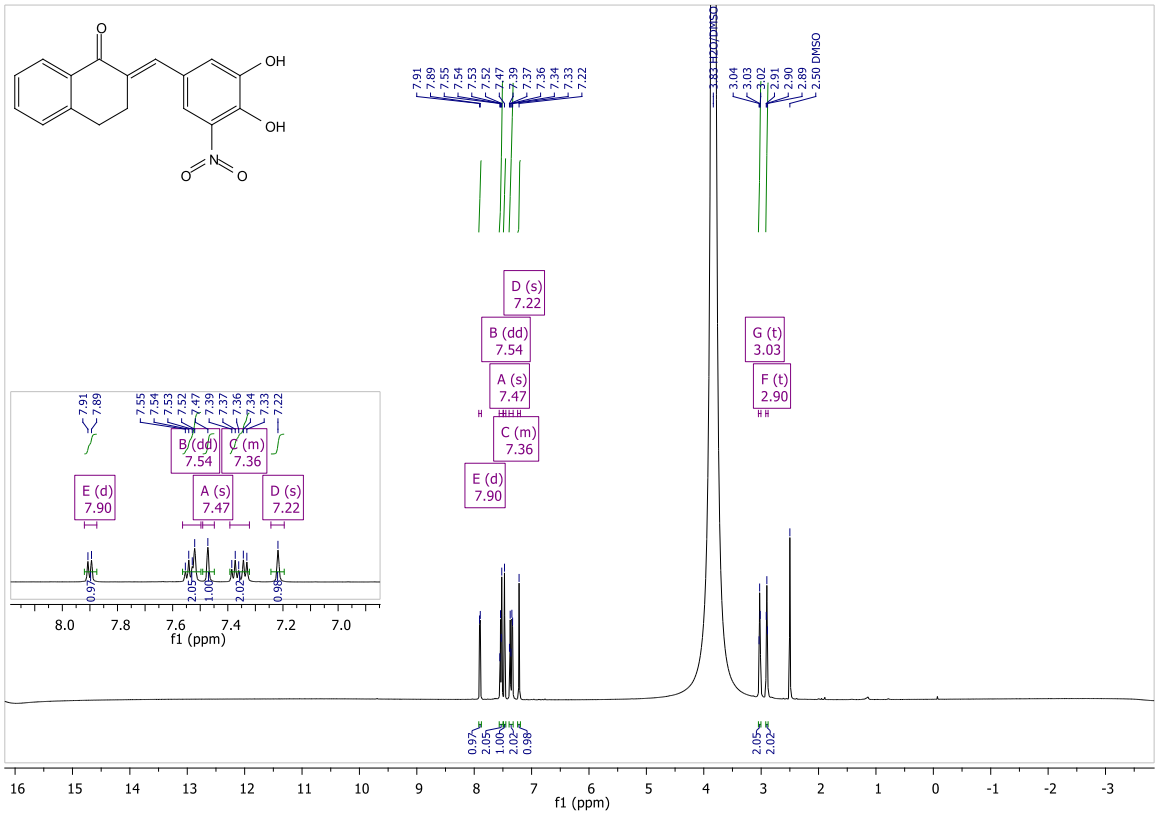

(2*E*)-2-(3,4-Dihydroxy-5-nitrobenzylidene)-3,4-dihydronaphthalen-1(2*H*)-one (I) [^{13}C NMR]

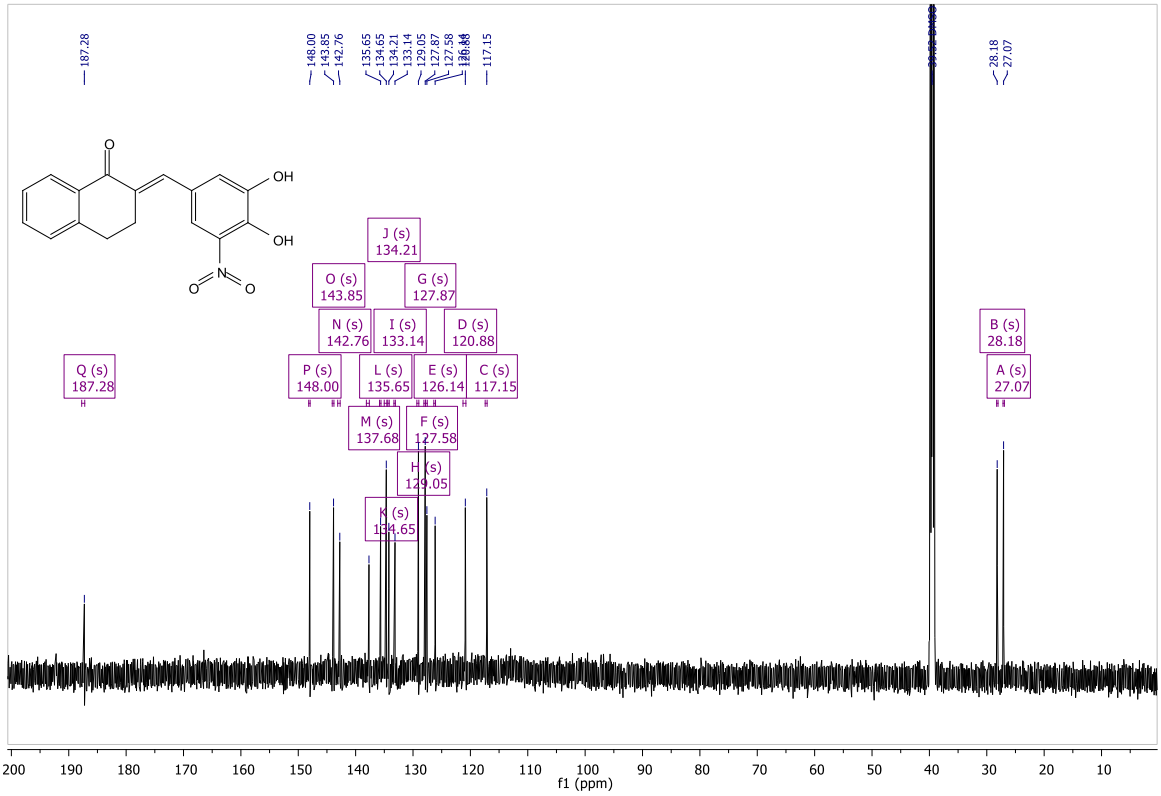

(2*E*)-2-(3,4-Dihydroxy-5-nitrobenzylidene)-6,7-dimethoxy-3,4-dihydronaphthalen-1(2*H*)-one (J) [^{1}H NMR]

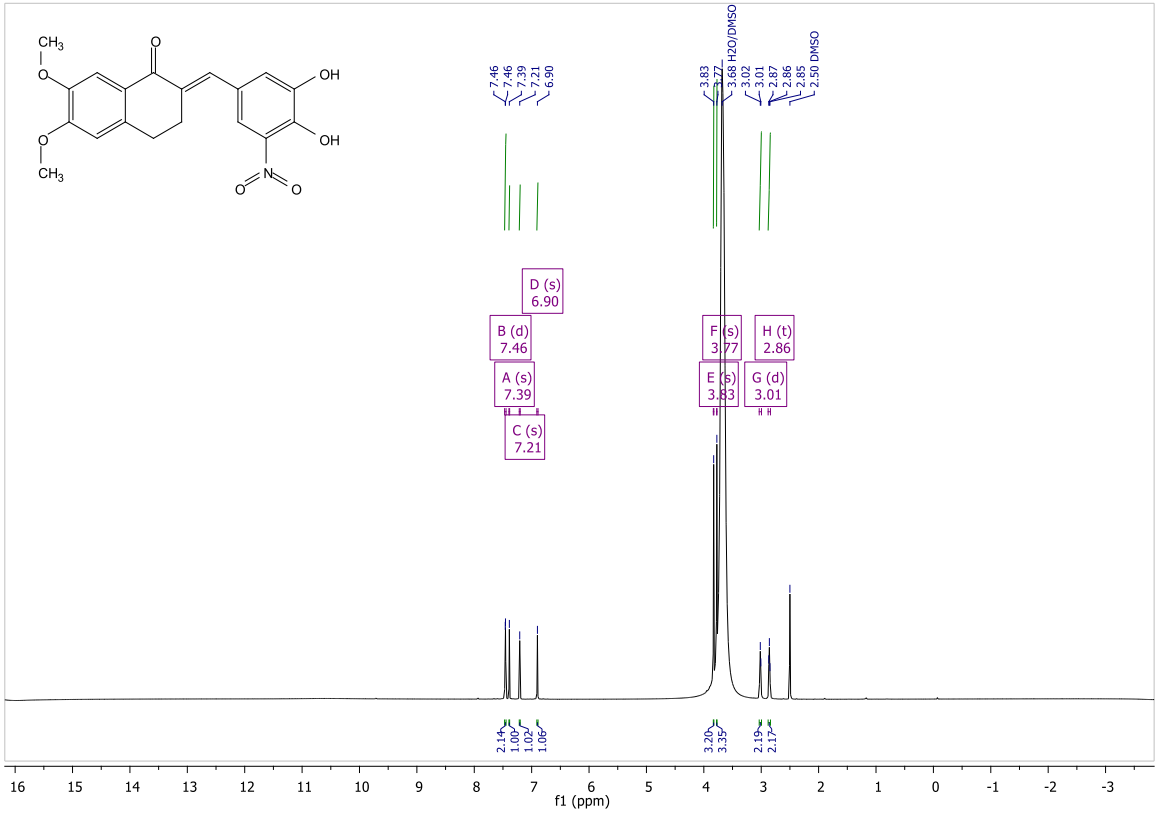

(2*E*)-2-(3,4-Dihydroxy-5-nitrobenzylidene)-6,7-dimethoxy-3,4-dihydronaphthalen-1(2*H*)-one (J) [^{13}C NMR]

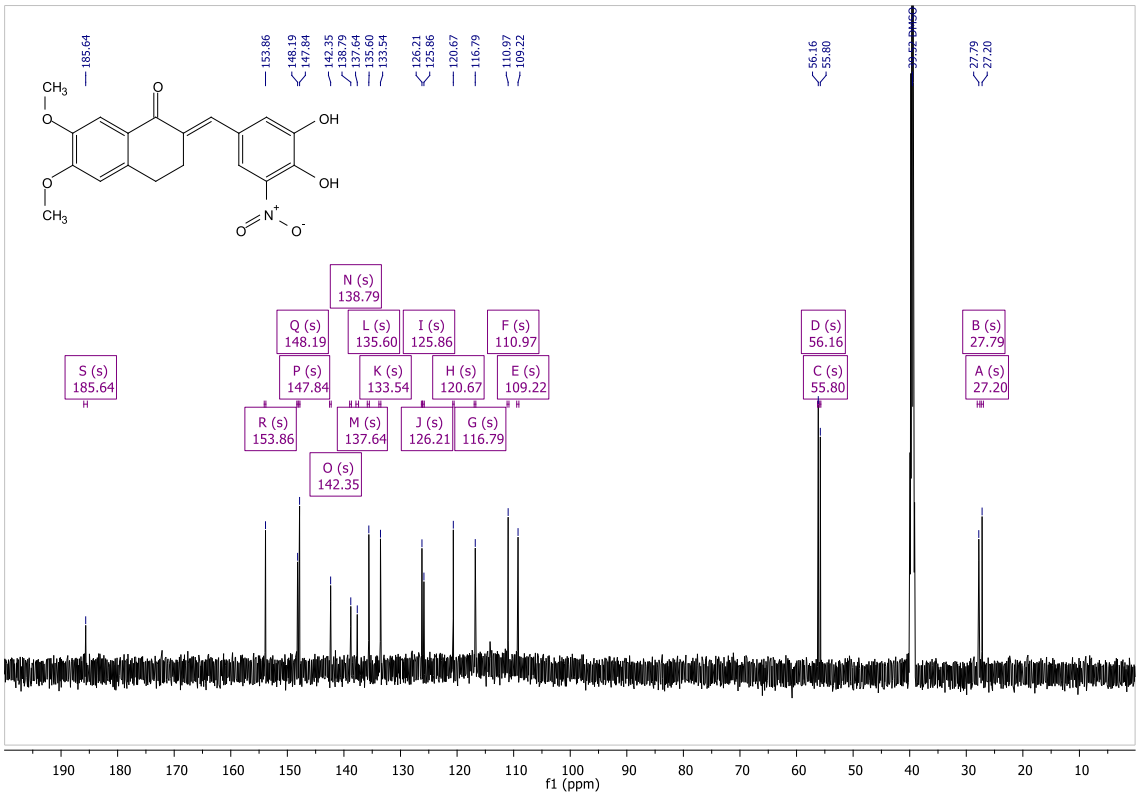

(2*E*)-2-(3,4-Dihydroxy-5-nitrobenzylidene)-6-methoxy-3,4-dihydronaphthalen-1(2*H*)-one (K) [^{1}H NMR]

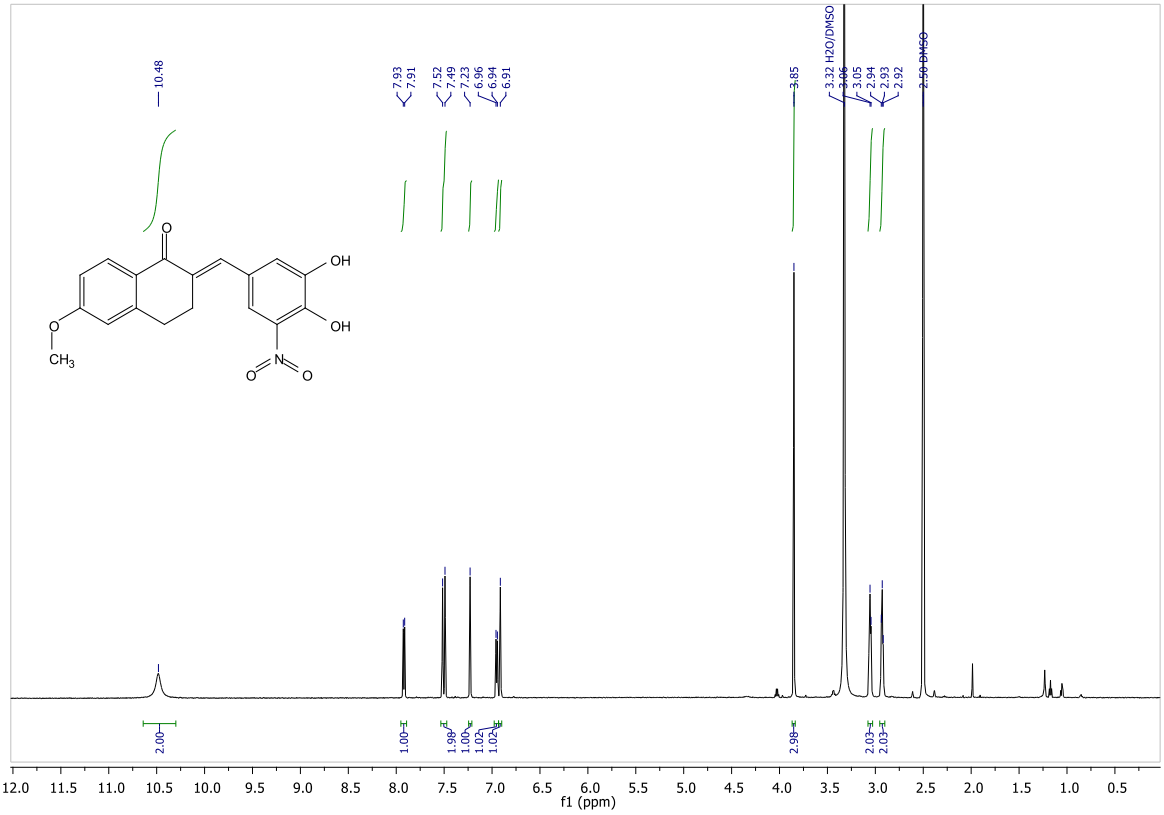

(2*E*)-2-(3,4-Dihydroxy-5-nitrobenzylidene)-6-methoxy-3,4-dihydronaphthalen-1(2*H*)-one (K) [^{13}C NMR]

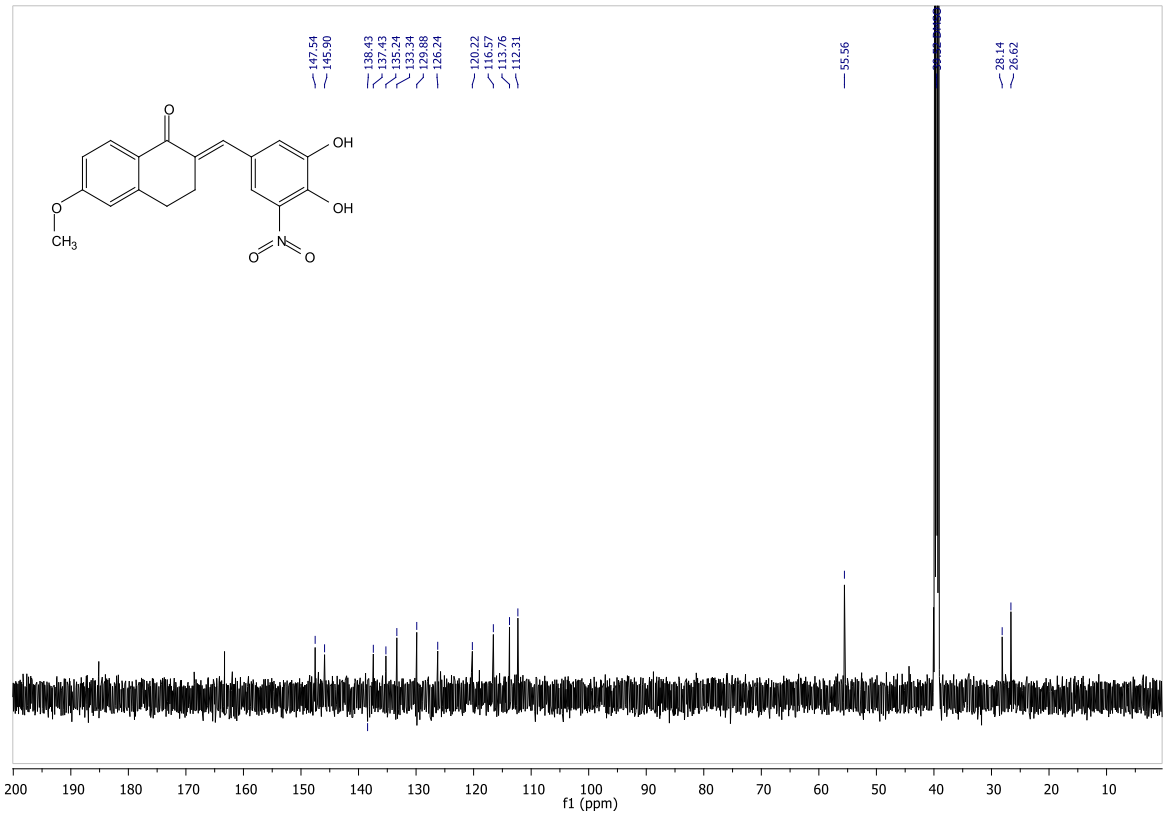

(2*E*)-2-(3,4-Dihydroxy-5-nitrobenzylidene)-5-methoxy-3,4-dihydronaphthalen-1(2*H*)-one (L) [^{1}H NMR]

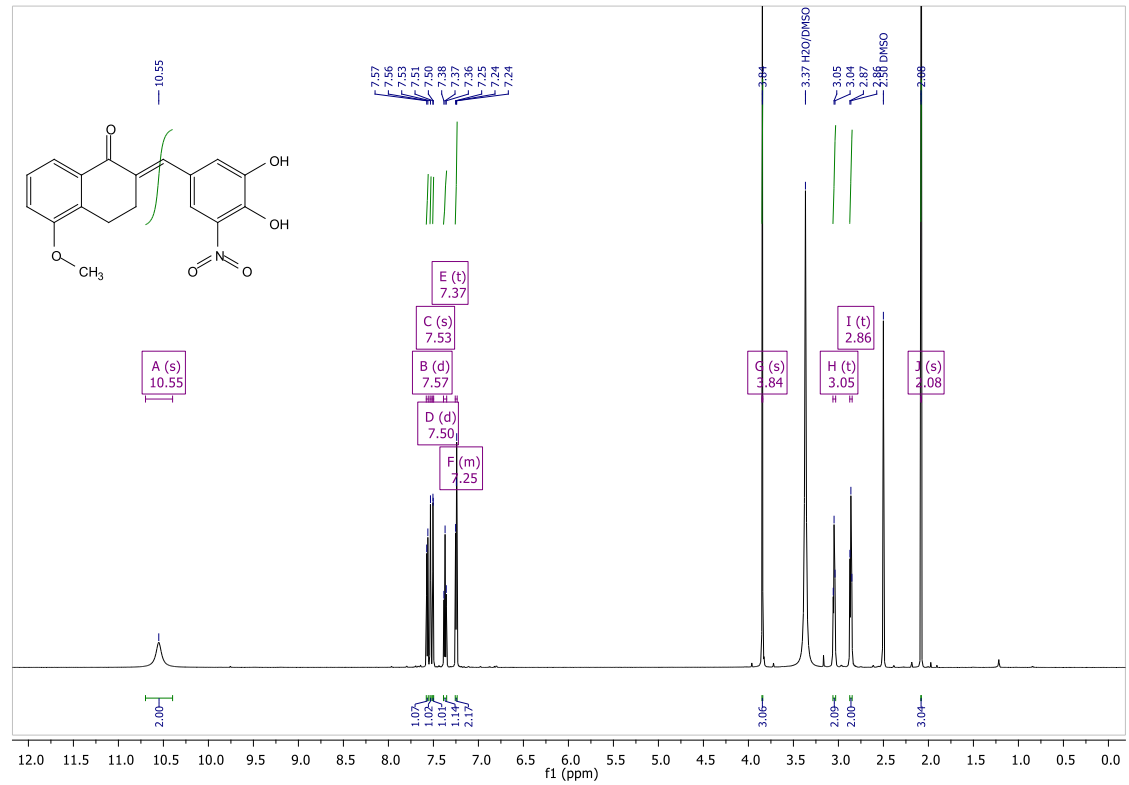

(2*E*)-2-(3,4-Dihydroxy-5-nitrobenzylidene)-5-methoxy-3,4-dihydronaphthalen-1(2*H*)-one (L) [^{13}C NMR]

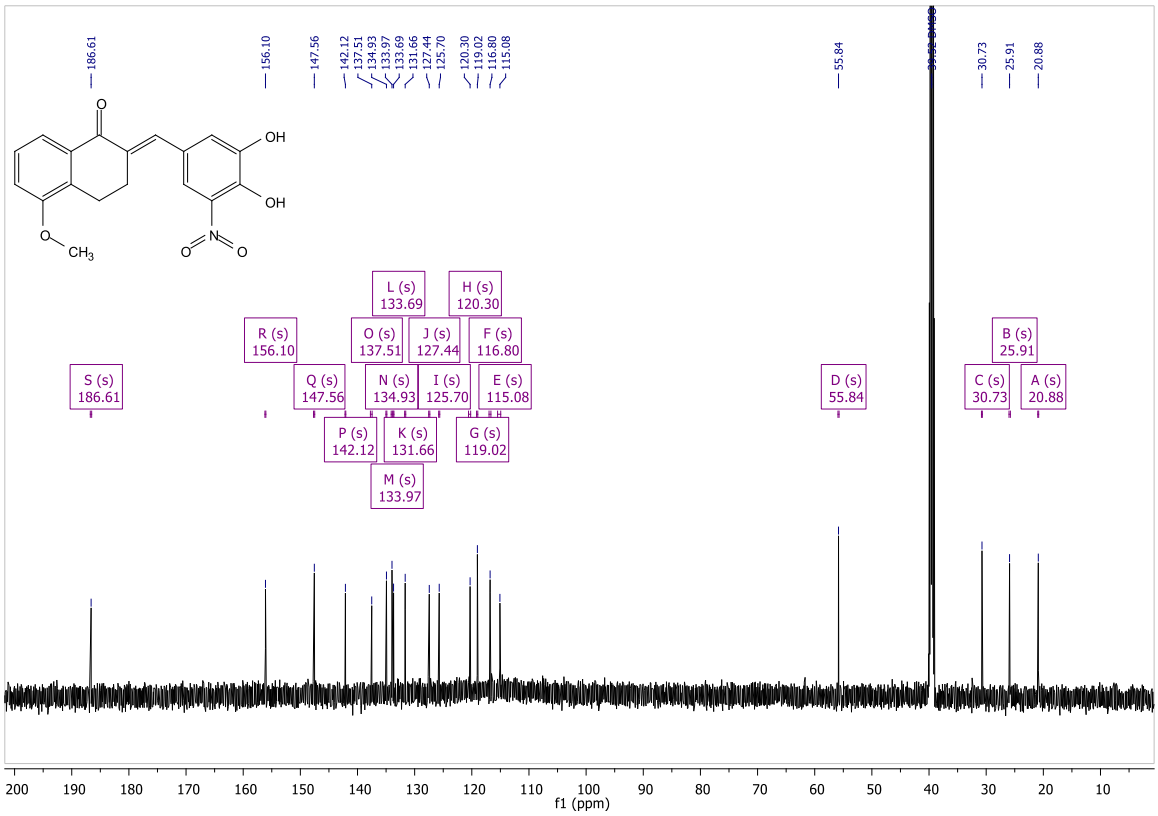

(2*E*)-2-(3,4-Dihydroxy-5-nitrobenzylidene)-7-methoxy-3,4-dihydronaphthalen-1(2*H*)-one (M) [^{1}H NMR]

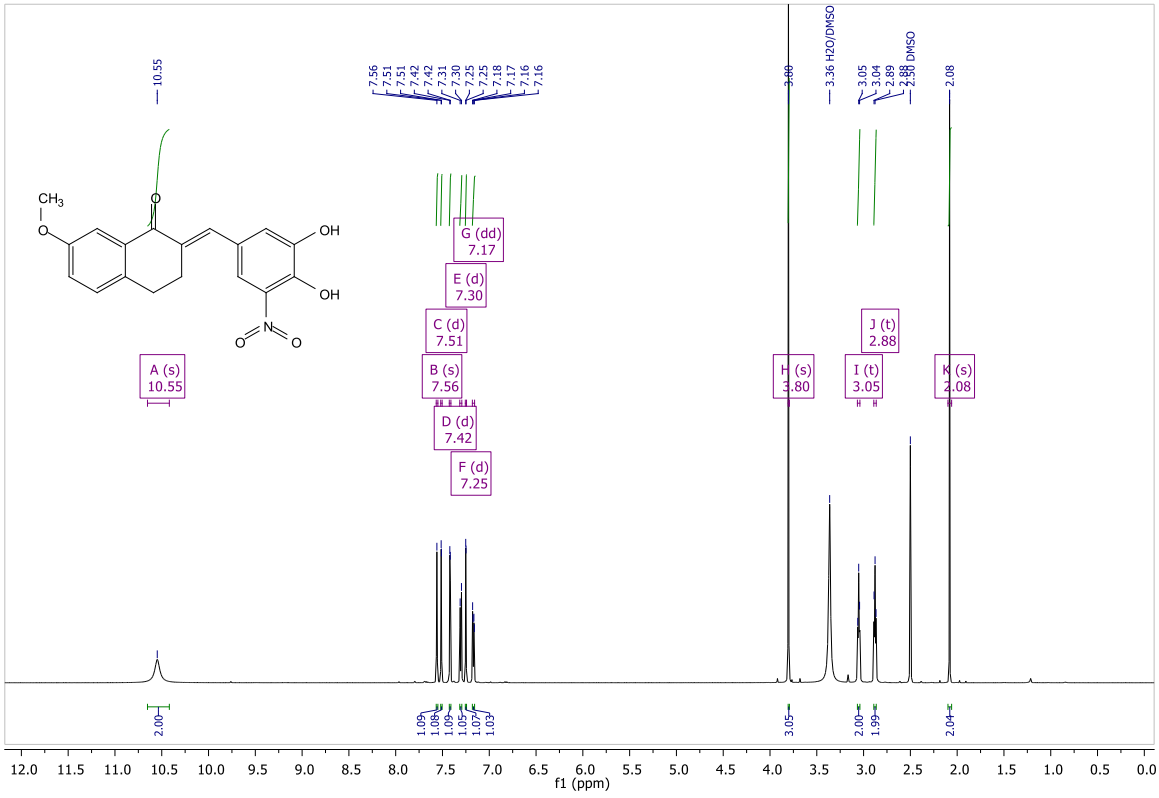

(2*E*)-2-(3,4-Dihydroxy-5-nitrobenzylidene)-7-methoxy-3,4-dihydronaphthalen-1(2*H*)-one (M) [^{13}C NMR]

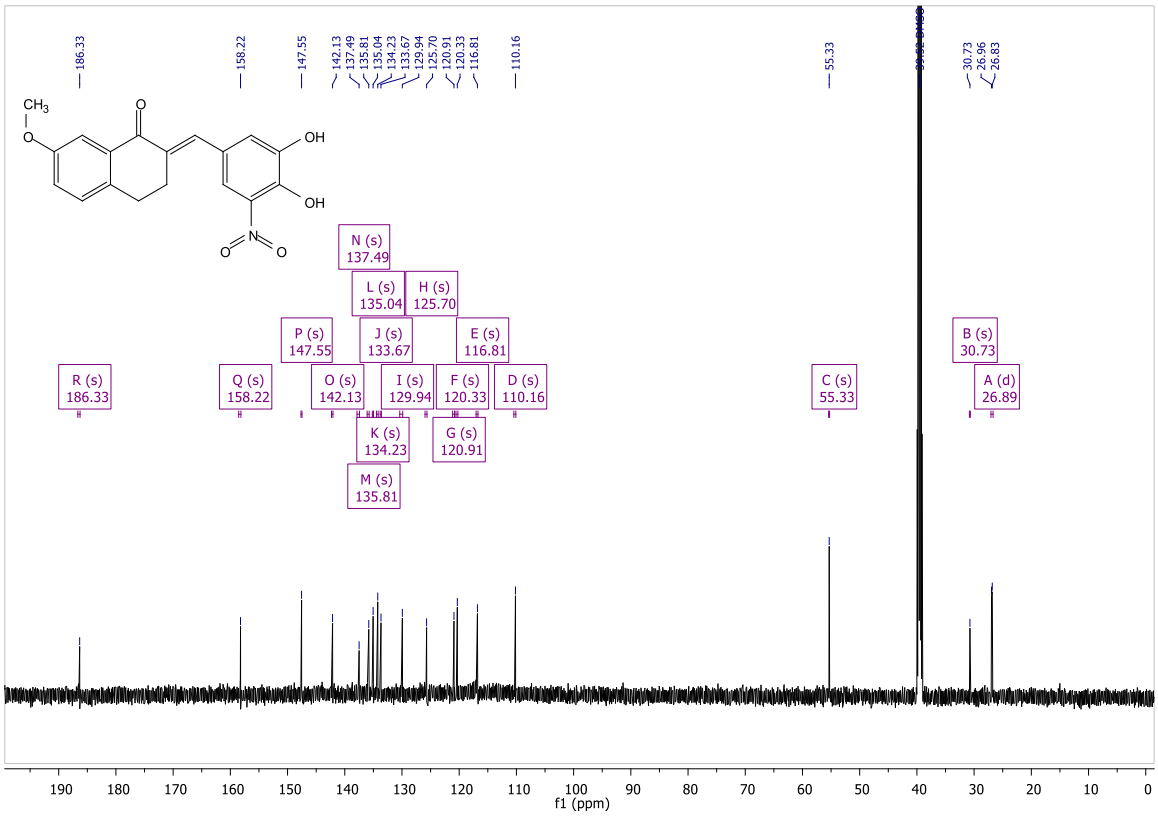

(2*E*)-6-Amino-2-(3,4-dihydroxy-5-nitrobenzylidene)-3,4-dihydronaphthalen-1(2*H*)-one (N) [^{1}H NMR]

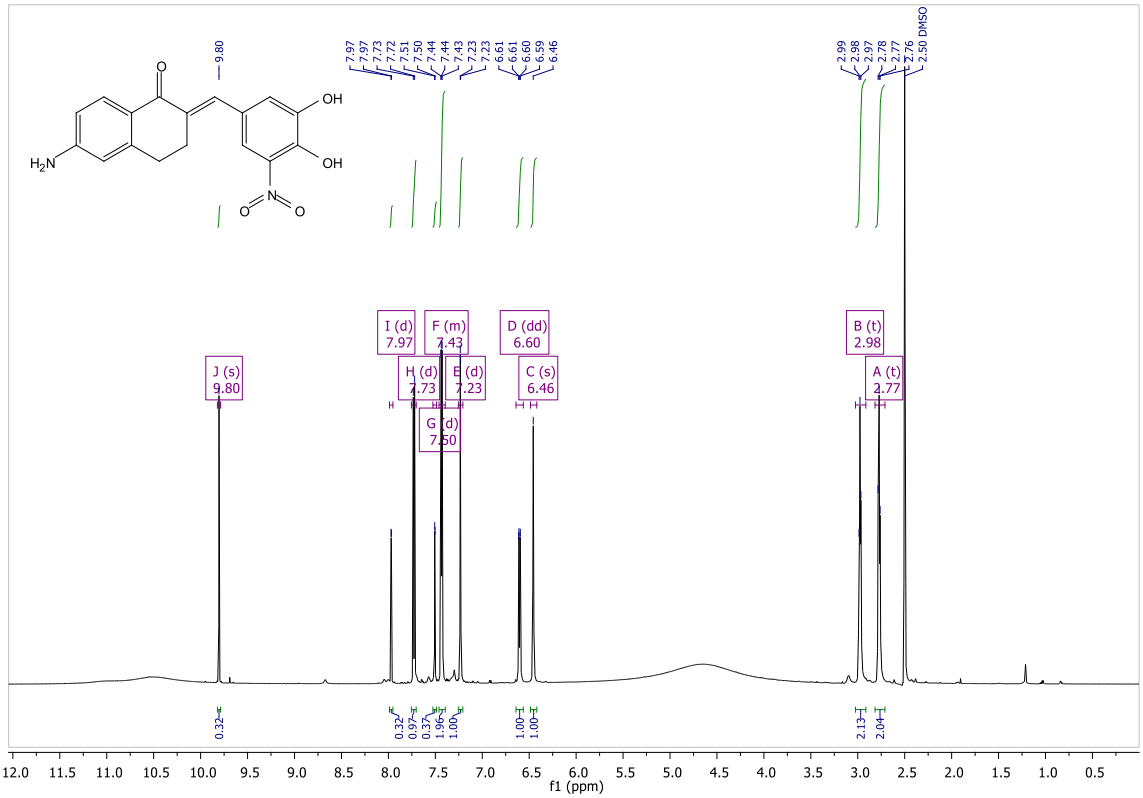

(2*E*)-6-Amino-2-(3,4-dihydroxy-5-nitrobenzylidene)-3,4-dihydronaphthalen-1(2*H*)-one (N) [^{13}C NMR]

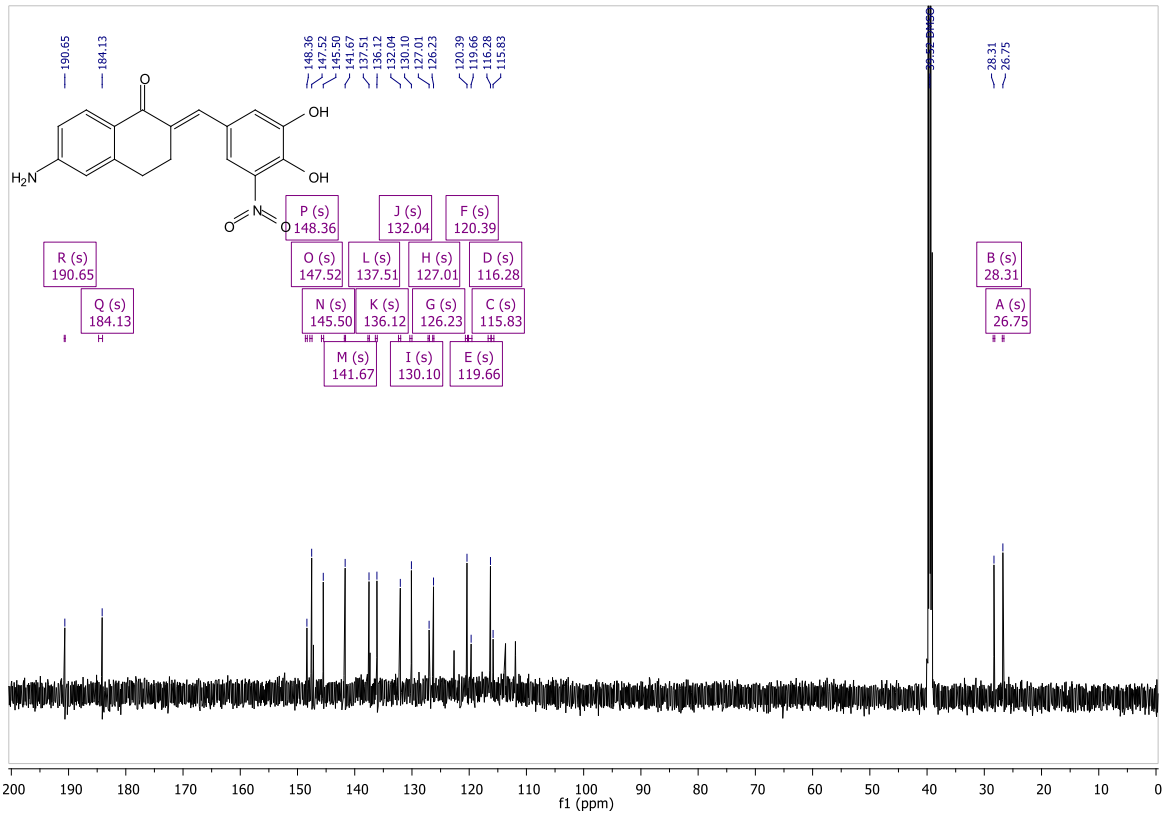

(2*E*)-3-(3,4-Dihydroxy-5-nitrophenyl)-1-phenylprop-2-en-1-one (O) [^{1}H NMR]

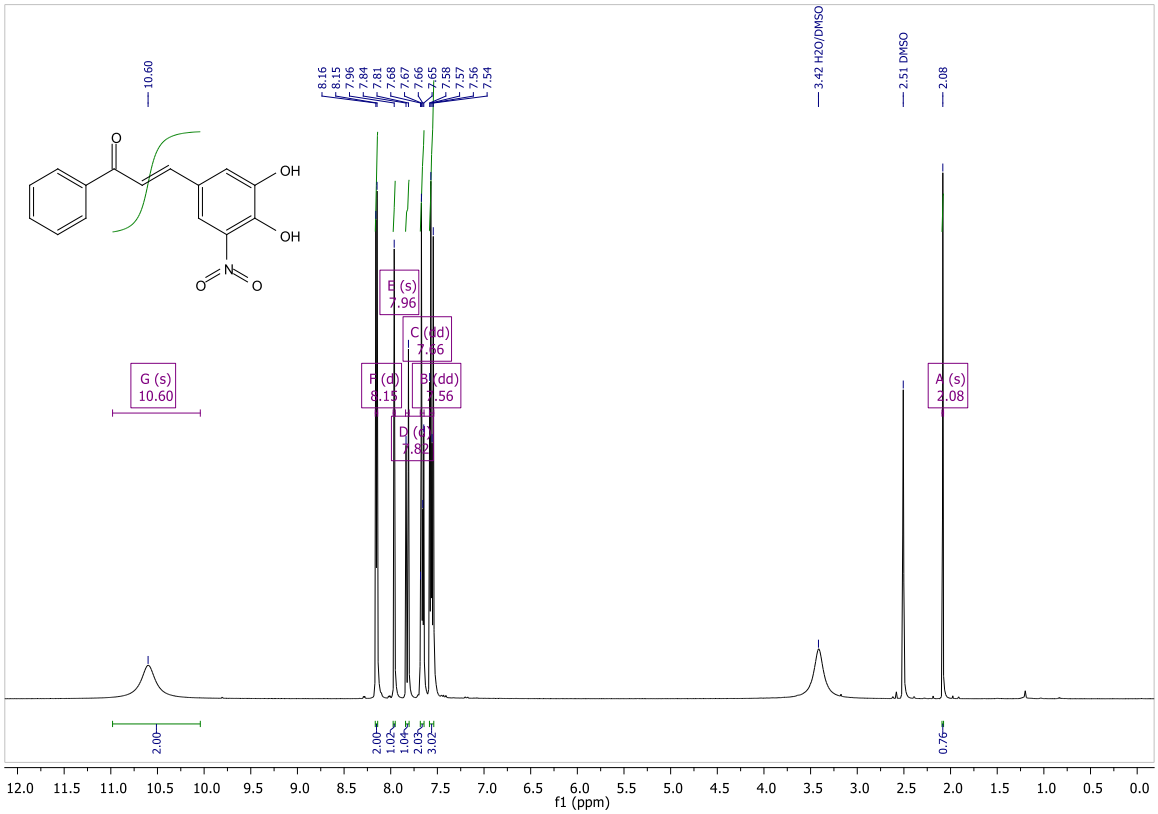

(2*E*)-3-(3,4-Dihydroxy-5-nitrophenyl)-1-phenylprop-2-en-1-one (O) [^{13}C NMR]

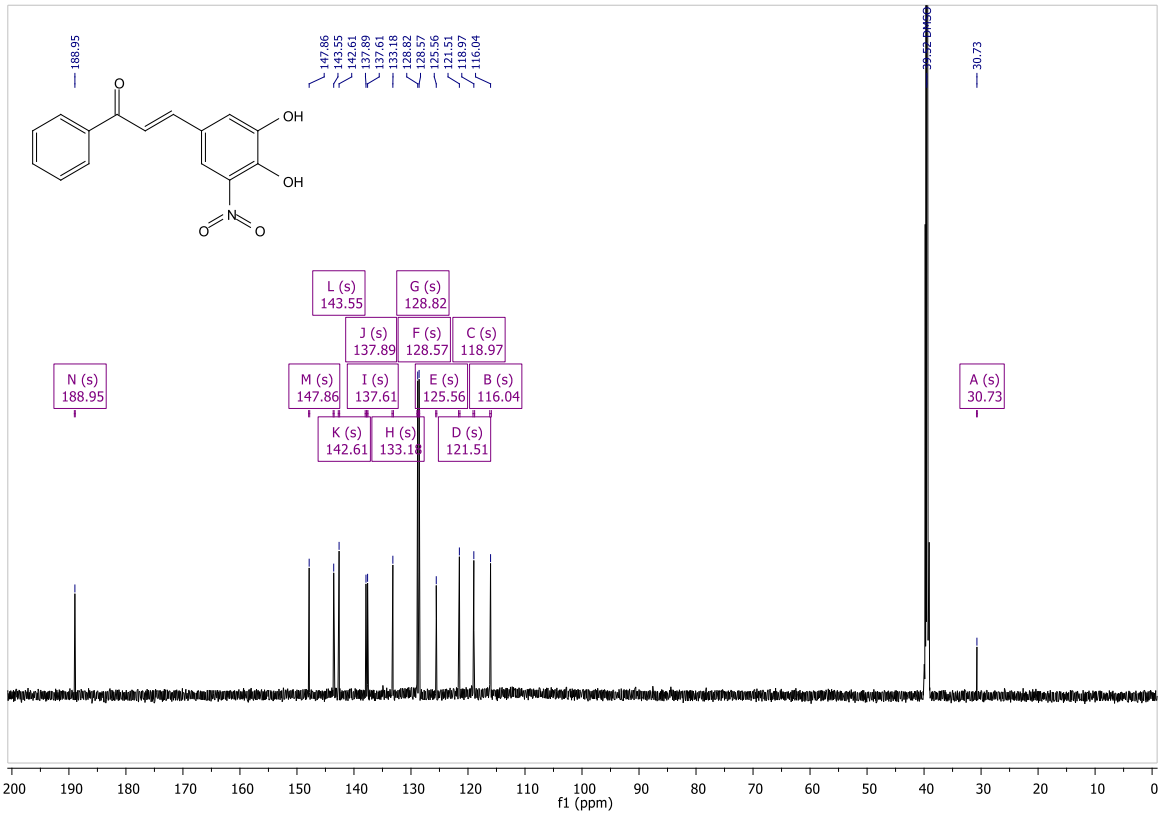

(2*Z*)-2-Bromo-3-(3,4-dihydroxy-5-nitrophenyl)-1-phenylprop-2-en-1-one (Q) [^{1}H]

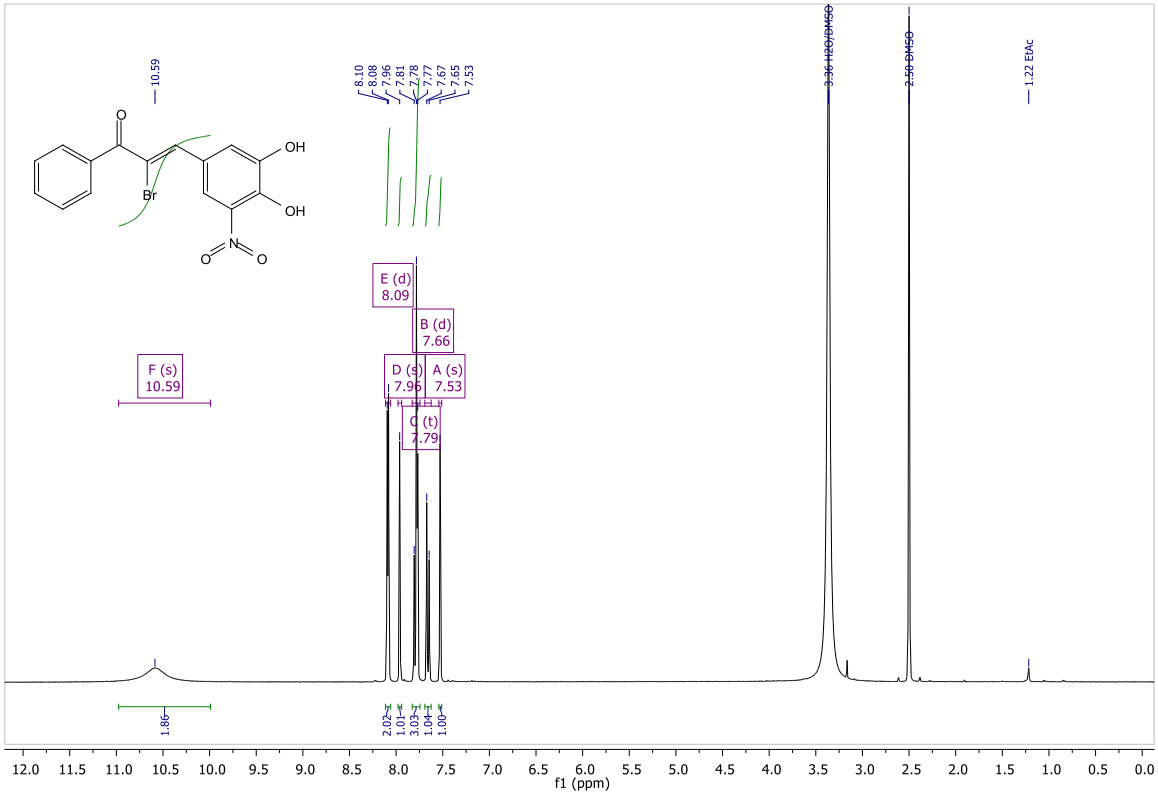

(2*Z*)-2-Bromo-3-(3,4-dihydroxy-5-nitrophenyl)-1-phenylprop-2-en-1-one (Q) [^{13}C NMR]

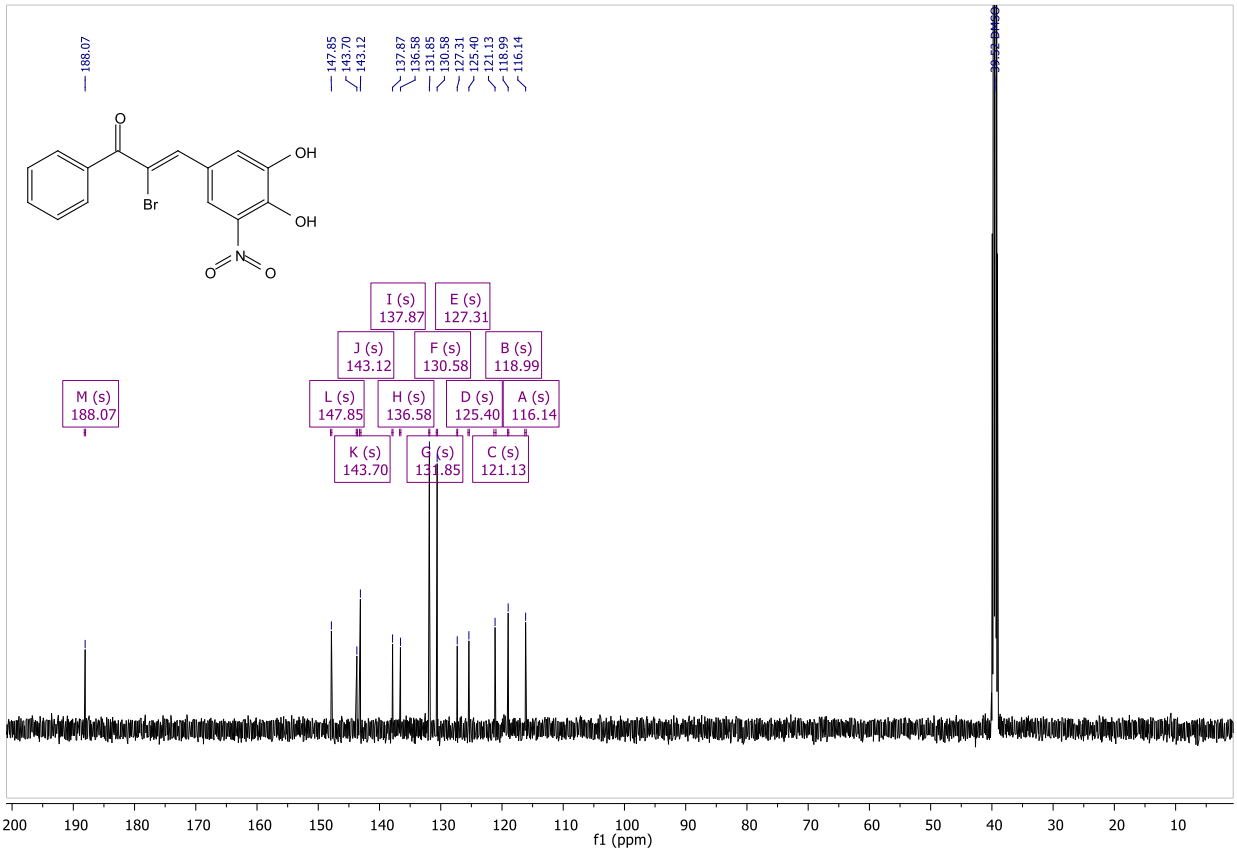

ANNEXURE B MS SPECTRA

(2*E*)-2-(3,4-Dihydroxy-5-nitrobenzylidene)-2,3-dihydro-1*H*-inden-1-one (A)

Acquisition Parameter

Source Type	APCI	Ion Polarity	Positive	Set Nebulizer	1.6 Bar
Focus	Not active	Set Capillary	4000 V	Set Dry Heater	200 °C
Scan Begin	50 m/z	Set End Plate Offset	-500 V	Set Dry Gas	8.0 l/min
Scan End	1600 m/z	Set Collision Cell RF	100.0 Vpp	Set Divert Valve	Waste

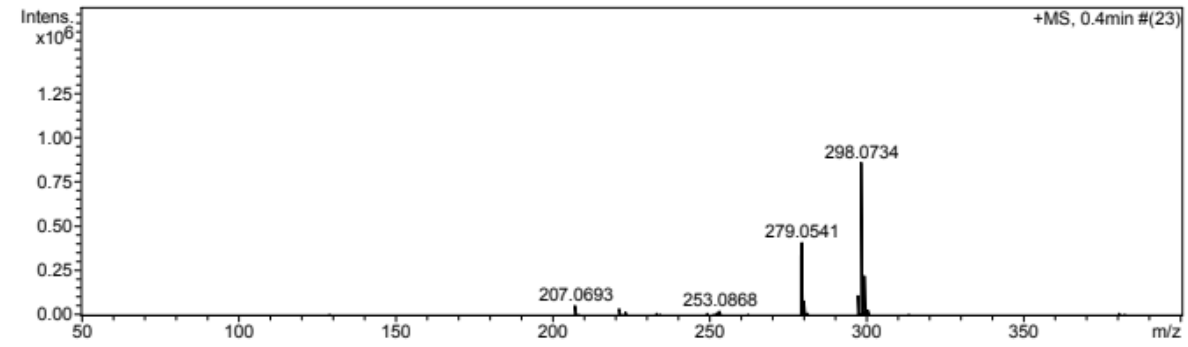

(2*E*)-2-(3,4-Dihydroxy-5-nitrobenzylidene)-5,6-dimethoxy-2,3-dihydro-1*H*-inden-1-one (B)

Acquisition Parameter

Source Type	APCI	Ion Polarity	Positive	Set Nebulizer	1.6 Bar
Focus	Not active	Set Capillary	4000 V	Set Dry Heater	200 °C
Scan Begin	50 m/z	Set End Plate Offset	-500 V	Set Dry Gas	8.0 l/min
Scan End	1600 m/z	Set Collision Cell RF	100.0 Vpp	Set Divert Valve	Waste

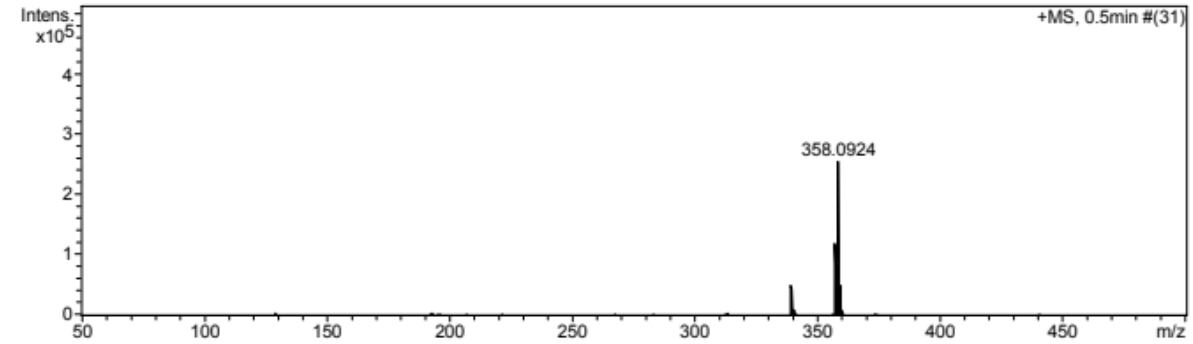

(6*E*)-6-(3,4-Dihydroxy-5-nitrobenzylidene)-6,7-dihydro-5*H*-indeno[5,6-*d*][1,3]dioxol-5-one (C)

Acquisition Parameter

Source Type	APCI	Ion Polarity	Positive	Set Nebulizer	1.6 Bar
Focus	Not active	Set Capillary	4000 V	Set Dry Heater	200 °C
Scan Begin	50 m/z	Set End Plate Offset	-500 V	Set Dry Gas	8.0 l/min
Scan End	1600 m/z	Set Collision Cell RF	100.0 Vpp	Set Divert Valve	Waste

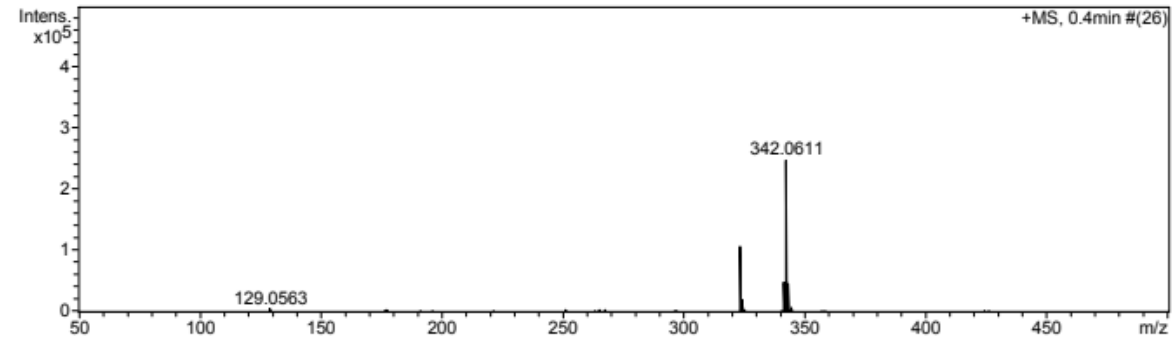

(2*E*)-2-(3,4-Dihydroxy-5-nitrobenzylidene)-5-methoxy-2,3-dihydro-1*H*-inden-1-one (D)

Acquisition Parameter

Source Type	APCI	Ion Polarity	Positive	Set Nebulizer	1.6 Bar
Focus	Not active	Set Capillary	4000 V	Set Dry Heater	200 °C
Scan Begin	50 m/z	Set End Plate Offset	-500 V	Set Dry Gas	8.0 l/min
Scan End	1600 m/z	Set Collision Cell RF	100.0 Vpp	Set Divert Valve	Waste

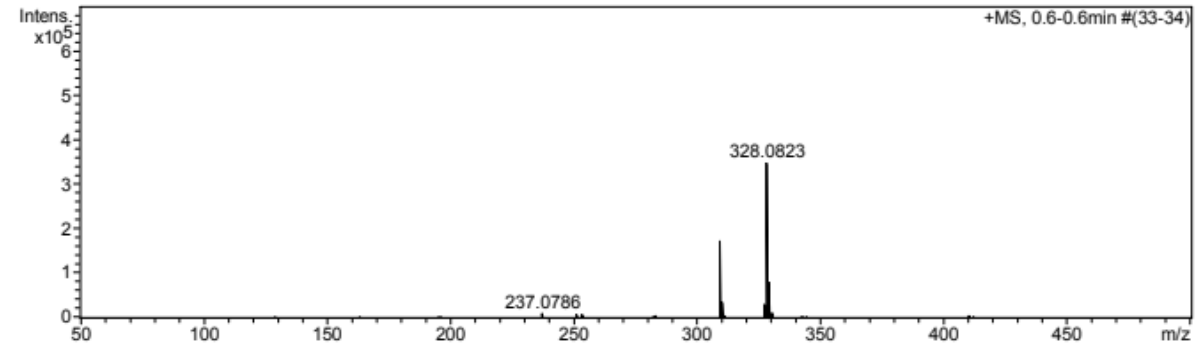

(2*Z*)-2-(3,4-Dihydroxy-5-nitrobenzylidene)-6-hydroxy-1-benzofuran-3(2*H*)-one (E)

Acquisition Parameter

Source Type	APCI	Ion Polarity	Positive	Set Nebulizer	1.6 Bar
Focus	Not active	Set Capillary	4000 V	Set Dry Heater	200 °C
Scan Begin	50 m/z	Set End Plate Offset	-500 V	Set Dry Gas	8.0 l/min
Scan End	1600 m/z	Set Collision Cell RF	100.0 Vpp	Set Divert Valve	Waste

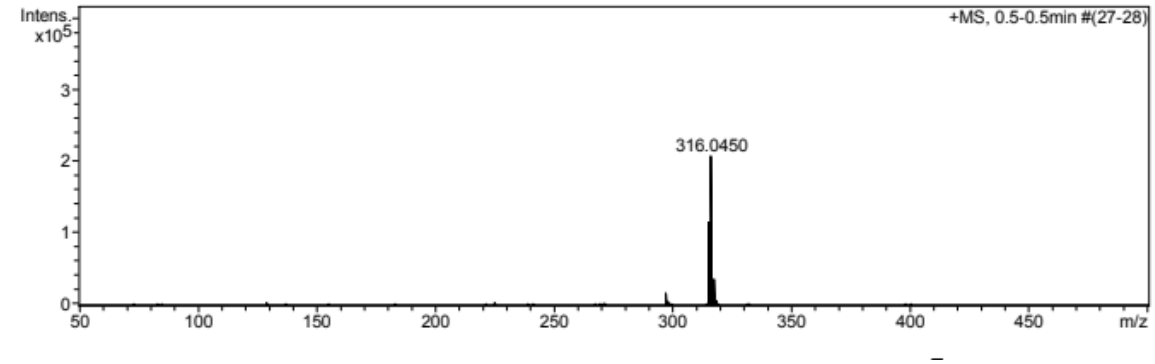

(2*E*)-2-(3,4-Dihydroxy-5-nitrobenzylidene)-5-hydroxy-2,3-dihydro-1*H*-inden-1-one (F)

Acquisition Parameter

Source Type	APCI	Ion Polarity	Positive	Set Nebulizer	1.6 Bar
Focus	Not active	Set Capillary	4000 V	Set Dry Heater	200 °C
Scan Begin	50 m/z	Set End Plate Offset	-500 V	Set Dry Gas	8.0 l/min
Scan End	1600 m/z	Set Collision Cell RF	100.0 Vpp	Set Divert Valve	Waste

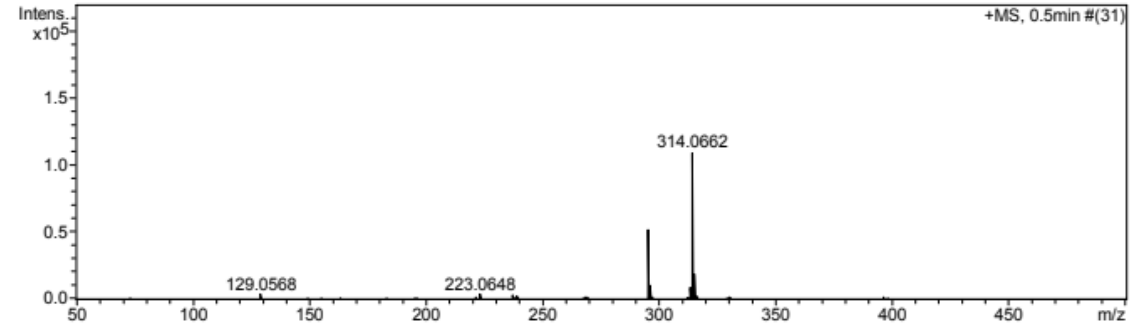

(3*E*)-3-(3,4-Dihydroxy-5-nitrobenzylidene)-2,3-dihydro-4*H*-chromen-4-one (G)

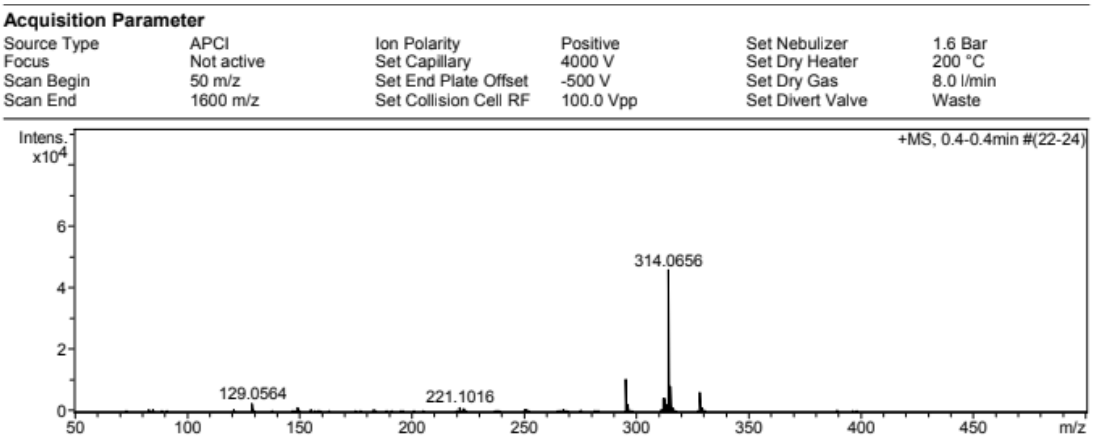

(3*Z*)-3-(3,4-Dihydroxy-5-nitrobenzylidene)-2,3-dihydro-4*H*-thiochromen-4-one (H)

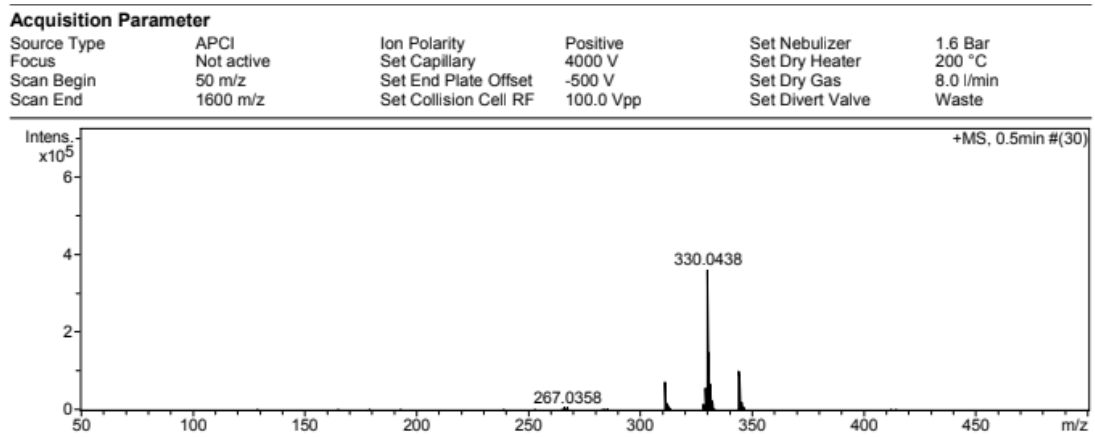

(2*E*)-2-(3,4-Dihydroxy-5-nitrobenzylidene)-3,4-dihydronaphthalen-1(2*H*)-one (I)

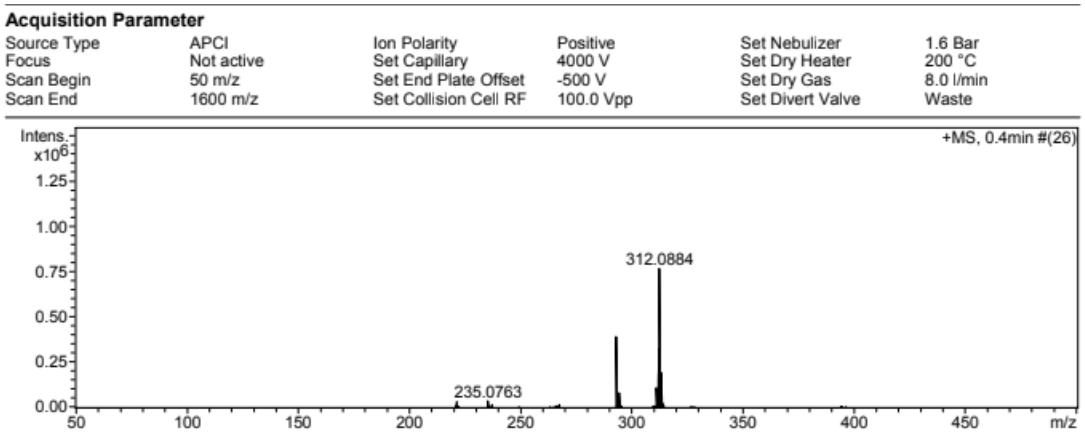

(2*E*)-2-(3,4-Dihydroxy-5-nitrobenzylidene)-6,7-dimethoxy-3,4-dihydronaphthalen-1(2*H*)-one (J)

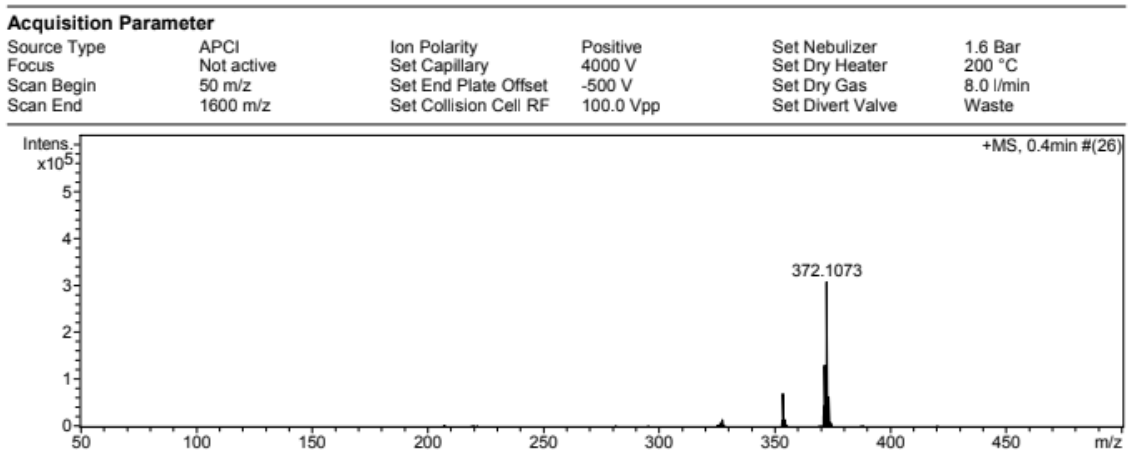

(2*E*)-2-(3,4-Dihydroxy-5-nitrobenzylidene)-6-methoxy-3,4-dihydronaphthalen-1(2*H*)-one (K)

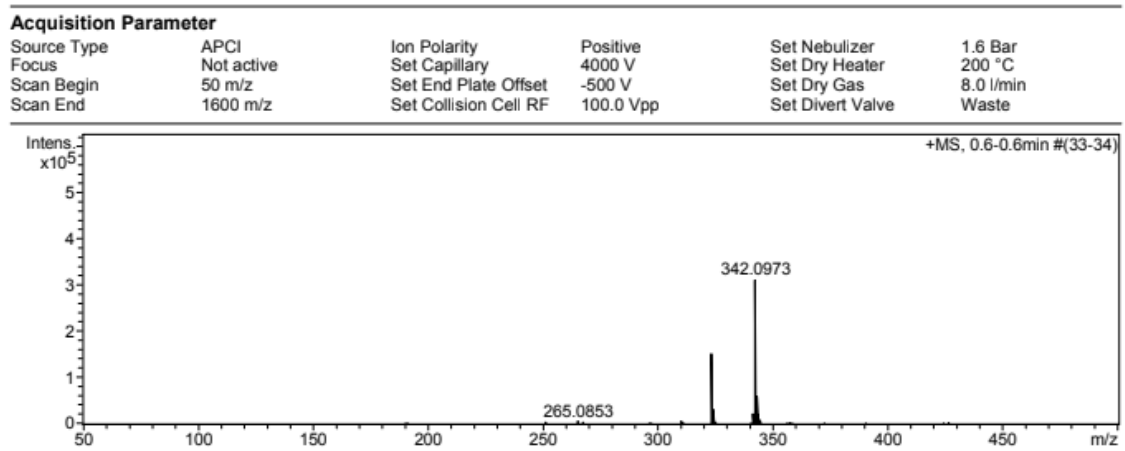

(2*E*)-2-(3,4-Dihydroxy-5-nitrobenzylidene)-5-methoxy-3,4-dihydronaphthalen-1(2*H*)-one (L)

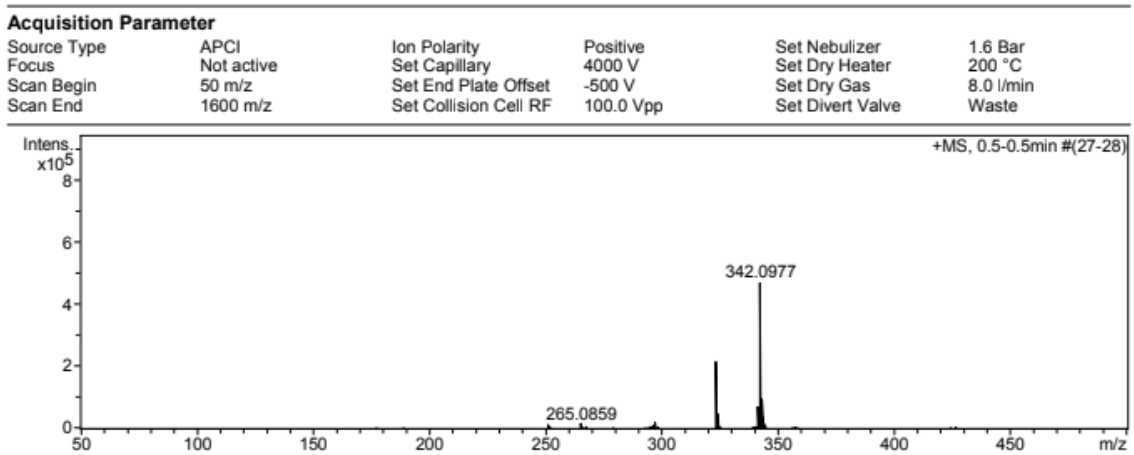

(2*E*)-2-(3,4-Dihydroxy-5-nitrobenzylidene)-7-methoxy-3,4-dihydronaphthalen-1(2*H*)-one (M)

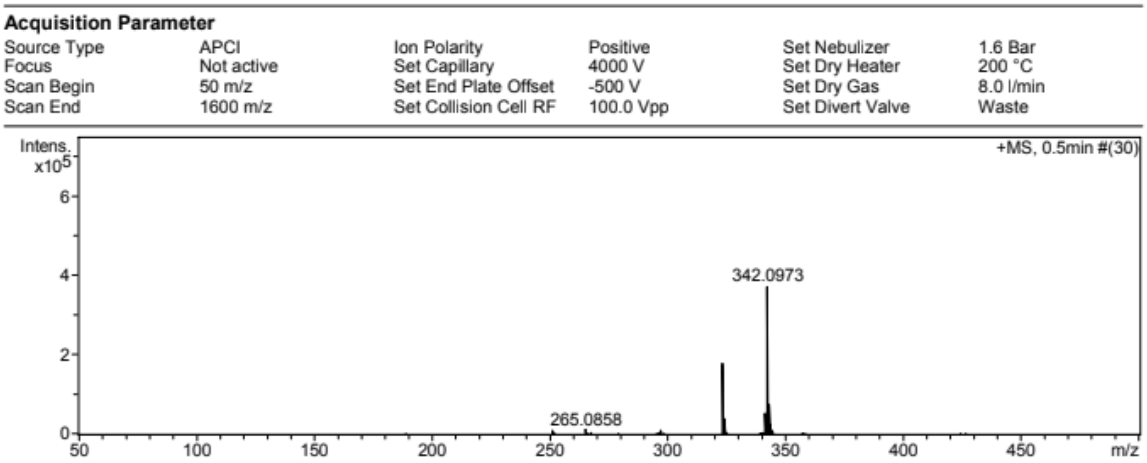

(2*E*)-6-Amino-2-(3,4-dihydroxy-5-nitrobenzylidene)-3,4-dihydronaphthalen-1(2*H*)-one (N)

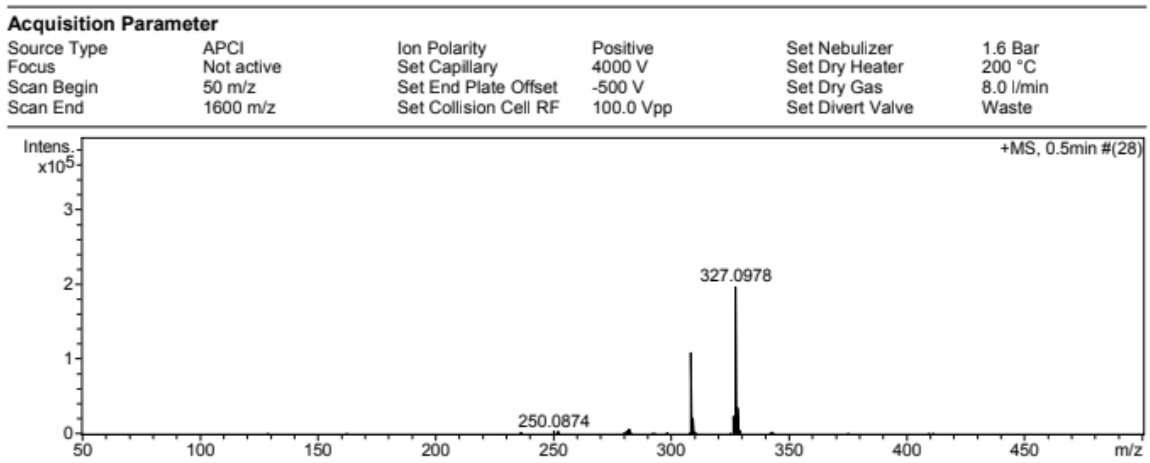

(2*E*)-3-(3,4-Dihydroxy-5-nitrophenyl)-1-phenylprop-2-en-1-one (O)

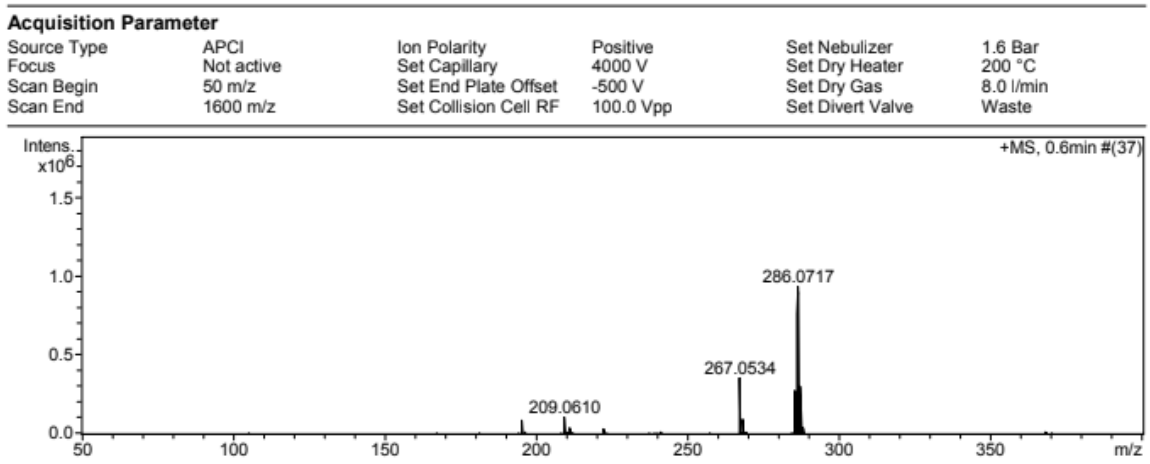

(2*Z*)-2-Bromo-3-(3,4-dihydroxy-5-nitrophenyl)-1-phenylprop-2-en-1-one (Q)

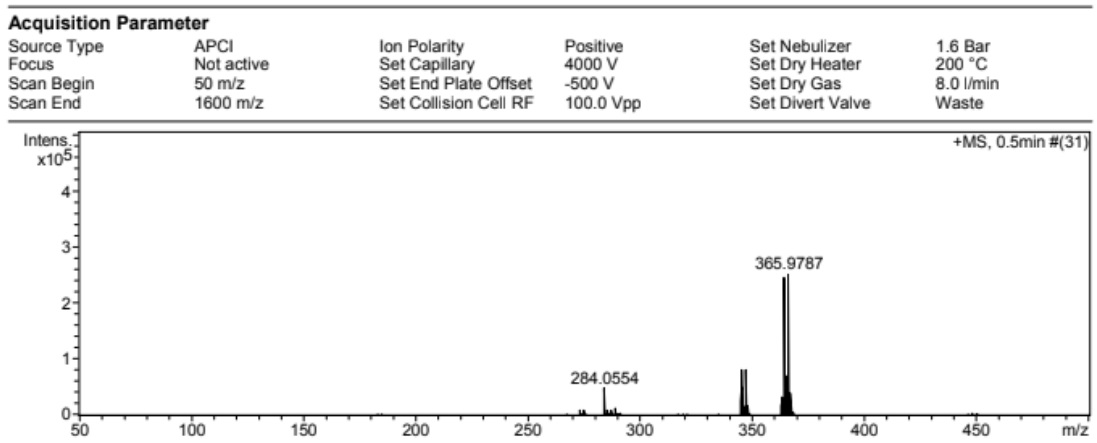

(2*E*)-3-(3,4-Dihydroxy-5-nitrophenyl)-1-(4-methoxyphenyl)prop-2-en-1-one (R)

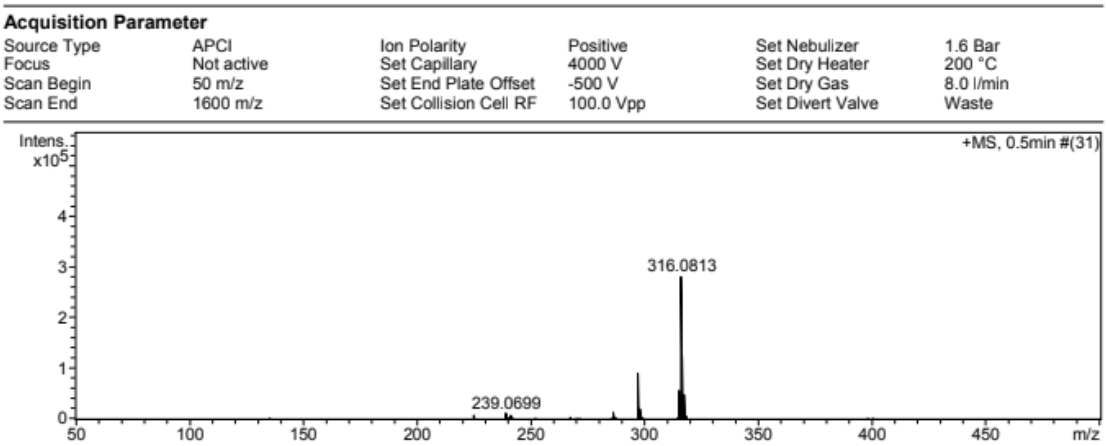

(2*Z*)-2-Bromo-3-(3,4-dihydroxy-5-nitrophenyl)-1-(4-isocyanophenyl)prop-2-en-1-one (T)